Nonlinear Vibration Analysis of Viscoelastic Plates with Fractional Damping

By

Shamim Mashrouteh

A Thesis Submitted in Partial Fulfillment

of the Requirements for the Degree of

Master of Applied Science

Mechanical Engineering

in

The Faculty of Engineering and Applied Science
Department of Mechanical Engineering

University of Ontario Institute of Technology

June 2017

Abstract

Fractional calculus has the history as long as the classical calculus, but up to recent years, less attention has been paid to this method due to its complexity and difficulties in dealing with fractional derivatives and fractional integrals. In the present study, the nonlinear vibration analysis of a rectangular composite plate with fractional viscoelastic properties has been analytically investigated. The plate is modeled based on the von Kármán plate theory, and the Caputo's fractional derivative has been utilized to mathematically model the viscoelastic behavior of the plate with higher accuracy. Galerkin procedure has been implemented to derive the time-dependent ordinary differential equations of motion. The first two orthogonal mode shapes are considered, and variational iteration method is applied to analyze the nonlinear free vibration of the system. The method of multiple time-scales is utilized to investigate the nonlinear forced vibration of the plate when subjected to an external harmonic force. Primary resonances of the system have been studied and analytical expressions for the frequency-amplitude relationships of each mode are derived. Parametric studies have been performed to examine the effect of various parameters, specifically the fractional derivative order as a key factor, on the damped free vibration response and the forced vibration frequency response.

Dedication

To my mother and my father who have always been encouraging me to continue with their greatest love and support.

Acknowledgement

I would like to acknowledge all people whom without their help and support this work could not be completed at all.

First of all, I would like to thank my research supervisor, Professor Ebrahim Esmailzadeh, who has been the best support for me not only as an academic supervisor, but also as a father in all different stages of my life during my master program.

Also, I would like to thank Dr. Davood Younesian who not only greatly supervised me during my undergraduate researches but also guided me with his precious advice and supports in my master program.

I would also thank Dr. Fereydoon Diba for being a supportive friend both in life and academic aspects.

And at the end, I want to thank my lovely parents, my mother Tahereh, and my father Saeed for all of their endless sacrifices whom without them, I would not be able to take one single step in this path.

I also deeply appreciate the research funding and support provided by the Natural Science Engineering Research Council of Canada (NSERC) for making this research possible.

Table of Contents

Nomenclatures

A	Initial displacement , amplitude
a	Length of the plate
b	Width of the plate
C	Non-dimensional damping coefficient
c	Damping coefficient
D	Elastic rigidity
E_x	Elastic modulus in x direction
E_y	Elastic modulus in y direction
$\bar{E}$	Non-dimensional elasticity ratio
F	Non-dimensional in-plane stress function
f	In-plane stress function
G	Shear modulus
h	Thickness of plate
J^{α}	The Reiman-Liouville fractional integral operator of order α
k	Coefficient of fractional derivative
L	General linear operator
M_x	Stress resultant moment in x direction
M_y	Stress resultant moment in y direction
m	Mode shape number in y direction
N	General nonlinear operator
N_x	Stress resultant normal force in x direction

N_y	Stress resultant normal force in y direction
N_{xy}	Stress resultant shear force
n	Shape mode number in x direction
P	External force
Q	Non-dimensional external force
r	Aspect ratio
T	Non-dimensional time parameter
t	Time coordinate
u	Displacement in x direction
v	Displacement in y direction
W	Non-dimensional displacement in z direction
w	Displacement in z direction
X	Non-dimensional length parameter
x	System coordinate
Y	Non-dimensional width parameter
y	System coordinate
z	System coordinate

Greek Nomenclatures

α	Order of the fractional derivative
β	Coefficient of ordinary differential equation
Γ	Gamma Operator

γ_{xy}	Middle surface strain
δ	Variational operator
ε	Small dimensionless parameter
ε_x	Middle surface strain
ε_y	Middle surface strain
$\lambda(s)$	General Lagrange multiplier
v_x	Poisson ratio in x direction
v_y	Poisson ratio in y direction
ρ	Mass density
σ_i	Detuning parameter for mode shape i
σ_{xx}	Kirchhoff stress in x direction
σ_{yy}	Kirchhoff stress in y direction
ω_{nm}	Natural frequency of nm^{th} mode

List of Figures

List of Tables

Chapter 1 - Introduction

Plates are one of the most commonly used structures in engineering applications. They are basic structural elements used in vehicles, mechanical systems, aerospace, navy vessels, and ocean offshore structures [1]. Considering design process of many structural components such as turbine blades, aircraft propeller blades, compressor blades, and helicopter rotor blades, the definition of natural frequencies and vibration behavior are of high importance. It is extremely necessary to design the system with accurate natural frequencies to obtain a structure free of any type of resonances [2].

In a study performed on the Golden Gate bridge [3], it is found that the best method, which led to the simulation results in line with the experimental data, was the one based on fractional derivate. This method made it possible to investigate the damping properties with a higher accuracy comparing to the previously considered methods. This example among so many others encouraged the author to investigate the large deflection vibration analysis of a composite plate with fractional viscoelastic properties as a challenge. In the next sections, an introduction on fractional derivative, large displacement and vibration of plates will be presented.

1.1. Plate Classification

Considering different types of boundary conditions, systems which include rectangular plates can be categorized into three different groups of plates with (i) all simply-supported edges, (ii) plates with a pair of opposite simply-supported edges, and (iii) plates with other types of boundary conditions other than those two mentioned categories [1]. Problems of the first and second types can be analyzed analytically in terms of the well-known Navier and Levy solutions [4]. Nevertheless, finding the exact solution for the vibration of rectangular plates with the third category of boundary conditions is analytically difficult. Therefore, the Rayleigh and Rayleigh-Ritz methods have been utilized by researchers to determine the natural frequencies of such structures.

The vibration analysis of rectangular plates with various boundary conditions has been investigated, by many researchers, using a set of characteristic orthogonal polynomials based on the Rayleigh-Ritz method. This is one of the most conventional methods used due to its high versatility and conceptual simplicity [5]. The orthogonal polynomials have been generated by using a Gram-Schmidt process in order to satisfy the geometric boundary conditions of the accompanying beam problems [6]. Another conventional technique is the Galerkin method, which is based on the orthogonality of mode shapes of the system under vibration. In this method, the displacement function is assumed as the summation of linear functions, which would satisfy the boundary conditions of the system [7].

In the present study, the Galerkin procedure has been considered to derive the time dependent ordinary differential equations of motion.

1.2. Large Deflection of Rectangular Plate

Vibration analysis of flexible structures such as plates, commonly used in engineering industries, is important and their critical vibration behavior must be considered in the design process of engineering systems.

Any known theory which will be used to model a specified structure has a significant effect on both the accuracy of the defined stresses and the natural frequencies of the system. This theory should be capable of presenting the nonlinear dynamic and vibration behavior of the structure, materials, boundary conditions and the loadings of the system [2]. As an example, the presence of transverse shear strain is very significant for modeling a composite plate, which can be seen by comparing the results obtained based on the classical plate theories with those obtained based on the theories that consider the transverse shear strains [2]. A noteworthy point is that when the amplitude of vibration is larger than the thickness of the plate, it is significant to consider the interaction of the normal modes with the in-plane ones [2].

Based on publications available, there is an agreement among researchers that the internal energy waste would occur mainly because of the action of forces on the in-plane surface where the flexural work could be neglected [8]. Based on the von Kármán theory, the in-plane displacements are infinitesimal and the strain relationships depend only on the main deflection of the plate, which has the same

value of the thickness of the plate [9]. In other words, when comparing the plates with smaller deflections with those having larger deflections, it can be shown that the vibration behavior of plates with larger deflection are not influenced by the external loads [10]. However, they would depend only on the mid-plane stretching of the plate [10].

1.3. Non-Isotropic and Composite Plates

A non-isotropic plate exhibits different properties in different directions which can be modeled using the general elasticity theory [11]. One of the large subcategories of non-isotropic plates are orthotropic plates. The orthotropic behavior of plates may be the result of using materials with such constitutive relations, modeling composite plates as orthotropic plates, changing isotropic plates structure by metallurgical process along perpendicular directions, and stiffening panels unequally along two orthogonal directions [1].

Composite materials represent properties such as high strength and high stiffness to weight ratio, high corrosion resistance, and high thermal stability. Such properties make composite materials suitable for structures, which need complex shape, impact resistance, and high strength and stiffness. Good examples of these type of structures are aerospace, marine and automotive structures [11].

1.4. Fractional Differential

To determine a successful response of a viscoelastic damped structure, under specific loadings, one will face two problems. The first one is being able to describe the mechanical properties of the viscoelastic material based on the mathematical rational behavior. Solving the first problem successfully will then allow one to effectively tackle the second problem, which is solving the time-dependent equation of motion of the viscoelastic structure. One of the best approaches to solve the above-mentioned problems is to utilize the fractional derivative model for defining the stress-strain relationship of viscoelastic solid structures [12]. Modeling the viscoelastic behavior of materials using fractional damping will facilitate researchers to simulate accurately a real-world problem.

Early investigations on the mechanical properties of viscoelastic materials showed that the stress relaxation phenomenon is related to fractional power as time changes. An important point is that as the frequency changes into fractional powers, the mechanical properties of the frequency dependence materials would vary and could be modeled as a differential fractional order. Fractional derivatives can be used to relate the time-dependent stress and strain in viscoelastic materials and such relationship has been observed and validated experimentally for some metals and glasses [12].

To better understand the concept of fractional derivative, it is of benefit to introduce the Caputo's definition which has been defined after modifying the Reiman-Liouville definition. The advantage of Caputo's definition on the Reiman-Liouville is the

capability of dealing with the initial value problems properly where in most physical cases the initial conditions are given in terms of the field parameters and their integer order [13].

As a first definition, we would need to define a real function $f(x)$, $x > 0$, which is assumed to be in the space C_μ, $\mu \in R$ if there exists a real number p which $p > \mu$, such that $f(x) = x^p f_1(x)$, where $f_1(x) \in C[0, \infty)$, and it is said to be in the space C_μ^m if $f^{(m)} \in C_\mu, m \in N$, [13].

The Reiman-Liouville fractional integral operator of order $\alpha \geq 0$, of a function $f \in C_\mu, \mu \geq -1$, is defined as [13]:

$$J^\alpha f(x) = \frac{1}{\Gamma(\alpha)} \int_0^x (x-t)^{\alpha-1} f(t) dt \, , \; \alpha > 0 \, , \; x > 0 \, , \tag{1-1}$$

$$J^0 f(x) = f(x) . \tag{1-2}$$

Detailed properties of the J^α operator can be found in [14, 15], but here some of the most important ones (when considering the assumptions $f \in C_\mu, \mu \geq -1, \alpha, \beta \geq 0$, and $\gamma > 0$) have been listed as [13]:

$$J^\alpha J^\beta f(x) = J^{\alpha+\beta} f(x), \tag{1-3}$$

$$J^\alpha J^\beta f(x) = J^\beta J^\alpha f(x), \tag{1-4}$$

and

$$J^\alpha x^\gamma = \frac{\Gamma(\gamma+1)}{\Gamma(\alpha+\gamma+1)} x^{\alpha+\gamma} , \tag{1-5}$$

The reason, which is resulted in defining a modified definition of fractional differential operator was to point out certain disadvantages of the Riemann-Liouville derivative in modeling the real-world problems with fractional differential equations. Hence, the Caputo's definition was introduced as a modified fractional differential operator by Caputo's theory of viscoelasticity.

The Caputo's fractional derivative of $f(x)$ is defined as [13]:

$$D_*^{\alpha} f(x) = J^{m-\alpha} D^m f(x) = \frac{1}{\Gamma(m-\alpha)} \int_0^x (x-t)^{m-\alpha-1} f^{(m)}(t) dt , \qquad (1\text{-}6)$$

For $m-1 < \alpha \leq m,\ \ m \in \mathbb{N},\ \ x > 0,\ \ f \in C_{-1}^{m}$.

Following are some of the most basic properties of the Caputo's fractional derivatives which have been mentioned in Ref. [13]:

If $m-1 < \alpha \leq m,\ \ m \in \mathbb{N},\ \ x > 0$, and $f \in C_{\mu}^{m},\ \ \mu \geq -1,$

then

$$D_*^{\alpha} J^{\alpha} f(x) = f(x) , \qquad (1\text{-}7)$$

$$J^{\alpha} D_*^{\alpha} f(x) = f(x) - \sum_{k=0}^{m-1} f^{(k)}(0^+) \frac{x^k}{k!} , \ \ x > 0 \qquad (1\text{-}8)$$

As an immediate extension of the ordinary derivative, in the fractional derivative modeling, as the fractional order α moves close to one, the Gamma function tends to the Dirac δ function, which results in the fractional derivative behaves like an ordinary derivative. Considering Eq. (1-6), if $\alpha \to 1$, for $m = 1$, one could obtain the following relationship [3]:

$$\frac{1}{\Gamma(1-\alpha)}(x-t)^{-\alpha} \Rightarrow \delta(x-t) \tag{1-9}$$

Therefore, the fractional derivative tends to become an ordinary derivative $\dot{x}$. At this stage, the mathematical model of the viscoelastic plate would be transformed into the Kelvin-Voigt model in which, the viscous damping element acts linearly, but the elastic element behaves nonlinearly [3].

1.5. Methodology

Approximating or solving nonlinear problems has always been known to be a difficult task. On the other hand, most of the available analytical methods simplifies the problems by linearizing the real model, which can result in losing some information or getting answers that describe the problem either incorrectly or with some errors [16]. The importance of solving a nonlinear equation, which describes a real-world problem as accurate as possible, and reducing the simplifications have resulted in many publications on various methods for solving nonlinear differential equations. Some of these methods such as the Variational Iteration Method and the Multiple Time-Scales Method have been briefly discussed in the following sections.

1.5.1. Variational Iteration Method

The variational iteration method has originally been applied to solve various models having nonlinear differential equations. The main advantage of this method is its capability to solve nonlinear equations conveniently and accurately. Based on the published literatures, the application of this method has been expanded into different

type of equations, such as the nonlinear wave equations, nonlinear oscillations, nonlinear fractional equations, and many other nonlinear problems arise in engineering applications. The main feature of this method is that the initial approximation can be chosen based on the unknown parameters and can be found in the solution process. Also, the initial solution can be defined easily based on the initial conditions of the problem, or by linearization of the main nonlinear problem [17].

In order to create an overall understanding on the basic concept of the variational iteration method, one could consider the following general nonlinear differential equation [18]:

$$L\{u\} + N\{u\} = g(x) \tag{1-10}$$

Where L is a general linear operator, N is a general nonlinear operator, and g(x) is either a non-homogeneous term or an external force. Based on the variational iteration method [18-20], a correction function advection partial differential equation can be defined as:

$$u_{n+1}(x) = u_n(x) + \int_0^x \lambda(\xi)\big(L\,u_n(\xi) + N\,\tilde{u}_n(\xi) - g(\xi)\big)\,d\xi \tag{1-11}$$

Where $\lambda(s)$ is a general Lagrange multiplier, which can be find on the basis of variational principle [21] and the exact procedure for finding it will be explained in details in Section 4. 2. Also, $\tilde{u}_n$ is considered as a restricted variation term.

1.5.2. Multiple Time-Scales Method

Some natural phenomena have more than one time scale or related length characteristic and failing to recognize the dependency of a system on more than one time scale is a common non-uniformity in perturbation expansion. The method of multiple time-scales is a well-known technique for solving nonlinear equations that depends on simultaneous different time scales. The response of a nonlinear oscillator, subjected to a harmonic excitation as an ideal energy source, depends on both the excitation frequency and amplitude of vibration. The system response consists of a free vibration part, which decays with time, and a steady-state part that has the same frequency as the excitation one., The resonant phenomenon occurs when the frequency of the external excitation approaches to the natural frequency of the system [22]. In the following sections, the application of this method will be explained in detail.

1.6. Thesis Outline

Content of this thesis is presented in the next five chapters and a summary of each chapter is outlined below.

An extensive literature survey is performed in Chapter 2. The most important aspects of this research, which previously studied by researchers, are summarized in this chapter. Different types of plates, the proposed theories and various applications of the fractional derivatives are presented in Chapter 2. Applications of the variational iteration method and the multiple time-scales method in engineering problems,

especially in solving the nonlinear differential equations for vibration of plates, beams, and Nano-beams are examined. The fractional derivation modeling, briefly introduced in Chapter 1, is examined in different engineering fields such as biomedical engineering, mechanical vibration, and civil engineering.

Chapter 3 covers the nonlinear vibration of a composite plate, which is modeled on the basis of the Kirchhoff stress theory and the von Kármán plate theory. The plate is assumed to have an orthotropic behavior with the fractional viscoelastic properties. The partial differential equations for the displacement of the plate and the in-plane stress functions are developed. The Galerkin procedure is utilized and the time-dependent ordinary differential equations for each natural vibration modes of the system are obtained.

The nonlinear free vibration analysis of the composite plate with the fractional viscoelastic properties is studied in Chapter 4. The variational iteration method is applied to solve the nonlinear equations of motion and also to obtain the numerical time response of the system under different conditions. To investigate the exact behavior of the plate with the fractional viscoelastic properties, the order of the fractional derivative is chosen as the key parameter; and the plate sensitivity to this parameter under different conditions has been examined. A detailed parametric study to assess the effect of the aspect ratio and the elasticity ratio is performed.

In Chapter 5, the nonlinear forced vibration of a plate with the fractional viscoelastic properties subjected to a harmonic external force is analyzed. The mathematical modeling based on the procedure outlined in Chapter 3 is developed and the method

of multiple time-scales is utilized to solve the nonlinear forced vibration equations. Analytical frequency-amplitude relationships for each mode of vibration are derived and detailed numerical studies based on the obtained formulas are performed. The effects of variation of important parameters, namely, the fractional derivative order α; coefficient of the fractional derivative k, aspect ratio r, and the elasticity ratio $\bar{E}$ are fully discussed.

The final chapter is devoted to the conclusion, wherein all the results obtained are summarized and fully discussed in order to draw the contribution of this research. Furthermore, few research ideas as the continuation of this work are suggested in Chapter 6.

Chapter 2 - Literature Review

2. 1. Large Deflection of Plates

Vibration analysis of a rectangular plate attached to a plate cavity has been investigated by Sadri and Younesian [23, 24]. The effect of the interaction between the air cavity and the isotropic plate has been modeled based on the von Kármán plate theory and the Galerkin procedure has been applied to derive the ordinary differential equations. The method of multiple time-scales has been utilized to study the primary, secondary, and the combination resonance cases [23].

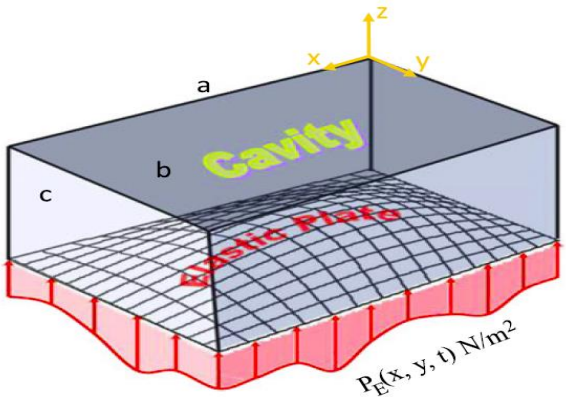

Figure 2-1- Schematic model of plate and air cavity [23]

They showed that the effect of excitation amplitude on the stable zone for the primary resonances can be neglected. They also concluded that for the superharmonic resonance case, the excitation amplitude has an increasing influence while for the subharmonic resonance has a decreasing effect [23]. In another study, they applied the variational iteration method to analytically solve the nonlinear ordinary differential equations of the system. They obtained the nonlinear natural frequency of the system by implementing the harmonic balance method [24].

Large oscillation of triangular plates is another interesting topic in the area of nonlinear vibration analysis. In a study performed by Nowinski and Ismail [25] large amplitude vibration of a triangular plate, based on the von Kármán plate theory, has been investigated. A similar study on nonlinear vibration of a triangular plate was performed by Askari et al. [26]. They tried different stiffeners attached to the plate in order to reduce the undesirable large deflections. Adding the stiffeners to the plate changed their system from an isotropic plate into an orthotropic one. They derived the governing equations of motion based on the von Kármán plate theory and applied the Galerkin method to obtain ordinary time-dependent equations of motion. Different solution methods of energy balance method (EBM), variational approach (VA), and the multiple time-scale method (MSM) were tested in their investigations as shown in **Figure 2-2**. They showed that the second-order variational approach has the highest accuracy and the first-order variational approach has the lowest accuracy among the mentioned methods.

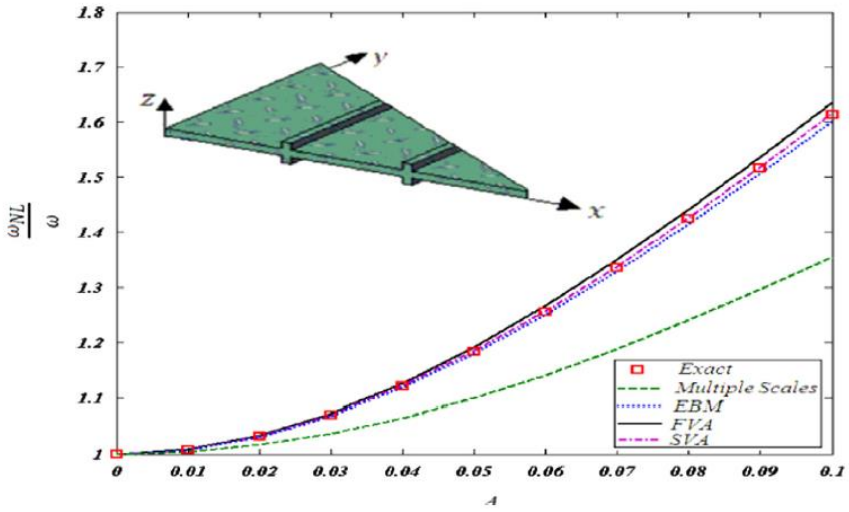

Figure 2-2- Frequency ratio of triangular orthotropic plate [26]

2. 2. Non-Isotropic plates

Most of the materials subjected to stress have either elastic behavior or nearly elastic one. Under elastic behavior, the strain remains unchanged when loading, unlike materials which follow the viscoelastic behavior. Viscoelastic materials exhibit elastic reaction upon loading but a slow and continuous increase will occur for their strain. These materials are significantly affected by the rate of strain or stress. Composite materials such as wood, epoxies, natural and synthetic fibers, among others, show this type of behavior [27].

The usage of composite materials such as fiber reinforced plastics has been increased during recent years due to the different behavior of these materials comparing with the conventional isotropic materials behavior. Composite materials are ideal for applications in which high strength-weight and stiffness-weight ratios are required.

For example, an aircraft or space structures which are sensitive to weight benefit most by using composite materials [28].

In general, the word composite as a material point of view, explains that two or more materials are combined on a microscopic scale to make a useful new material. Most important properties improved in composite materials are listed below [28]:

- Strength
- Stiffness
- Corrosion resistance
- Weight
- Wear resistance
- attractiveness

In a study implemented by Woo and Meguid [29], large deflection of composite plates and shallow shells under a temperature field and transverse mechanical load were investigated. They assumed that functionally graded materials change continuously through the thickness of the plate. They modeled the plates and shells based on the von Kármán plate theory for large deflections. They studied the effects of various material properties and used different materials volume fractions (alumina-aluminum, aluminum-zirconia) in their numerical simulations. For each combination of functionally graded plates, the dimensionless deflection, bending moment and stresses were computed and the influence of different parameters were investigated [29].

Nonlinear vibration analysis of a composite plate embedded with shape memory alloys under influence of initial deflection and stresses based on the von Kármán plate theory has been studied by Park et al. [30]. They showed that higher initial strain of the shape memory alloy fibers result in higher stiffness of composite plate [30].

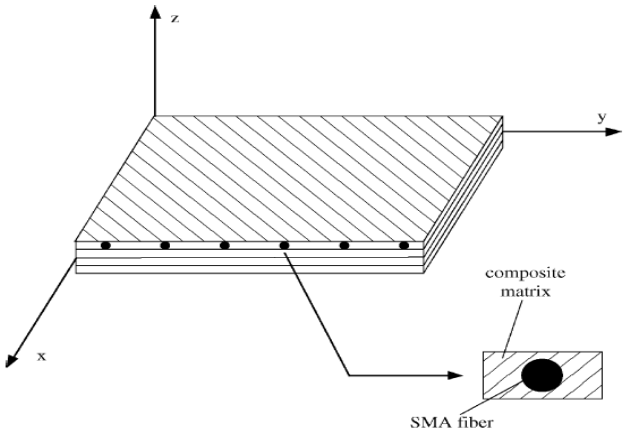

Figure 2-3- Schematic composite plate reinforced with SMA [30]

They also indicated that using the shape memory alloyed fibers would decrease the critical temperature and the thermal large deflections [30].

Large-amplitude vibration of a nanocomposite plate, reinforced by carbon nanotubes, in the thermal environment resting on an elastic foundation was studied by Wang and Shen [31]. Two different distribution of carbon nanotubes for the plate were assumed, namely, (i) uniformly distributed and (ii) functionally-graded reinforcement. They developed the equations of motion based on the shear deformation plate theory and assumed that the material properties are temperature-dependent. The numerical results obtained by improved perturbation technique showed that as the carbon nanotubes volume fraction increased, the natural frequencies of the systems will increase. Also, the natural frequencies have decreased when either the temperature increased or the stiffness of the foundation decreased [31].

Chen et al. [32] studied a transversely magneto-elector-elastic medium by using two separate states of equations for the displacements and stresses. They assumed a non-

isotropic plate with inhomogeneous properties along thickness. In order to study the free vibration of this system, they applied an approximate laminate model that would develop two independent classes of vibration equations. The first class had the natural frequency related only to the elastic properties of the plate. Additionally, they considered the magneto-electric coupling effect between the laminate layers, which were neglected during the previous studies.

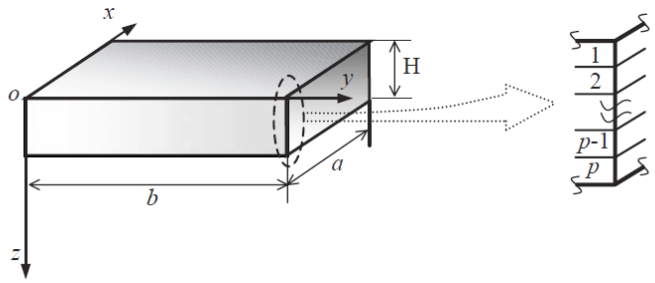

Figure 2-4- Magneto-elector-elastic medium and laminate model [32]

The second class of their vibration modeling consisted of the in-plane and out-of-plane displacements, non-zero elastic properties, and the magnetic potentials. They successfully confirmed the accuracy of their modeling by comparing it with the available results in literature [32].

2. 3. Variational Iteration Method

Wu and lee [33] investigated fractional differential equations investigated by variational iteration method. They considered the fractional terms in their approach instead of assuming its term as a restricted variation term. They modeled the fractional term of the equations based on the Modified Reimann-Liouville derivatives.

Different examples were solved in their work from which, one of them was the following fractional diffusion equation [33]:

$$\frac{\partial^{\alpha} u(x,t)}{\partial t^{\alpha}} = \frac{x^2}{2}\frac{\partial^2 u(x,t)}{\partial x^2} \quad , 0 < \alpha \leq 1, \tag{2-1}$$

Where the boundary conditions were defined as $u(0,t) = 0$ and $u(1,t) = f(t)$, and the initial condition as $u(x,0) = x^2$. Based on He's method of variational iteration [34], they found the Lagrange multiplier as $\lambda(\xi) = -1$. Subsequently, they obtained the following iteration formula for solving Eq. (2-1) [33]:

$$u_{n+1}(\mathrm{x},t) = u_n(\mathrm{x},t) - \frac{1}{\Gamma(1+\alpha)}\int_0^t \left(\frac{\partial^{\alpha} u_n(\mathrm{x},\xi)}{\partial \xi^{\alpha}} - \frac{x^2}{2}\frac{\partial^2 u_n(\mathrm{x},\xi)}{\partial x^2} \right) (d\xi)^{\alpha}, \tag{2-2}$$

After applying n number of iterations, they came up with the general solution as:

$$u_n(\mathrm{x},t) = \sum_{k=0}^{n} \frac{x^2\, t^{k\alpha}}{\Gamma(1+k\alpha)}. \tag{2-3}$$

In another study on the application of variational iteration method for nonlinear time-fractional equations, reported by Odibit and Momani [13], the nonlinear time-fractional advection partial differential equation was solved. Consider the following time-fractional form for the equation as [13]:

$$D^{\alpha}{}_t\, u(x,t) + u(x,t)\, u_x(x,t) = x + x\, t^2 \,, \quad t > 0 \,, x \in R \,, 0 < \alpha \leq 1, \tag{2-4}$$

Assuming the initial condition $u(x,0) = 0$, the Lagrange multiplier was defined as $\lambda(\xi) = -1$ which resulted into the following fractional iteration formula [13]:

$$u_{n+1}(x,t) = u_n(x,t) - \int_0^t \left(\frac{\partial^\alpha u_n(x,\xi)}{\partial \xi^\alpha} + u_n(x,\xi)\left((u_n)_x(x,\xi)\right) - x - x\xi^2 \right) d\xi\,, \qquad (2\text{-}5)$$

In order to solve the variational iteration formula with the initial approximate solution $u_0(x,t) = 0$, they came up with the following solutions for the first and the second iterations [13]:

$$u_0(x,t) = 0\,, \qquad (2\text{-}6)$$

$$u_1(x,t) = x\left(t + \frac{t^3}{3}\right), \qquad (2\text{-}7)$$

and

$$u_2(x,t) = x\left(2t + \frac{t^3}{3} - \frac{2t^5}{15} - \frac{t^7}{63} - \frac{t^{2-\alpha}}{\Gamma(3-\alpha)} - \frac{t^{4-\alpha}}{\Gamma(5-\alpha)}\right), \qquad (2\text{-}8)$$

To validate the obtained solution, they compared the numerical results of Eq. (2-8) with those obtained from the decomposition method and showed that both variational iteration method and the Adomain decomposition methods provide the solutions easily with computable components [13].

In another study performed by Das [35], the vibration behavior of large membranes was obtained by using the variational iteration method. The governing equation of motion was modeled as a fractional calculus version of the standard vibration equation with the radial velocity of $u(r,t)$ with the fractional time derivative of order $1 < \alpha \leq 2$ and c being the wave velocity [35].

$$\frac{\partial^2 u}{\partial r^2}+\frac{1}{r}\frac{\partial u}{\partial r}=\frac{1}{c^2}\frac{\partial^\alpha u}{\partial t^\alpha}\ ,\ r\geq 0\ ,\ t\geq 0\ ,1<\alpha\leq 2\ , \tag{2-9}$$

In order to apply the variational iteration method, the Lagrange multiplier was defined as $\lambda(\xi)=\xi-t$, and the following iteration formula was obtained [35]:

$$\begin{aligned} u_{n+1}(r,t)=u_n(r,t)+\int_0^t(\xi-t)\Bigg(&\frac{\partial^2 u_n(r,\xi)}{\partial\xi^2}\\ &-c^2\frac{\partial^{2-\alpha}}{\partial t^{2-\alpha}}\left(\frac{\partial^2\tilde{u}_n(r,\xi)}{\partial r^2}+\frac{1}{r}\frac{\partial\tilde{u}_n(r,\xi)}{\partial r}\right)\Bigg)d\xi \end{aligned} \tag{2-10}$$

By having the approximate initial solutions, which satisfied the initial conditions of the system, the exact solution of the nonlinear equation of motion could easily be obtained only after two iterations. In order to validate the obtained solution, Das compared the results obtained using the variational method by those obtained from the modified decomposition method and confirmed the accuracy and power of the variational iteration method for solving such nonlinear equations [35].

In a study performed by Yaghoobi and Torabi [36], the nonlinear vibration equation of motion of a functionally graded beam, placed on an elastic foundation, was solved by applying the variational iteration method. The beam was subjected to an axial force and modeled based on the Euler-Bernoulli beam theory and von Kármán geometric nonlinearity theory. They analytically examined several case studies with different types of boundary conditions. They specifically investigated the accuracy of the variational iteration method by comparing their time response results found using the variational iteration method and the numerical simulation. They proved the top

capability of variational iteration method in solving nonlinear equations for a wide range of applications [36].

2. 4. Method of Multiple Time-Scales

Internal resonance, as well as the external resonance of a beam, resting on an elastic foundation, were investigated based on the multiple time-scales method [37]. They modeled a railway track resting on ballast foundation as the nonlinear elastic foundation, which was under excitation of passing trains. The method of multiple time-scales was used to find the response of the free and forced vibrations and to investigate different resonance cases, such as the internal resonances of three-to-one or the external resonances when the frequency of the external force would become close to the natural frequency of the system.

Nonlinear forced vibration analysis of an orthotropic plate with part through crack was studied by Joshi et al. [38]. They modeled the plate based on the Berger formulation for the in-plane forces, which resulted in a cubic nonlinear equation of motion. After applying the Galerkin procedure, they obtained the well-known duffing equation. In order to find the pick amplitude and the frequency response of the system, they applied the multiple time-scales method and the effect of different parameters, such as the crack length and the location of crack, on the frequency response and vibration behavior of the system were investigated.

Another study on the nonlinear oscillation and frequency response of a system based on the multiple time-scales method was performed by Askari et al. [39]. They modeled a non-uniform carbon nanotube based on the Euler-Bernoulli beam theory. By applying the Galerkin procedure, they obtained the nonlinear ordinary differential equation of their system and by implementing the method of multiple time-scales, they found the frequency response of the free-form nanotube analytically. They could also examine the effect of different parameters on the nonlinear vibration behavior of the system using the analytical solution found by the multiple time-scales method.

The damped vibration of a rectangular plate under the condition of the one-to-one internal resonance and the internal combination of resonances have been investigated by Rossikhin and Shitikova [40]. The damping properties of the plate were defined based on the Riemann-Liouville fractional derivative. The method of multiple time-scales was utilized to determine the in-plane and the out-of-plane displacements by expanding the amplitude of vibration into power series of different time scales and also by expanding the fractional derivative into the fractional power of differentiation operators. They studied the energy exchange phenomena, which was caused by the condition of internal resonance of free vibration. They concluded that the fractional viscoelasticity has two different effects on the energy exchange of the system. On one hand, resulted in producing unsteady energy exchange and on the other hand, resulted in damping of the energy of the system.

Another study was performed by Rossikhin and Shitikova on the nonlinear vibration behavior of a thin plate under internal two-to-one resonance [41]. They considered a

plate embedded in a nonlinear viscoelastic medium with the fractional viscoelastic properties. They solved the coupled nonlinear equations of motion by utilizing the method of multiple time-scales and proposed a new approach that resulted in decoupling the linear part of the equations of motion. By this new approach introduced in their research, they could find a new internal resonance as one-to-one-to-two resonance. They found that the internal resonance phenomena in thin plates could be very critical with high possibility of happening. They also showed that the type of internal resonance depends on the order of the fractional derivative and the smallness of the viscosity of the system [41, 42].

2. 5. Fractional Derivative Applications

The history of fractional derivatives goes back to the same time as the classical calculus, but they are not so popular due to the difficulties of dealing with the fractional derivatives and integrals. Although several researchers have been working on this area, the physical meaning of fractional derivative is quite an open question yet [43].

Based on the available publications on viscoelastic materials with memory [44, 45], such materials have been mainly modeled in terms of the stress and strain by Kevin model, Maxwell model, Voigt model among others, with an integer order of derivatives or integrals. Comparing the results of the models with derivative of fractional order with those having derivative of integer order indicate that the modeling of materials with memory effect by integer order will decrease the accuracy of simulation.

The early investigation showed that viscoelastic materials act between viscosity and elasticity, therefore it is logical to model their behavior with fractional derivatives in the form of Eqs. (1-1) and (1-6). The acceptable range for fractional order α can be considered from the value of $\alpha = 0$, which describes the Hook's law, to the value of $\alpha = 1$, which follows the Newton's law.

In a study performed by Bagley and Torvik [12], a generalized form of both Caputo's and Scott-Blair's models for the fractional derivative has been introduced as [12]:

$$\sigma(t) + \sum_{m=1}^{M} b_m D^{\beta} m(\sigma(t)) = E_0 \varepsilon(t) + \sum_{n=1}^{N} E_n D^{\alpha} n(\varepsilon(t)) \,, \tag{2-11}$$

Where E is the bar modulus of elasticity and α, β and b are the model parameters. $\varepsilon(t)$ and $\sigma(t)$ are the strain history and stress history functions, respectively. This model was modified based on the mechanical properties observed for 30 materials. Observations showed that the fractional derivative relationship of both Scott-Blair's model with the modified model presented in Eq. (2-11) are almost identical [12]. Other results from experimental observations indicate that many viscoelastic materials can be modeled only by considering the first iteration of Eq. (2-11) [12].

Studies on the fractional modeling have shown that Scott-Bair's model, which is basically a material model, can be used for modeling biological kinetics with memory and cognitive dynamic in psychology. Such modeling proved to work properly after being tested by Hermann Ebbinghaus in 1885. The data found from memorizing tests, including different learning materials and learning times of day, have been fitted with the fractional models based on the Scott-Bair's model [43].

Mechanical response of living cells are known for being too complicated due to their complex cellular structure. Such complex and heterogeneous characteristics of the living cells haves caused many difficulties in modeling and cannot be solved by simple linear modeling of viscoelasticity. As an example, when considering an isolated human breast cell, investigations revealed that the relaxation phenomenon of these cells are not simply exponential and cannot be modeled by the standard linear solid theory. Instead of using the standard linear model, researchers have suggested to consider the Fractional Zener model of viscoelasticity, which introduces a new parameter for the fractional time-derivative of the response.

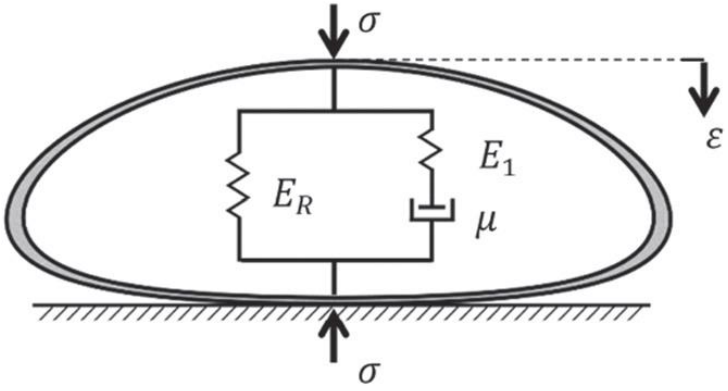

Figure 2-5- Schematic of Standard Linear model of cancer cell [46]

The schematic diagram of Standard Linear Solid is shown in **Figure 2-5**. Since this model failed to simulate the time-dependent derivative, therefore the viscous damper shown in **Figure 2-5** has been replaced by a fractional element, shown in **Figure 2-6**.

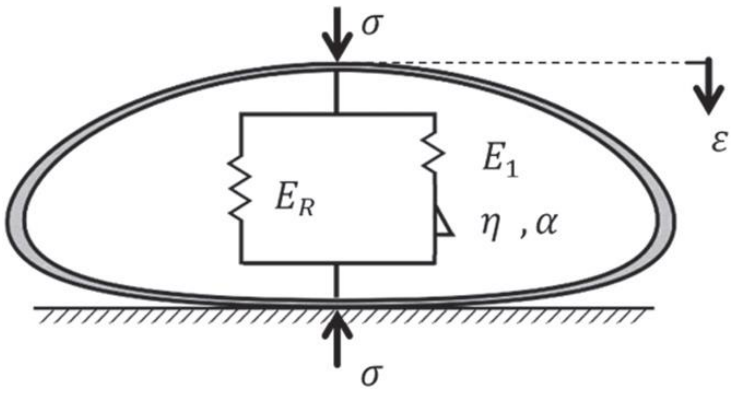

Figure 2-6- Schematic of Fractional Zener model of cancer cell [46]

The strain dependency on the zeroth or first derivative has been replaced by the fractional order derivation as:

$$\sigma(t) = \eta \frac{d^{\alpha}}{dt^{\alpha}}(\varepsilon) = \eta D^{\alpha}(\varepsilon), \qquad (2\text{-}12)$$

The results obtained from this investigation showed an excellent increase in the data found from experiments with those found from the Fractional Zener modeling. The best range of fractional order for the malignant population of cells was reported to be an average value of 0.48 ± 0.06 , while for the benign cells this was reported as 0.51 ± 0.07.

Studies on the viscoelastic features of soft biological tissues provide many useful information in medical diagnosis. Magnetic Resonance Elastography (MRE), which is known as a noninvasive elasticity imaging technique, renovates viscoelastic material properties using the dynamic displacement images. The results obtained from this technique are highly sensitive to the model chosen for simulating the viscoelasticity of the material. Therefore, choosing the best possible model can improve the capability

and accuracy of MRE. Typically, the well-known Voigt and Kelvin model with a derivative of integer order has been used for modeling the viscoelasticity, which cannot represent the material properties of biological tissues over a wide spectral range.

A recently introduced fractional derivative model has been reported to have approximate material properties with higher accuracy [47]. In an investigation performed by Meral et al. [47], the viscoelastic properties of materials CF-11 and also Gelatin subjected to harmonic mechanical loadings have been compared for two fractional and integer derivative models. They developed a fractional order for the materials being used in MRE and showed a better performance of the fractional order of Voigt model than the integer model. It is believed that such investigation will result in a better understanding of human soft-tissue viscoelastic properties and lead to improve analytical applications.

In an study perfomed by Kaul [48] an accurate model for prediction of the dynamic behavior of an isolator has been introduced based on the Maxwell-Voigt model with fractional damping and time delay. He compared his model with the conventional Maxwell-Voigt model and discovered that the Voigt model in highly sensitive to fractional damping and since the accuracy of isolator models are critical for a successful dynamic behavior prediction, choosing the model with fractional damping will make it possible to model the system with higher accuracy in comparison with using the traditional modeling.

On the effect of fractional damping on the solution of plate equations, an investigation has been performed by Horbach et al. [49] on the optimal decay rate and asymptotic profile for the plate equation. They showed that the decay rate depends on the fractional power of the damping term and they derived the exact decay rate analytically for the optimal condition.

Vibration characteristic of a plate made with the Zener viscoelastic material modelled with the Caputo fractional derivative has been studied by Litewka and Lewandowski [50]. The goal of their investigation was to identify properties of viscoelastic materials with the fractional damping. They used the von Kármán plate theory and by considering the shear effects and rotary inertia, solved the problem in the frequency domain. They surprisingly found some unexpected results which showed the influence of relaxation time on the damping properties of the fractional Zener viscoelastic material and the frequency resonance in the nonlinear geometrical regime.

2. 6. Thesis Contribution

The literature review performed that research improvements will depend on the accuracy of the mathematical modeling of the real-world problems.

Developing a mathematical model with least simplifications, from the vibration and viscoelastic behavior point of view, and obtaining the analytical solutions are the main goal of this study. The composite plate is modeled based on the von Kármán plate theory and the Caputo's fractional derivative and the time-dependent differential

equations are developed using the Galerkin procedure. The free vibration of the system is investigated by utilizing the variational iteration method and by using parametric studies, the vibration behavior of the system under different conditions are examined. Also, the method of multiple time-scales is applied to investigate the nonlinear forced vibration of the system. The frequency-amplitude relationship, for each natural modes of vibration of the system, are analytically derived and the numerical results for different values of the fractional derivative order, fractional derivative coefficient, aspect ratio, and the elasticity ratio of plate are presented.

Based on the sensitivity of vibration behavior to the fractional derivative order, and from a design point of view, any types of resonance or undesired vibration behavior can be avoided by choosing an optimum value of fractional derivative order.

Chapter 3 - Vibration of Viscoelastic Plates

3. 1. Introduction

Vibration analysis of a composite plate with fractional viscoelastic properties is investigated in this chapter. The system is schematically presented and mathematically modeled based on the von Kármán plate theory and it is assumed to be an orthotropic nonhomogeneous plate. In order to make the solution methods and the analytical results being independent of any specific physical variables, the non-dimensional parameters are introduced, which can facilitate the analyses to be applicable for all possible case studies. By deriving the non-dimensional partial differential equations for displacement and the in-plane stress function of the system, the Galerkin procedure is utilized to obtain the governing time-dependent ordinary differential equation of motion for each mode of vibration. The first four modes of vibration that consist of two orthogonal modes in both x and y directions have been considered. Variational iteration method is utilized for the free vibration analysis and the Multiple Time-Scales method is considered for the forced vibration investigation, which will be discussed in detail in the following chapters.

3. 2. Mathematical Modeling

Mathematical modeling of the rectangular plate with fractional viscoelasticity is derived in this section. **Figure 3-1** shows the schematic model of a composite rectangular plate with the simply-supported boundary conditions on all four edges.

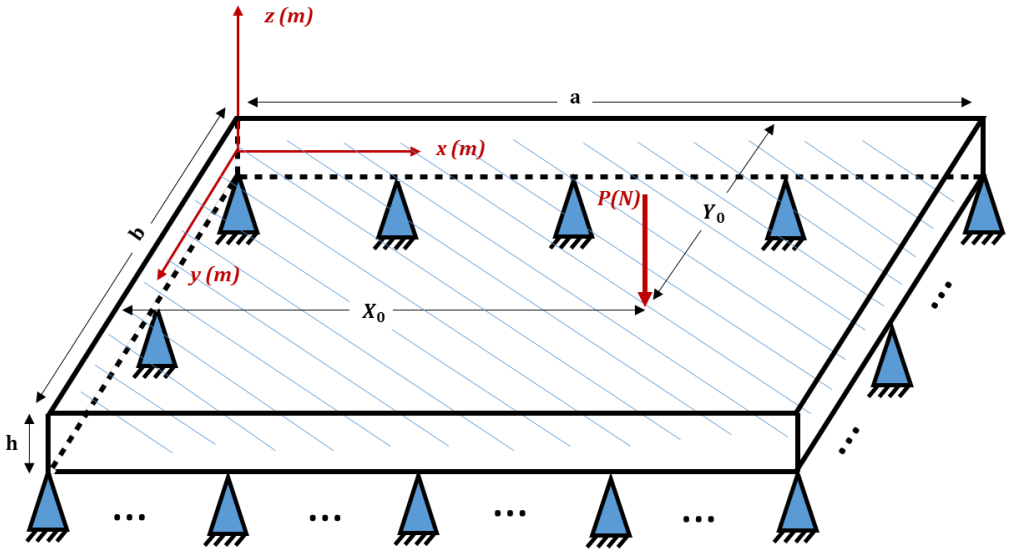

Figure 3-1- Schematic representation of viscoelastic composite plate

Initially, one could consider the displacements of an arbitrary point on the middle surface of a rectangular plate are indicated by the coordinates u, v and w in the x, y and z directions, respectively. For larger deflections of w, where it has the same range of magnitudes as the thickness of the plate h, using the linear theories would decrease the accuracy of the results. Therefore, the von Kármán plate theory has been developed in the Cartesian coordinate. Here, few of the assumptions of this theory have been listed [9]:

a) The plate is thin, hence $h \ll a$, $h \ll b$.

b) The slope of each point is small $|\partial w/\partial x| \ll 1$, $|\partial w/\partial y| \ll 1$.

c) The strain components are all small enough so that the linear elasticity theories are applicable.

d) The in-plane displacements u and v are too small, and therefore, all the nonlinear terms of the strain-displacement relationships can be neglected except those terms that will depend on w.

The corresponding displacements of an arbitrary point of the plate, at a distance z from the middle surface, are assumed u_1, u_2 and u_3, for which they can be written as functions of u, v, and w:

$$u_1 = u(x, y, t) - z\frac{\partial w}{\partial x}, \tag{3-1}$$

$$u_2 = v(x, y, t) - z\frac{\partial w}{\partial y}, \tag{3-2}$$

and

$$u_3 = w(x, y, t). \tag{3-3}$$

Considering those displacements u_1, u_2 and u_3 and by substituting them into the Green's strain tensor [9], the strain components of an arbitrary point of the rectangular plate can be written as:

$$\varepsilon_{xx} = \varepsilon_{x,0} + zk_x, \tag{3-4}$$

$$\varepsilon_{yy} = \varepsilon_{y,0} + zk_y, \tag{3-5}$$

and

$$\gamma_{xy} = \gamma_{xy,0} + zk_{xy}. \tag{3-6}$$

Where $\varepsilon_{x,0}$, $\varepsilon_{y,0}$ and $\gamma_{xy,0}$ are the middle surface strains and k_x, k_y and k_{xy} represent the changes in the curvature and the torsion of the middle surface, respectively [9]. They are defined as:

$$\varepsilon_{x,0} = \frac{\partial u(x,y,t)}{\partial x} + \frac{1}{2}\left(\frac{\partial w(x,y,t)}{\partial x}\right)^2, \tag{3-7}$$

$$\varepsilon_{y,0} = \frac{\partial v(x,y,t)}{\partial x} + \frac{1}{2}\left(\frac{\partial w(x,y,t)}{\partial y}\right)^2, \tag{3-8}$$

$$\gamma_{xy,0} = \frac{\partial u(x,y,t)}{\partial y} + \frac{\partial v(x,y,t)}{\partial x} + \frac{\partial w(x,y,t)}{\partial x}\frac{\partial w(x,y,t)}{\partial y}, \tag{3-9}$$

and

$$k_x = -\frac{\partial^2 w(x,y,t)}{\partial x^2}, \quad k_y = -\frac{\partial^2 w(x,y,t)}{\partial y^2}, \quad k_{xy} = -2\frac{\partial^2 w(x,y,t)}{\partial x \partial y}. \tag{3-10}$$

The Kirchhoff stresses for the nonhomogeneous and orthotropic materials have been defined as [10]:

$$\sigma_{xx} = \frac{E_x}{1-\nu_x\nu_y}\left(\varepsilon_{xx} + \nu_y\varepsilon_{yy}\right), \tag{3-11}$$

$$\sigma_{yy} = \frac{E_x}{1-\nu_x\nu_y}\left(\varepsilon_{yy} + \nu_x\varepsilon_{xx}\right), \tag{3-12}$$

and

$$\tau_{xy} = G\gamma_{xy}. \tag{3-13}$$

By substituting Eqs. (3-4)-(3-10) into Eqs. (3-11)-(3-13), the stress expressions for the orthotropic rectangular plate can be obtained as:

$$\sigma_{xx} = -\frac{E_x z}{1-\nu_x\nu_y}\left(\frac{\partial^2 w(x,y,t)}{\partial x^2} + \nu_y\frac{\partial^2 w(x,y,t)}{\partial y^2}\right), \tag{3-14}$$

$$\sigma_{yy} = -\frac{E_y z}{1-\nu_x\nu_y}\left(\frac{\partial^2 w(x,y,t)}{\partial y^2} + \nu_x\frac{\partial^2 w(x,y,t)}{\partial x^2}\right), \tag{3-15}$$

and

$$\tau_{xy} = -2Gz\frac{\partial^2 w(x,y,t)}{\partial x\partial y}. \tag{3-16}$$

In order to obtain the equations of motion of the system, based on the von Kármán plate theory, one needs to use the strain-displacement relationship, Eqs. (3-11)-(3-13), to define the forces and moments per unit length, which are acting on the plate as shown in **Figure 3-2**.

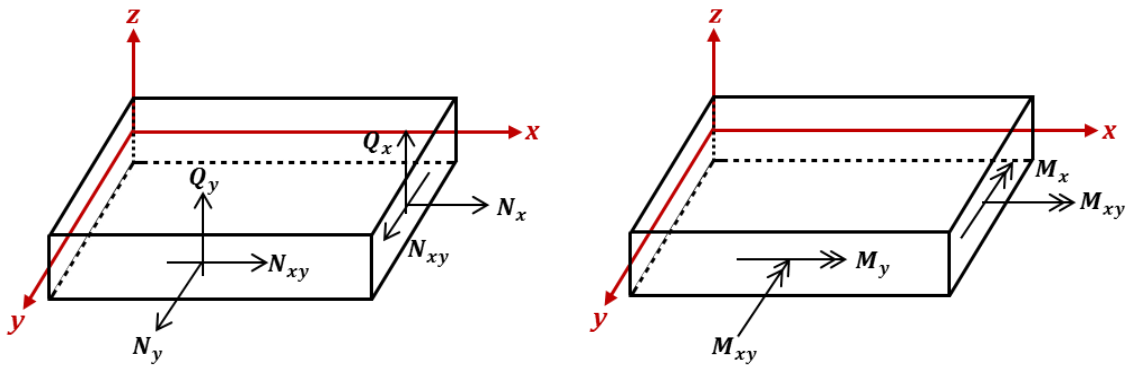

Figure 3-2- Schematic model of forces and moments of plate element

The stress resultant forces and moments per unit length acting on the plate can be defined as:

$$N_x = \frac{E_x h}{1-\nu_x \nu_y}\left(\frac{\partial u}{\partial x}+\frac{1}{2}\left(\frac{\partial w}{\partial x}\right)^2+\nu_y\left(\frac{\partial v}{\partial y}+\frac{1}{2}\left(\frac{\partial w}{\partial y}\right)^2\right)\right), \tag{3-17}$$

$$N_y = \frac{E_y h}{1-\nu_x \nu_y}\left(\frac{\partial v}{\partial y}+\frac{1}{2}\left(\frac{\partial w}{\partial y}\right)^2+\nu_x\left(\frac{\partial u}{\partial x}+\frac{1}{2}\left(\frac{\partial w}{\partial x}\right)^2\right)\right), \tag{3-18}$$

$$N_{xy} = Gh\left(\frac{\partial u}{\partial y}+\frac{\partial v}{\partial x}+\frac{\partial w}{\partial x}\frac{\partial w}{\partial y}\right), \tag{3-19}$$

$$M_x = -\frac{E_x h^3}{12\left(1-\nu_x \nu_y\right)}\left(\frac{\partial^2 w}{\partial x^2}+\nu_y \frac{\partial^2 w}{\partial y^2}\right), \tag{3-20}$$

$$M_y = -\frac{E_y h^3}{12\left(1-\nu_x \nu_y\right)}\left(\frac{\partial^2 w}{\partial y^2}+\nu_x \frac{\partial^2 w}{\partial x^2}\right), \tag{3-21}$$

and

$$M_{xy} = \frac{Gh^3}{6}\left(\frac{\partial^2 w}{\partial x \partial y}\right). \tag{3-22}$$

The three-dimensional equations of equilibrium of the plate, considering the moments and forces defined earlier, can be written as:

$$\frac{\partial^2 M_x}{\partial x^2} + 2\frac{\partial^2 M_{xy}}{\partial x \partial y} + \frac{\partial^2 M_y}{\partial y^2} = -q - N_x \frac{\partial^2 w}{\partial x^2} - 2N_{xy}\frac{\partial^2 w}{\partial x \partial y} - N_y \frac{\partial^2 w}{\partial y^2}, \tag{3-23}$$

$$\frac{\partial N_x}{\partial x} + \frac{\partial N_{xy}}{\partial y} = 0, \tag{3-24}$$

and

$$\frac{\partial N_{xy}}{\partial x} + \frac{\partial N_y}{\partial y} = 0, \tag{3-25}$$

where q is the transverse load. For a plate with the fractional viscoelasticity this can be defined as:

$$q = p - \rho h \frac{\partial^2 w(x,y,t)}{\partial t^2} - k\frac{\partial^\alpha w(x,y,t)}{\partial t^\alpha} - ch\frac{\partial w(x,y,t)}{\partial t}, \tag{3-26}$$

in which p is the external load and α is the order of the fractional derivative, which can vary from zero to one, $0 \leq \alpha < 1$. Also, ρ and c are the mass density and damping coefficient of the plate, respectively.

The corresponding Eqs. (3-24) and (3-25) can be satisfied by introducing the in-plane stress function f defined as [9]:

$$N_x = \frac{\partial^2 f(x,y,t)}{\partial y^2}, \quad N_y = \frac{\partial^2 f(x,y,t)}{\partial x^2}, \quad N_{xy} = \frac{\partial^2 f(x,y,t)}{\partial x \partial y}, \tag{3-27}$$

By substituting Eqs. (3-17) - (3-22) and Eqs. (3-26) and (3-27) into Eqs. (3-23) - (3-25) and implementing some mathematical simplifications, the following expressions that would only involve f and w can be written as:

$$D_x \frac{\partial^4 w(x,y,t)}{\partial x^4} + 2H \frac{\partial^4 w(x,y,t)}{\partial x^2 \partial y^2} + D_y \frac{\partial^4 w(x,y,t)}{\partial y^4} + k \frac{\partial^\alpha w(x,y,t)}{\partial t^\alpha} =$$

$$-\rho h \frac{\partial^2 w(x,y,t)}{\partial t^2} - ch \frac{\partial w(x,y,t)}{\partial t} + p + \frac{\partial^2 w(x,y,t)}{\partial x^2} \frac{\partial^2 f(x,y,t)}{\partial y^2} \tag{3-28}$$

$$-2 \frac{\partial^2 w(x,y,t)}{\partial x \partial y} \frac{\partial^2 f(x,y,t)}{\partial x \partial y} + \frac{\partial^2 w(x,y,t)}{\partial y^2} \frac{\partial^2 f(x,y,t)}{\partial x^2}$$

$$\frac{1}{E_x h} \frac{\partial^4 f(x,y,t)}{\partial x^4} + \left(\frac{1}{Gh} - \frac{2\nu_x}{E_x h}\right) \frac{\partial^4 f(x,y,t)}{\partial x^2 \partial y^2} + \frac{1}{E_y h} \frac{\partial^4 f(x,y,t)}{\partial y^4} =$$

(3-29)

$$\left(\frac{\partial^2 w(x,y,t)}{\partial x \partial y}\right)^2 - \frac{\partial^2 w(x,y,t)}{\partial x^2} \frac{\partial^2 w(x,y,t)}{\partial y^2}$$

In Eqs. (3-28) and (3-29), the flexural rigidities in the x and y directions and also the torsional rigidity for the orthotropic plate with a uniform thickness have been replaced as:

$$D_x = \frac{E_x h^3}{12\left(1-\nu_x \nu_y\right)} \tag{3-30}$$

$$D_y = \frac{E_y h^3}{12\left(1-\nu_x \nu_y\right)} \tag{3-31}$$

$$D_{xy} = \frac{E_x \nu_y h^3}{12(1-\nu_x \nu_y)} \tag{3-32}$$

$$G_{xy} = \frac{G h^3}{12} \tag{3-33}$$

and

$$H = D_{xy} + 2G_{xy} \tag{3-34}$$

In order to expand the solutions and the results further into a more general method that would be applicable for any possible case-study, the following dimensionless parameters have been defined:

$$X = \frac{x}{a},\ \mathrm{Y} = \frac{y}{b},\ r = \frac{a}{b},\ W = \frac{w}{h},\ F = \frac{f}{D_x},\ \bar{E} = \frac{E_y}{E_x},$$

$$C = ch\sqrt{\frac{a^4}{D_x \rho h}},\ Q = p\left(\frac{a^4}{D_x h}\right),\ T = t\sqrt{\frac{D_x}{\rho h a^4}},$$

$$\alpha_1 = \nu_y + 2\frac{G}{E_x},\ \alpha_2 = \frac{E_x}{G} - \frac{2\nu_x}{1-\nu_x \nu_y},\ \alpha_3 = 12(1-\nu_x \nu_y)$$

Substituting the non-dimensional parameters into Eqs. (3-28) and (3-29), the non-dimensional partial differential equations of motion of the plate can be rewritten as:

$$\frac{\partial^4 W}{\partial X^4} + 2\alpha_1 r^2 \frac{\partial^4 W}{\partial X^2 \partial Y^2} + \bar{E} r^4 \frac{\partial^4 W}{\partial Y^4} + K \frac{\partial^\alpha W}{\partial T^\alpha} + \frac{\partial^2 W}{\partial T^2} + C \frac{\partial W}{\partial T} = Q + \frac{\partial^2 W}{\partial X^2}\frac{\partial^2 F}{\partial X^2} - 2\frac{\partial^2 W}{\partial X \partial Y}\frac{\partial^2 F}{\partial X \partial Y} + \frac{\partial^2 W}{\partial Y^2}\frac{\partial^2 F}{\partial X^2} \tag{3-35}$$

$$\frac{\partial^4 F}{\partial X^4} + \alpha_2 \frac{\partial^4 F}{\partial X^2 \partial Y^2} + \frac{r^4}{\bar{E}} \frac{\partial^4 F}{\partial Y^4} = \left(\frac{\partial^2 W}{\partial X \partial Y} \right)^2 - \frac{\partial^2 W}{\partial X^2}\frac{\partial^2 W}{\partial Y^2} \tag{3-36}$$

3. 3. Galerkin Procedure

In order to obtain the ordinary differential equation of motion for each modes of vibration, the Galerkin method is applied. For implementing this method, the displacement function $W(X, Y, T)$ and the in-plane stress function $F(X, Y, T)$ must be defined in such a way that they will satisfy the boundary conditions of the system. Considering the simply-supported boundary conditions at all edges of the plate, one could assume approximate solutions for the displacement function and the in-plane stress function of the plate in the following forms:

$$W(X, \mathrm{Y}, T) = \sum_{n=1}^{\infty}\sum_{m=1}^{\infty}\left(W_{nm} \sin(n\pi X)\sin(m\pi Y)\right) \tag{3-37}$$

$$F(X, \mathrm{Y}, T) = \sum_{r=1}^{\infty}\sum_{s=1}^{\infty}\left(F_{rs} \cos(r\pi X)\cos(s\pi Y)\right) \tag{3-38}$$

in which W_{nm} and F_{rs} are the time dependent functions of the displacement and the in-plane stress function, respectively.

In deriving the ordinary differential equation of motion for the nm^{th} mode of the system, Eqs. (3-37) and (3-38) must be substituted into Eqs. (3-35) and (3-36). By multiplying the obtained equations by $\sin(n\pi X)\sin(m\pi Y)$ and $\sin(r\pi X)\sin(s\pi Y)$, respectively, and integrating them over the area of the plate, the ordinary differential equations for the nm^{th} mode of the system can be derived after some mathematical simplifications as:

$$\begin{aligned}\ddot{W}_{11}+\mathrm{C}\dot{W}_{11}+k\,D^{(\alpha)}W_{11}+\omega_{11}{}^{2}W_{11}+\beta_{11}W_{11}{}^{3}+\beta_{12}W_{11}W_{12}{}^{2}\\+\beta_{13}W_{11}W_{21}{}^{2}+\beta_{14}W_{11}W_{22}{}^{2}+\beta_{15}W_{12}W_{21}W_{22}=f_{11}Q\end{aligned} \tag{3-39}$$

$$\begin{aligned}\ddot{W}_{12}+\mathrm{C}\dot{W}_{12}+k\,D^{(\alpha)}W_{12}+\omega_{12}\,W_{12}+\beta_{12}W_{12}W_{11}{}^{2}+\beta_{22}W_{12}{}^{3}\\+\beta_{23}W_{12}W_{21}{}^{2}+\beta_{24}W_{12}W_{22}{}^{2}+\beta_{25}W_{11}W_{21}W_{22}=f_{12}Q\end{aligned} \tag{3-40}$$

$$\begin{aligned}\ddot{W}_{21}+\mathrm{C}\dot{W}_{21}+k\,D^{(\alpha)}W_{21}+\omega_{21}{}^{2}W_{21}+\beta_{31}W_{21}W_{11}{}^{2}+\beta_{32}W_{21}W_{12}{}^{2}\\+\beta_{33}W_{21}{}^{3}+\beta_{34}W_{21}W_{22}{}^{2}+\beta_{35}W_{11}W_{12}W_{22}=f_{21}Q\end{aligned} \tag{3-41}$$

and

$$\begin{aligned}\ddot{W}_{22}+\mathrm{C}\dot{W}_{22}+k\,D^{(\alpha)}W_{22}+\omega_{22}{}^{2}W_{22}+\beta_{42}W_{22}W_{11}{}^{2}+\beta_{42}W_{22}W_{12}{}^{2}\\+\beta_{43}W_{22}W_{21}{}^{2}+\beta_{44}W_{22}{}^{3}+\beta_{45}W_{11}W_{12}W_{21}=f_{22}Q\end{aligned} \tag{3-42}$$

where $D^{(\alpha)}W_{nm}(\mathrm{t})$ is the Caputo fractional derivative:

$$D^{(\alpha)}W_{nm}(t)=\frac{1}{\Gamma(1-\alpha)}\int_{0}^{t}(t-\xi)^{-\alpha-1}W_{nm}(\xi)d\xi\ ,\quad 0\le\alpha<1 \tag{3-43}$$

The coefficients β_{ij}, ($i = m + n$ and $j = 1,2, \ldots ,5.$), f_{nm}, and ω_{nm} have all been defined in Appendix A in the form of Eqs. (A-1)-(A-28).

Chapter 4 - Nonlinear Free Vibration Analysis

4. 1. Introduction

The goal of this chapter is to investigate the free vibration analysis of a rectangular composite plate with the fractional viscoelastic damping using the variational iteration method. The fractional derivation has been modeled using the Caputo's model, which has been explained in Chapters 1 and 2. In order to utilize the variational iteration method, first the appropriate Langrage coefficient has been obtained and based on the initial conditions of the system, the initial approximations for time-dependent response have been chosen. Then by following the necessary steps for solving the damped vibration equations of motion, based on the variational iteration method, the time response of the system for each mode has been obtained. The order of the fractional derivation is the key parameter in this study, which is varying between zero and one. By implementing the first iteration, the time-dependent response of the system for each natural vibration mode has been derived and the effect of physical parameters have been investigated in the result section.

4. 2. Free Vibration of Plate with Fractional Viscoelasticity

The general mathematical model for the plate with fractional viscoelastic damping was explained in detail in Chapter 3 - . Based on the von Kármán plate theory and the Galerkin procedure, one can have the free vibration time-dependent governing equations of motion of the system as:

$$\begin{aligned}\ddot{W}_{11}(t)+C\dot{W}_{11}(t)+k\,D^{(\alpha)}W_{11}(t)+\omega_{11}{}^2W_{11}(t)+\beta_{11}W_{11}(t)^3+\beta_{12}W_{11}(t)W_{12}(t)^2\\ +\beta_{13}W_{11}(t)W_{21}(t)^2+\beta_{14}W_{11}(t)W_{22}(t)^2+\beta_{15}W_{12}(t)W_{21}(t)W_{22}(t)=0\end{aligned} \quad (4\text{-}1)$$

$$\begin{aligned}\ddot{W}_{12}(t)+C\dot{W}_{12}(t)+k\,D^{(\alpha)}W_{12}(t)+\omega_{12}{}^2W_{12}(t)+\beta_{12}W_{12}(t)W_{11}(t)^2+\beta_{22}W_{12}(t)^3\\ +\beta_{23}W_{12}(t)W_{21}(t)^2+\beta_{24}W_{12}(t)W_{22}(t)^2+\beta_{25}W_{11}(t)W_{21}(t)W_{22}(t)=0\end{aligned} \quad (4\text{-}2)$$

$$\begin{aligned}\ddot{W}_{21}(t)+C\dot{W}_{21}(t)+k\,D^{(\alpha)}W_{21}(t)+\omega_{21}{}^2W_{21}(t)+\beta_{31}W_{21}(t)W_{11}(t)^2\\ +\beta_{32}W_{21}(t)W_{12}(t)^2+\beta_{33}W_{21}(t)^3+\beta_{34}W_{21}(t)W_{22}(t)^2+\beta_{35}W_{11}(t)W_{12}(t)W_{22}(t)=0\end{aligned} \quad (4\text{-}3)$$

and

$$\begin{aligned}\ddot{W}_{22}(t)+C\dot{W}_{22}(t)+k\,D^{(\alpha)}W_{22}(t)+\omega_{22}{}^2W_{22}(t)+\beta_{42}W_{22}(t)W_{11}(t)^2\\ +\beta_{42}W_{22}(t)W_{12}(t)^2+\beta_{43}W_{22}(t)W_{21}(t)^2+\beta_{44}W_{22}(t)^3+\beta_{45}W_{11}(t)W_{12}(t)W_{21}(t)=0\end{aligned} \quad (4\text{-}4)$$

in which all the coefficients can be found in Appendix A as Eqs. (A- 1)- (A- 28).

4. 3. Solution Method

The variational iteration method, which has been explained in general at Section 2. 3 will be utilized specifically for solving the nonlinear vibration equation of motion with

the fractional derivative of order α in this section. In order to apply the variational iteration method, the governing equations of motion should be considered in the following form [21]:

$$L(W_{nm}(t)) + N(W_{nm}(t)) = 0 \tag{4-5}$$

where $L = \frac{\partial^2}{\partial t^2} + C\frac{\partial}{\partial t} + {\omega_{nm}}^2$ is the linear operator and N is the nonlinear operator.

In order to define the Lagrange multiplier for the first vibration mode of the system, one needs to write the correction functional equation for the first mode as:

$$\begin{aligned} W_{11(n+1)}(t) = W_{11(n)}(t) + \int_0^t \lambda_{11}(\tau)\Big(&\ddot{W}_{11(\mathrm{n})}(\mathrm{t}) + \mathrm{C}\dot{W}_{11(\mathrm{n})}(\mathrm{t}) + K_{11}D^{(\alpha)}\tilde{W}_{11(\mathrm{n})}(\mathrm{t}) \\ &+ {\omega_{11}}^2 W_{11(\mathrm{n})}(\mathrm{t}) + \beta_{11}\tilde{W}_{11(\mathrm{n})}(\mathrm{t})^3 + \beta_{12}\tilde{W}_{11(\mathrm{n})}(\mathrm{t})\tilde{W}_{12(\mathrm{n})}(\mathrm{t})^2 + \beta_{13}\tilde{W}_{11(\mathrm{n})}(\mathrm{t})\tilde{W}_{21(\mathrm{n})}(\mathrm{t})^2 \\ &+ \beta_{14}\tilde{W}_{11(\mathrm{n})}(\mathrm{t})\tilde{W}_{22(\mathrm{n})}(\mathrm{t})^2 + \beta_{15}\tilde{W}_{12(\mathrm{n})}(\mathrm{t})\tilde{W}_{21(\mathrm{n})}(\mathrm{t})\tilde{W}_{22(\mathrm{n})}(\mathrm{t})\Big)d\tau \end{aligned} \tag{4-6}$$

For making the above correction functional equation stationary, the variational operator δ must be applied to Eq. (4-6) which, can be rewritten as:

$$\begin{aligned} \delta W_{11(n+1)}(t) &= \delta W_{11(n)}(t) + \delta\int_0^t \lambda_{11}(\tau)\begin{pmatrix} \ddot{W}_{11(\mathrm{n})}(\tau) + \mathrm{C}\dot{W}_{11(\mathrm{n})}(\tau) \\ + {\omega_{11}}^2 W_{11(\mathrm{n})}(\tau) + N\tilde{W}_{(\mathrm{n})}(\tau) \end{pmatrix} d\tau \\ &= \delta W_{11(n)}(t) + \lambda_{11}(\tau)\,\delta\dot{W}_{11(\mathrm{n})}(\tau)\Big|_{\tau=t} + (C\lambda_{11}(\tau) - \dot{\lambda}_{11}(\tau))\delta W_{11(\mathrm{n})}(\tau)\Big|_{\tau=t} \\ &\quad + \int_0^t (\ddot{\lambda}_{11}(\tau) - \mathrm{C}\dot{\lambda}_{11}(\tau) + {\omega_{11}}^2\lambda_{11}(\tau))\,\delta W_{11(n)}(\tau) \end{aligned} \tag{4-7}$$

Considering $\delta W(0)=0$, and by separating the terms with the same order of $\delta W_{11(n)}(t)$, the following stationary conditions can be obtained:

$$\ddot{\lambda}_{11}(\tau)-\mathrm{C}\,\dot{\lambda}_{11}(\tau)+\omega_{11}{}^{2}\lambda_{11}(\tau)=0 \tag{4-8}$$

$$1-\dot{\lambda}_{11}(\tau)+C\lambda_{11}(\tau)\big|_{\tau=t}=0 \tag{4-9}$$

and

$$\lambda_{11}(\tau)\big|_{\tau=t}=0 \tag{4-10}$$

Consequently, by solving Eqs. (4-8) to (4-9)-(4-10), the Lagrange multiplier for the first mode can be identified as follow:

$$\lambda_{11}(\tau)=\frac{2\,Sin\left(\frac{1}{2}\sqrt{4\omega_{11}{}^{2}-C^{2}}\,(\tau-t)\right)}{\sqrt{4\omega_{11}{}^{2}-C^{2}}}e^{0.5C(\tau-t)} \tag{4-11}$$

The same procedure needs to be followed in order to derive the Lagrange multiplier for the other three modes. Therefore, one can readily find the Lagrange multiplier for other modes of the system as:

$$\lambda_{12}(\tau)=\frac{2\,Sin\left(\frac{1}{2}\sqrt{4\omega_{12}{}^{2}-C^{2}}\,(\tau-t)\right)}{\sqrt{4\omega_{12}{}^{2}-C^{2}}}e^{0.5C(\tau-t)} \tag{4-12}$$

$$\lambda_{21}(\tau)=\frac{2\,Sin\left(\frac{1}{2}\sqrt{4\omega_{21}{}^{2}-C^{2}}\,(\tau-t)\right)}{\sqrt{4\omega_{21}{}^{2}-C^{2}}}e^{0.5C(\tau-t)} \tag{4-13}$$

and

$$\lambda_{22}(\tau)=\frac{2\,Sin\left(\frac{1}{2}\sqrt{4{\omega_{22}}^2-C^2}\,(\tau-t)\right)}{\sqrt{4{\omega_{22}}^2-C^2}}e^{0.5C(\tau-t)} \tag{4-14}$$

Consequently, the iteration formulas can be obtained as:

$$\begin{aligned}W_{11(n+1)}(t)=W_{11(n)}(t)+\int_0^t\left(\frac{Sin\left(\frac{1}{2}\sqrt{4{\omega_{11}}^2-C^2}\,(\tau-t)\right)}{\frac{1}{2}\sqrt{4{\omega_{11}}^2-C^2}}e^{0.5C(\tau-t)}\right)\\ \times\Big(\ddot{W}_{11(n)}(\tau)+C\dot{W}_{11(n)}(\tau)+k\,D^{(\alpha)}W_{11(n)}(\tau)+{\omega_{11}}^2W_{11(n)}(\tau)\\ +\beta_{11}W_{11(n)}(\tau)^3+\beta_{12}W_{11(n)}(\tau)W_{12(n)}(\tau)^2+\beta_{13}W_{11(n)}(\tau)W_{21(n)}(\tau)^2\\ +\beta_{14}W_{11(n)}(\tau)W_{22(n)}(\tau)^2+\beta_{15}W_{12(n)}(\tau)W_{21(n)}(\tau)W_{22(n)}(\tau)\Big)d\tau\end{aligned} \tag{4-15}$$

$$\begin{aligned}W_{12(n+1)}(t)=W_{12(n)}(t)+\int_0^t\left(\frac{Sin\left(\frac{1}{2}\sqrt{4{\omega_{12}}^2-C^2}\,(\tau-t)\right)}{\frac{1}{2}\sqrt{4{\omega_{12}}^2-C^2}}e^{0.5C(\tau-t)}\right)\\ \times\Big(\ddot{W}_{12(n)}(\tau)+C\dot{W}_{12(n)}(\tau)+k\,D^{(\alpha)}W_{12(n)}(\tau)+{\omega_{12}}^2W_{12(n)}(\tau)\\ +\beta_{12}W_{12(n)}(\tau)W_{11(n)}(\tau)^2+\beta_{22}W_{12(n)}(\tau)^3+\beta_{23}W_{12(n)}(\tau)W_{21(n)}(\tau)^2\\ +\beta_{24}W_{12(n)}(\tau)W_{22(n)}(\tau)^2+\beta_{25}W_{11(n)}(\tau)W_{21(n)}(\tau)W_{22(n)}(\tau)\Big)d\tau\end{aligned} \tag{4-16}$$

$$W_{21(n+1)}(t)=W_{21(n)}(t)+\int_0^t\left(\frac{Sin\left(\frac{1}{2}\sqrt{4\omega_{21}{}^2-C^2}\,(\tau-t)\right)}{\frac{1}{2}\sqrt{4\omega_{21}{}^2-C^2}}e^{0.5C(\tau-t)}\right)$$
$$\times\Big(\ddot{W}_{21(n)}(\tau)+\mathrm{C}\dot{W}_{21(n)}(\tau)+k\,D^{(\alpha)}W_{21(n)}(\tau)+\omega_{21}{}^2W_{21(n)}(\tau)$$
$$+\beta_{31}W_{21(n)}(\tau)W_{11(n)}(\tau)^2+\beta_{32}W_{21(n)}(\tau)W_{12(n)}(\tau)^2+\beta_{33}W_{21(n)}(\tau)^3$$
$$+\beta_{34}W_{21(n)}(\tau)W_{22(n)}(\tau)^2+\beta_{35}W_{11(n)}(\tau)W_{12(n)}(\tau)W_{22(n)}(\tau)\Big)d\tau \qquad (4\text{-}17)$$

and

$$W_{22(n+1)}(t)=W_{22(n)}(t)+\int_0^t\left(\frac{Sin\left(\frac{1}{2}\sqrt{4\omega_{22}{}^2-C^2}\,(\tau-t)\right)}{\frac{1}{2}\sqrt{4\omega_{22}{}^2-C^2}}e^{0.5C(\tau-t)}\right)$$
$$\times\Big(\ddot{W}_{22(n)}(\tau)+\mathrm{C}\dot{W}_{22(n)}(\tau)+k\,D^{(\alpha)}W_{22(n)}(\tau)+\omega_{22}{}^2W_{22(n)}(\tau)$$
$$+\beta_{41}W_{22(n)}(\tau)W_{11(n)}(\tau)^2+\beta_{42}W_{22(n)}(\tau)W_{12(n)}(\tau)^2+\beta_{43}W_{22(n)}(\tau)$$
$$\times W_{21(n)}(\tau)^2+\beta_{44}W_{22(n)}(\tau)^3+\beta_{45}W_{11(n)}(\tau)W_{12(n)}(\tau)W_{21(n)}(\tau)\Big)d\tau \qquad (4\text{-}18)$$

Based on the initial conditions of the system, one can assume the following solutions for the linear part of the main equation $L(W_{nm}(t))=0$, for the respective four different shape modes, one-one, one-two, two-one and two-two as:

$$W_{11(0)}(t)=A_{11}Cos(\omega_{11}t) \qquad (4\text{-}19)$$

$$W_{12(0)}(t)=A_{12}Cos(\omega_{12}t) \qquad (4\text{-}20)$$

$$W_{21(0)}(t)=A_{21}Cos(\omega_{21}t) \qquad (4\text{-}21)$$

And

$$W_{22(0)}(t) = A_{22} Cos(\omega_{22} t) \tag{4-22}$$

where A_{nm} is the initial displacement for each vibration mode of the system.

It is noteworthy to mention that the fractional derivatives $D^{(\alpha)} W_{nm(n)}(\tau)$ in Eqs. (4-15) to (4-18) have been replaced by the equivalent Caputo's model as:

$$D^{(\alpha)} W_{nm(0)}(\tau) = \frac{1}{\Gamma(1-\alpha)} \int_0^{\tau} (\tau - \xi)^{-\alpha-1} W_{nm(0)}(\xi) d\xi \quad , \quad 0 \le \alpha < 1 \tag{4-23}$$

In order to obtain the time response of the damped free vibration, the initial approximations as Eqs. (4-19)-(4-22) must be substituted into the iteration formulas of Eqs. (4-15)- (4-18). By integrating the resulted relationships over the desired time span, the time history responses for each mode of the system can be numerically obtained.

4. 4. Results and Discussions

In this section, the solution procedure presented in the previous section is examined in detail. Effects of various parameters on the free vibration of rectangular plate are investigated. The fractional differential order α is the key parameter in this section, which is considered in all results obtained.

The following table represents the numerical values for the parameters of the system used to obtain the numerical results. For this purpose, Boron Epoxy plate which was reported as a composite plate at [38] have been used as a case study.

Table 4-1. Numerical values of different parameters of the system

Parameter	Value	Parameter	Value
Elastic Modulus ($\boldsymbol{E_x}$) [38]	208 GPa	**Plate Length** ($\boldsymbol{a}$)	1 m
Elastic Modulus $(\boldsymbol{E_y})$ [38]	18.9 GPa	**PlateWidth** ($\boldsymbol{b}$)	0.3 m
Shear Modulus ($\boldsymbol{G}$) [38]	5.7 GPa	**Plate Height** ($\boldsymbol{h}$)	0.01 m
Poisson Ratio ($\boldsymbol{v_x}$) [38]	0.23	**Plate Mass Density** ($\boldsymbol{\rho}$) [38]	2000 kg/m^3
Poisson Ratio ($\boldsymbol{v_y}$) [38]	0.0208		

4.4.1. Effect of Order of Fractional Derivative, $\boldsymbol{\alpha}$

As mentioned in the last sections, based on the iteration formulas, Eqs. (4-15)-(4-18), derived in Section 4. 2, time responses of the plate are obtained by applying the first iteration.

Figure 4-1 to **Figure 4-4** represent the time response of the plate for the first mode to the fourth mode, respectively. For each mode, three different values of the fractional derivative order have been considered and the effect of this parameter α, has been investigated. **Figure 4-1** shows the time response of the first mode of the plate and can be seen that as the order of the fractional derivative increases, the fractional element acts more like a viscoelastic element and increases the damping effect of the system. On the other hand, the elastic effect of the fractional element increases for

small values of the fractional derivative and the system behaves more like forced vibration and will prevent the system to be completely damped. On the other hand, the system is creating an unstable energy transformation due to the fractional behavior of the viscoelasticity.

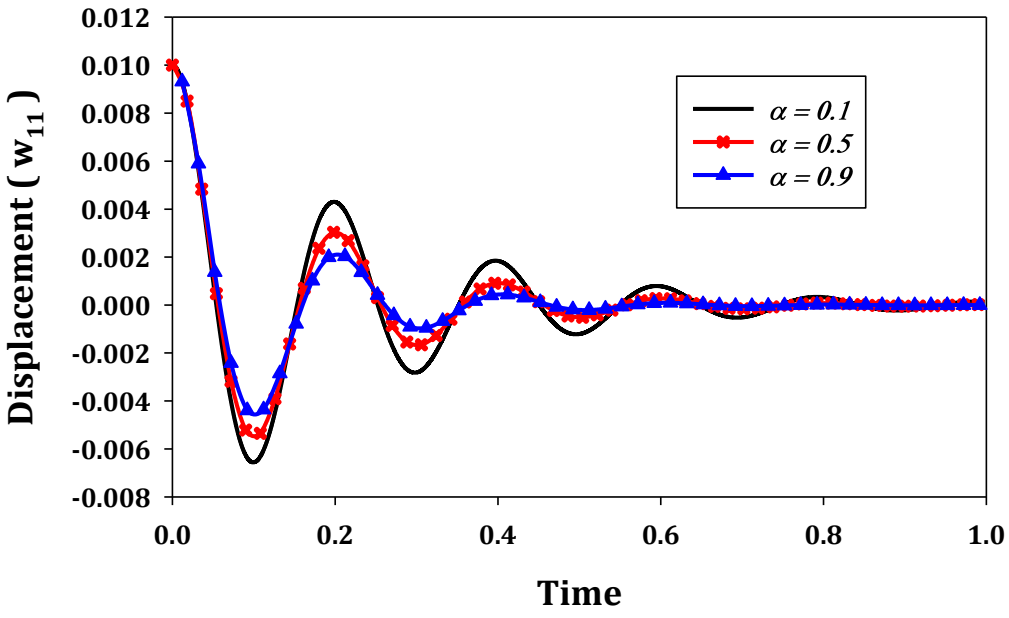

Figure 4-1- Time response of first mode under various values of α

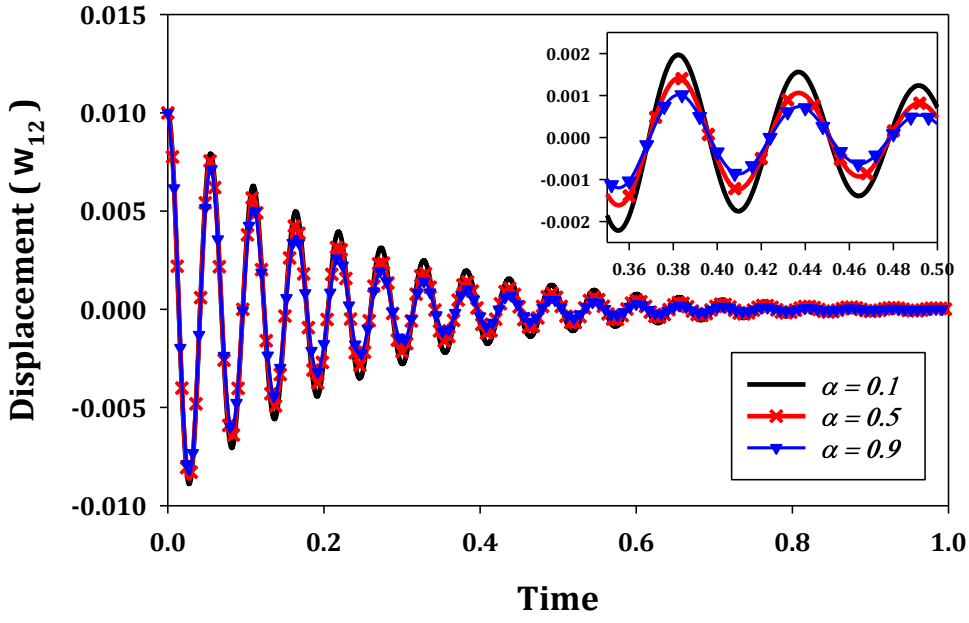

Figure 4-2- Time response of second mode under various values of α

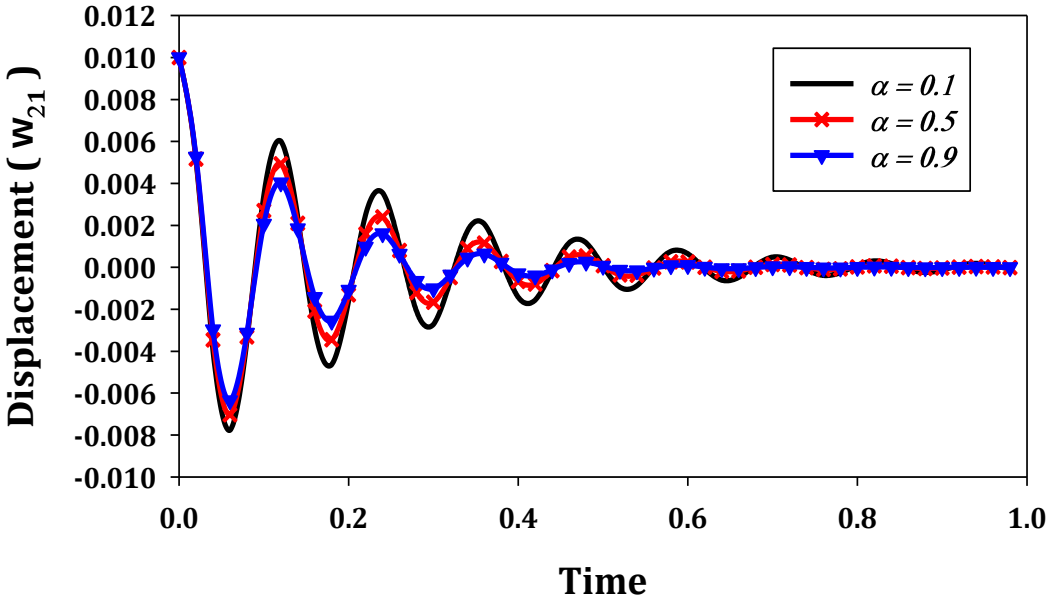

Figure 4-3- Time response of third mode under various values of α

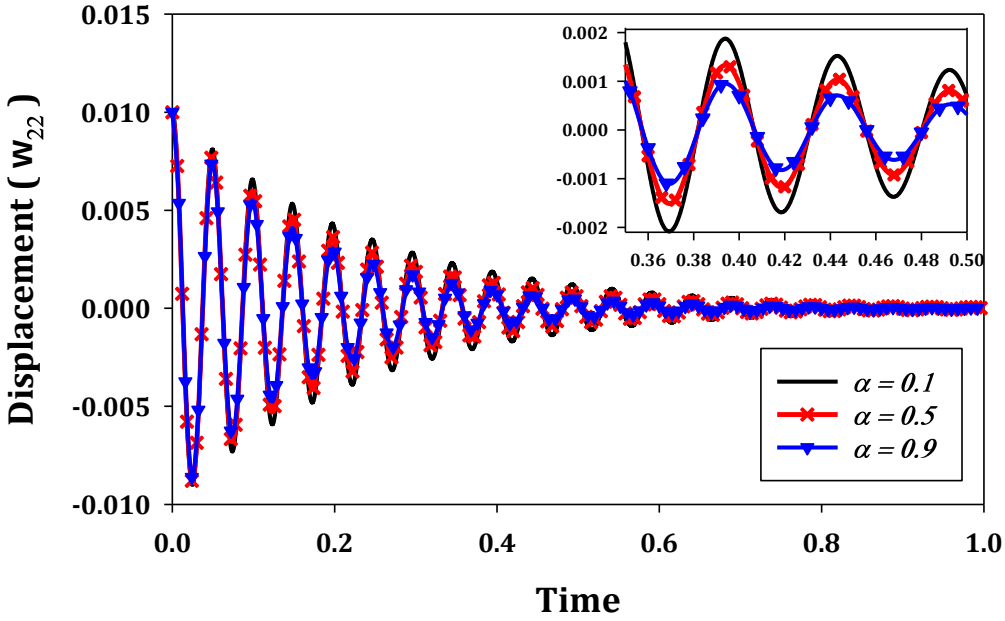

Figure 4-4- Time response of fourth mode under various values of α

By comparing **Figure 4-1** and **Figure 4-3** with respect to **Figure 4-2** and **Figure 4-4**, it can be seen that the effect of the fractional derivative order α on the system damping changes with the natural frequency for each mode. Changes in the magnitude of α have stronger effect on the damping of the first and third modes and has weaker effect of the damping of the second and fourth modes. Therefore, it can be concluded that the effect of parameter α depends on the frequency of the system.

4.4.2. Effect of Aspect Ratio, *r*

Effect of parameter *r*, defined as the aspect ratio, is studied in this section. Three different numerical values have been assumed for the aspect ratio and the results are shown in **Figure 4-5** to **Figure 4-8** which represent the effect of these various values on the time response of the system. These figures illustrate that as the aspect ratio of the plate increases, the natural frequency of the system increases, too. This behavior can be seen in all four different modes of the system but the intensity of this effect varies for each mode. To study the effect of the aspect ratio on the natural frequencies as clear as possible, the exact numerical values for the undamped natural frequencies of each mode have been presented in **Table 4-2**.

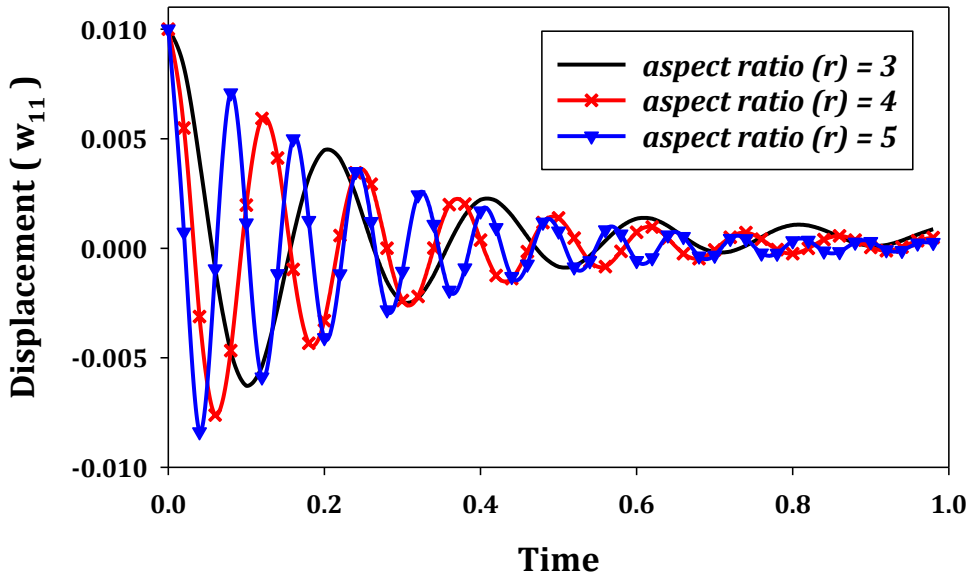

Figure 4-5- Aspect ratio effect on time response of mode one for $\alpha = 0.5$

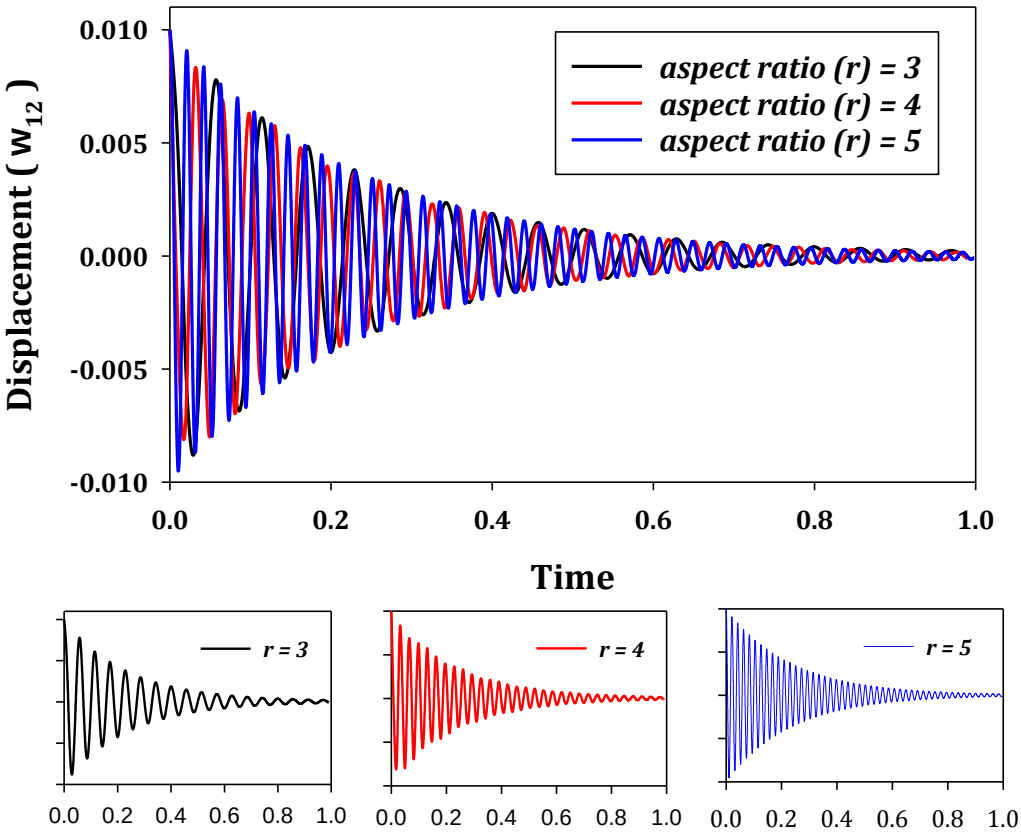

Figure 4-6- Aspect ratio effect on time response of mode two for $\alpha = 0.5$

Table 4-2 . Aspect ratio effect on natural frequencies for $\alpha = 0.5$

Natural Frequency	Aspect Ratio ($r = {}^{a}/_{b}$)		
	$r = 3$	$r = 4$	$r = 5$
First Mode (ω_{11})	31.92163071	53.16726317	80.95505613
Second Mode (ω_{12})	115.1168902	202.3335785	314.6100371
Third Mode (ω_{21})	53.64541183	70.67476488	95.49653903
Fourth Mode (ω_{22})	127.6865229	212.6690527	323.8202245

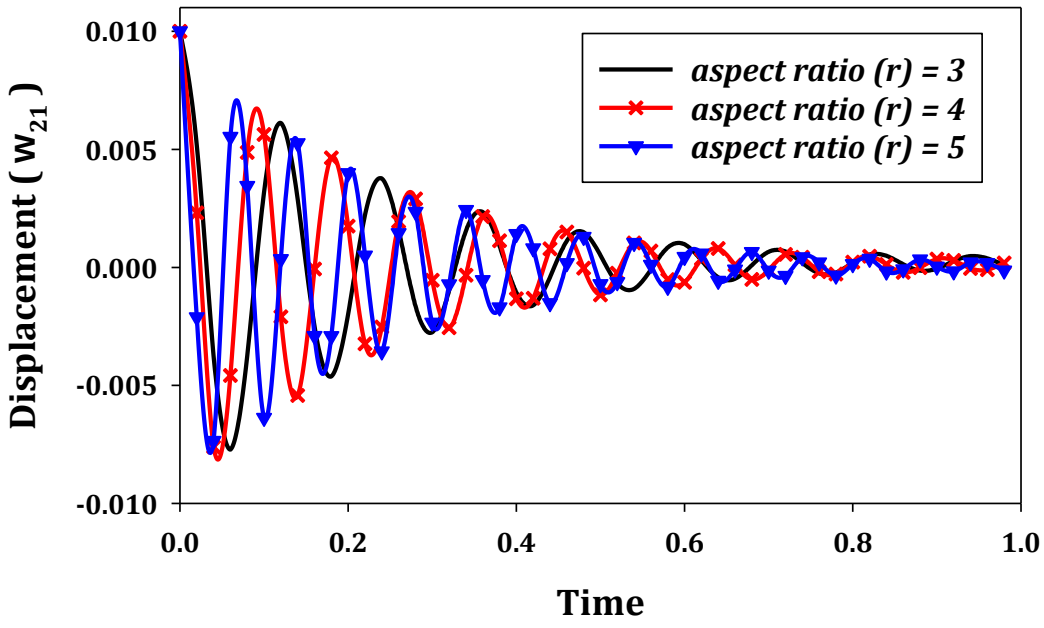

Figure 4-7- Aspect ratio effect on time response of mode three for $\alpha = 0.5$

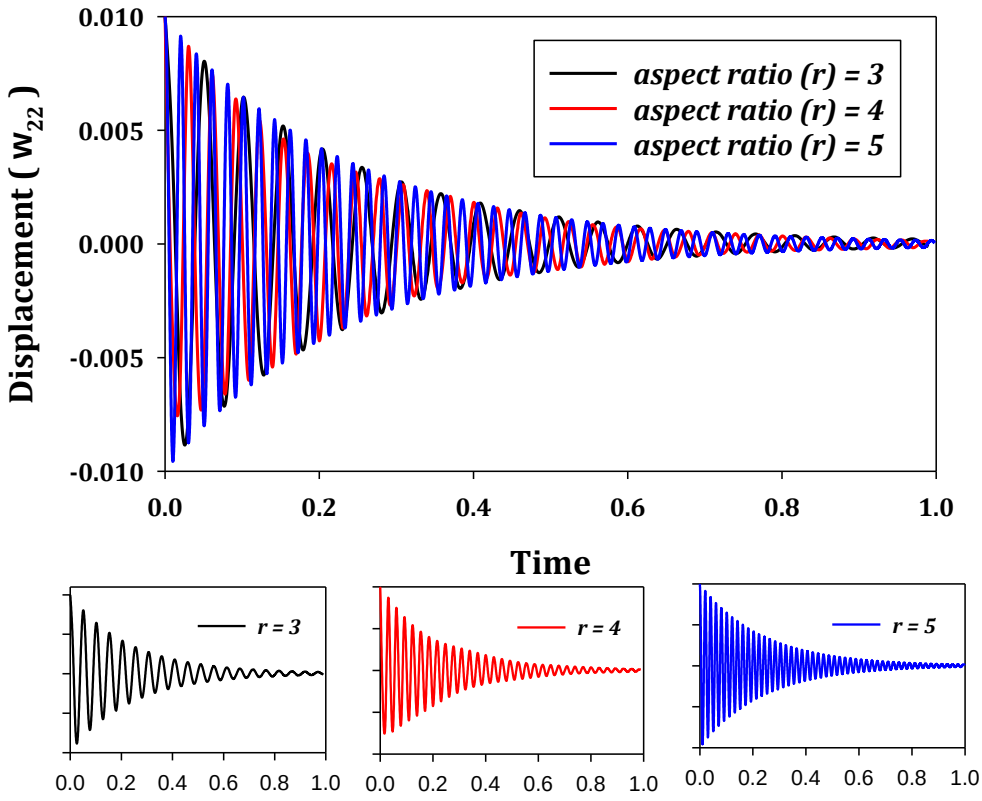

Figure 4-8- Aspect ratio effect on time response of mode four for $\alpha = 0.5$

4.4.3. Effect of Elasticity Ratio

Free vibration behavior of the system under different elasticity ratios and different orders of fractional derivative have been investigated in this section. **Figure 4-9** represents the effect of elasticity ratios for $E_x/E_y = 1$, 10 and 100 for the fractional derivative order of $\alpha = 0.1$. It can be seen that as the elasticity ratio increases, the natural frequency of the system decreases. Also, by comparing **Figure 4-9** to **Figure 4-11**, one could see that as the order of fractional derivative increases, the system damping will increase. The effect of the elastic ratio and the fractional order on other three modes of the system have also been studied and similar behavior as

explained for the first mode has been observed. The remaining numerical results related to this section have been included in Appendix B as **Figure B-1** to **Figure B-3**.

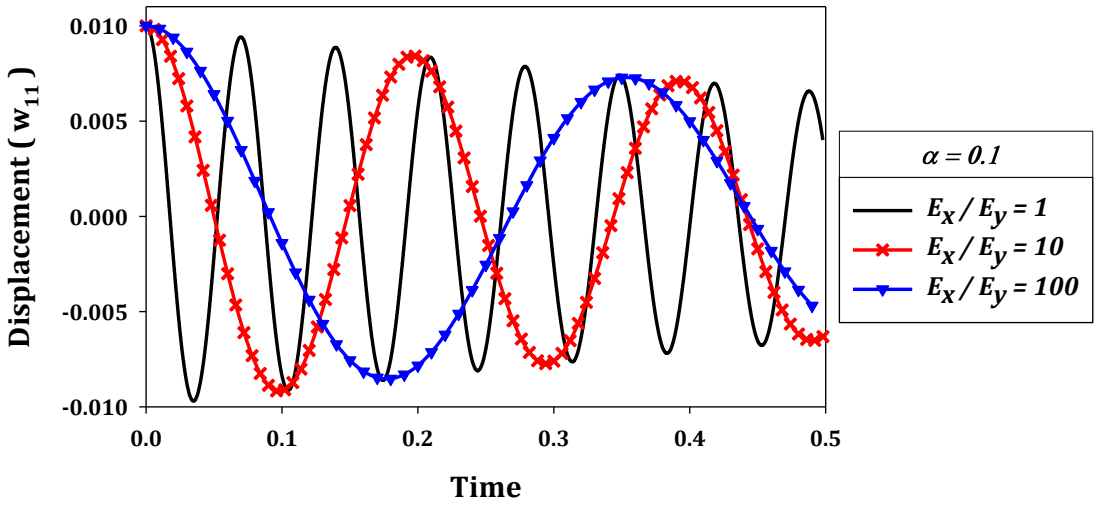

Figure 4-9- Effect of elasticity ratio on free vibration, first mode, $\alpha = 0.1$

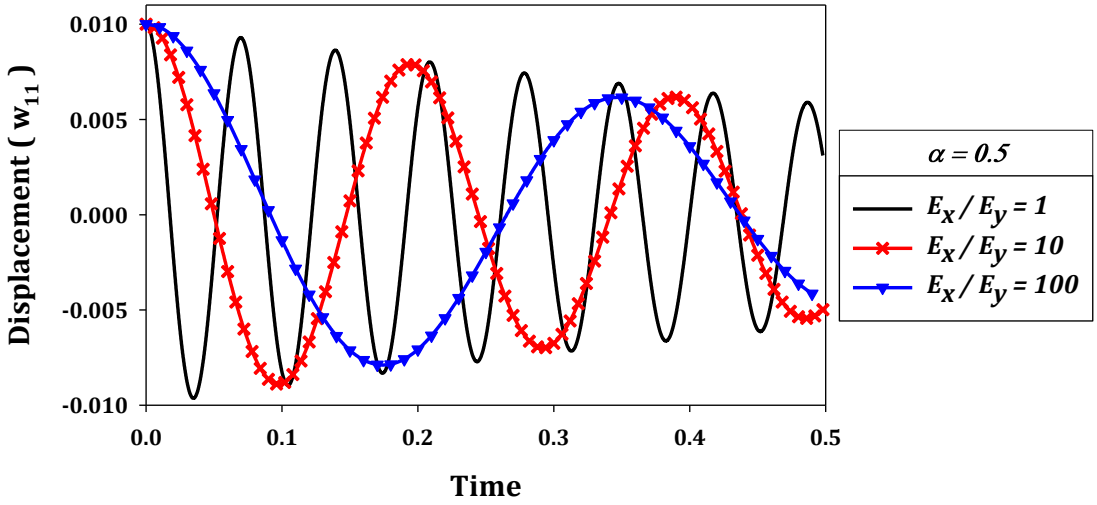

Figure 4-10- Effect of elasticity ratio on free vibration, first mode, $\alpha = 0.5$

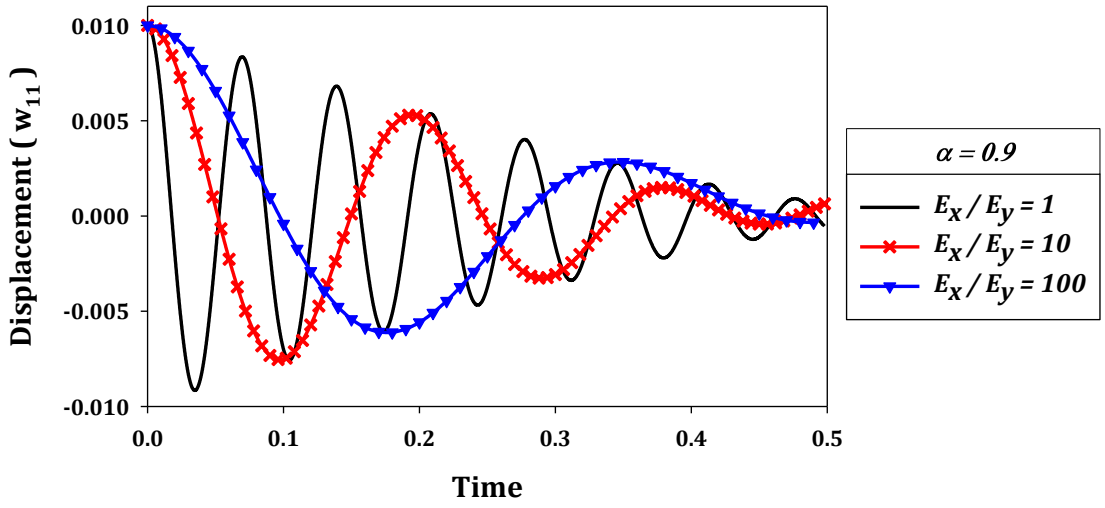

Figure 4-11- Effect of elasticity ratio on free vibration, first mode, $\alpha = 0.9$

In order to present a clear vision to the readers, the exact values of natural frequencies of each mode under different elasticity ratios have been presented in **Table 4-3**.

Table 4-3 . Effect of elasticity ratio on natural frequencies.

Natural Frequency	Elasticity Ratio(E_x/E_y)		
	1	**10**	**100**
First Mode (ω_{11})	90.11167098	31.92163071	17.57493196
Second Mode (ω_{12})	356.1879592	115.1168902	43.47530363
Third Mode (ω_{21})	99.89470929	53.64541183	46.55875789
Fourth Mode (ω_{22})	360.4466839	127.6865229	70.29972784

Chapter 5 - Nonlinear Forced Vibration Analysis

5. 1. Introduction

The nonlinear forced vibration analysis of a rectangular composite plate has been presented in this chapter. It has been assumed that the plate is subjected to a harmonic force, which is applied in the Z -direction to the $X-Y$ plane. Depending on the application of the plate, the harmonic excitation frequency may vary and since the natural frequency of the plate is constant, the resonance phenomena might happen occur with a high probability. The goal here is to investigate the frequency response of the system under different conditions, specifically the resonance phenomena in which the frequency of the external force moves closer to the natural frequencies of the system. For this purpose, the method of multiple time-scales has been chosen to solve the nonlinear equations and obtain the frequency response of the system. Analytical solutions have been derived for the plate with the fractional derivation viscoelasticity. The effect of the key parameter α and other physical parameters have been investigated in this chapter.

5. 2. Forced Vibration of Plate with Fractional Viscoelasticity

The governing equations of motion of the rectangular plate with the fractional derivative subjected to a harmonic external force, discussed in Section 3. 2, have been developed. Based on the von Kármán plate theory and by applying the Galerkin procedure one would arrive at:

$$\begin{aligned}\ddot{W}_{11} + \mathrm{C}\dot{W}_{11} + k\, D^{(\alpha)}W_{11} + \omega_{11}{}^{2}W_{11} + \beta_{11}W_{11}{}^{3} + \beta_{12}W_{11}W_{12}{}^{2} \\ + \beta_{13}W_{11}W_{21}{}^{2} + \beta_{14}W_{11}W_{22}{}^{2} + \beta_{15}W_{12}W_{21}W_{22} = f_{11}Q\end{aligned} \tag{5-1}$$

$$\begin{aligned}\ddot{W}_{12} + \mathrm{C}\dot{W}_{12} + k\, D^{(\alpha)}W_{12} + \omega_{12}\, W_{12} + \beta_{12}W_{12}W_{11}{}^{2} + \beta_{22}W_{12}{}^{3} \\ + \beta_{23}W_{12}W_{21}{}^{2} + \beta_{24}W_{12}W_{22}{}^{2} + \beta_{25}W_{11}W_{21}W_{22} = f_{12}Q\end{aligned} \tag{5-2}$$

$$\begin{aligned}\ddot{W}_{21} + \mathrm{C}\dot{W}_{21} + k\, D^{(\alpha)}W_{21} + \omega_{21}{}^{2}W_{21} + \beta_{31}W_{21}W_{11}{}^{2} + \beta_{32}W_{21}W_{12}{}^{2} \\ + \beta_{33}W_{21}{}^{3} + \beta_{34}W_{21}W_{22}{}^{2} + \beta_{35}W_{11}W_{12}W_{22} = f_{21}Q\end{aligned} \tag{5-3}$$

and

$$\begin{aligned}\ddot{W}_{22} + \mathrm{C}\dot{W}_{22} + k\, D^{(\alpha)}W_{22} + \omega_{22}{}^{2}W_{22} + \beta_{42}W_{22}W_{11}{}^{2} + \beta_{42}W_{22}W_{12}{}^{2} \\ + \beta_{43}W_{22}W_{21}{}^{2} + \beta_{44}W_{22}{}^{3} + \beta_{45}W_{11}W_{12}W_{21} = f_{22}Q\end{aligned} \tag{5-4}$$

where all coefficients can be found in Appendix A as Eqs. (A-1)-(A-28).

5. 3. Solution Method

The method of multiple time-scales has been utilized in this section to obtain the frequency response and vibration behavior of each mode of the system. For solving

the nonlinear ordinary differential equations of motion, Eqs. (5-1)-(5-4), by implementing the method of multiple time-scales, following approximate solutions can be written in terms of different time scales as [22]:

$$W_{11} = u_1(t,\varepsilon) = \varepsilon u_{1(1)}(T_0, T_2, ...) + \varepsilon^3 u_{1(3)}(T_0, T_2, ...) + ... \tag{5-5}$$

$$W_{12} = u_2(t,\varepsilon) = \varepsilon u_{2(1)}(T_0, T_2, ...) + \varepsilon^3 u_{2(3)}(T_0, T_2, ...) +, ... \tag{5-6}$$

$$W_{21} = u_3(t,\varepsilon) = \varepsilon u_{3(1)}(T_0, T_2, ...) + \varepsilon^3 u_{3(3)}(T_0, T_2, ...) +, ... \tag{5-7}$$

and

$$W_{22} = u_4(t,\varepsilon) = \varepsilon u_{4(1)}(T_0, T_2, ...) + \varepsilon^3 u_{4(3)}(T_0, T_2, ...) +, ... \tag{5-8}$$

where ε is a small dimensionless parameter, and the time scales are defined as [22]:

$$T_n = \varepsilon^n t \tag{5-9}$$

Therefore, the derivatives with respect to time are defined as [22, 40]:

$$\frac{d}{dt} = \frac{dT_0}{dt}\frac{d}{\partial T_0} + \frac{dT_1}{dt}\frac{d}{\partial T_1} + ... = D_0 + \varepsilon D_1 + \varepsilon^2 D_2 + ..., \tag{5-10}$$

$$\frac{d^2}{dt^2} = {D_0}^2 + 2\varepsilon D_0 D_1 + \varepsilon^2 ({D_1}^2 + 2D_0 D_2) + ..., \tag{5-11}$$

and

$$D^{(\alpha)} = \frac{d^\alpha}{dt^\alpha} = {D_0}^\alpha + \varepsilon\alpha {D_0}^{\alpha-1} D_1 + \varepsilon^2 \alpha(\alpha-1) {D_0}^{\alpha-2} D_2 + ...\tag{5-12}$$

where D_0^{α} is the fractional derivative with respect to T_0. Therefore, the fractional derivative is written in the form of the fractional power of differential operator [40]. Also, according to the method of multiple time-scales, the damping coefficient, fractional derivative coefficient and the external force terms must be developed as [22]:

$$C = \varepsilon^2 \tilde{C}\,, \tag{5-13}$$

$$k = \varepsilon^2 \tilde{k}\,, \tag{5-14}$$

and

$$Q = \varepsilon^3 q\,, \tag{5-15}$$

By substituting Eqs. (5-5)-(5-8) and Eqs. (5-10)-(5-15) into Eqs. (5-1)-(5-4), the following equations are resulted:

$$\begin{aligned}
&(D_0{}^2 + 2\varepsilon D_0 D_1 + \varepsilon^2 (D_1{}^2 + 2D_0 D_2) + \ldots) \times (\varepsilon u_{1(1)} + \varepsilon^3 u_{1(3)} + \ldots) \\
&\quad + \varepsilon^2 \tilde{C} \times (D_0 + \varepsilon D_1 + \varepsilon^2 D_2 + \ldots) \times (\varepsilon u_{1(1)} + \varepsilon^3 u_{1(3)} + \ldots) \\
&\quad + \varepsilon^2 \tilde{k} \times (D_0{}^{\alpha} + \varepsilon\alpha D_0{}^{\alpha-1} D_1 + \varepsilon^2 \alpha(\alpha-1) D_0{}^{\alpha-2} D_2 + \ldots) \\
&\quad \times (\varepsilon u_{1(1)} + \varepsilon^3 u_{1(3)} + \ldots) + \omega_{11}{}^2 \times (\varepsilon u_{1(1)} + \varepsilon^3 u_{1(3)} + \ldots) \\
&\quad + \beta_{11} (\varepsilon u_{1(1)} + \varepsilon^3 u_{1(3)} + \ldots)^3 \\
&\quad + \beta_{12} (\varepsilon u_{1(1)} + \varepsilon^3 u_{1(3)} + \ldots) \times (\varepsilon u_{2(1)} + \varepsilon^3 u_{2(3)} + \ldots)^2 \\
&\quad + \beta_{13} (\varepsilon u_{1(1)} + \varepsilon^3 u_{1(3)} + \ldots) \times (\varepsilon u_{3(1)} + \varepsilon^3 u_{3(3)} + \ldots)^2 \\
&\quad + \beta_{14} (\varepsilon u_{1(1)} + \varepsilon^3 u_{1(3)} + \ldots) \times (\varepsilon u_{4(1)} + \varepsilon^3 u_{4(3)} + \ldots)^2 \\
&\quad + \beta_{15} (\varepsilon u_{2(1)} + \varepsilon^3 u_{2(3)} + \ldots) \times (\varepsilon u_{3(1)} + \varepsilon^3 u_{3(3)} + \ldots) \\
&\quad \times (\varepsilon u_{4(1)} + \varepsilon^3 u_{4(3)} + \ldots) = f_{11} \varepsilon^3 q
\end{aligned} \tag{5-16}$$

$$
\begin{aligned}
&(D_0{}^2 + 2\varepsilon D_0 D_1 + \varepsilon^2 (D_1{}^2 + 2D_0 D_2) + \ldots) \times (\varepsilon u_{2(1)} + \varepsilon^3 u_{2(3)} + \ldots) \\
&\quad + \varepsilon^2 \tilde{C} \times (D_0 + \varepsilon D_1 + \varepsilon^2 D_2 + \ldots) \times (\varepsilon u_{2(1)} + \varepsilon^3 u_{2(3)} + \ldots) \\
&\quad + \varepsilon^2 \tilde{k} \times (D_0{}^{\alpha} + \varepsilon \alpha D_0{}^{\alpha-1} D_1 + \varepsilon^2 \alpha(\alpha-1) D_0{}^{\alpha-2} D_2 + \ldots) \\
&\quad \times (\varepsilon u_{2(1)} + \varepsilon^3 u_{2(3)} + \ldots) + \omega_{12}{}^2 \times (\varepsilon u_{2(1)} + \varepsilon^3 u_{2(3)} + \ldots) \\
&\quad + \beta_{21} \times (\varepsilon u_{2(1)} + \varepsilon^3 u_{2(3)} + \ldots) \times (\varepsilon u_{1(1)} + \varepsilon^3 u_{1(3)} + \ldots)^2 \\
&\quad + \beta_{22} \times (\varepsilon u_{2(1)} + \varepsilon^3 u_{2(3)} + \ldots)^3 \\
&\quad + \beta_{23} (\varepsilon u_{2(1)} + \varepsilon^3 u_{2(3)} + \ldots) \times (\varepsilon u_{3(1)} + \varepsilon^3 u_{3(3)} + \ldots)^2 \\
&\quad + \beta_{24} (\varepsilon u_{2(1)} + \varepsilon^3 u_{2(3)} + \ldots) \times (\varepsilon u_{4(1)} + \varepsilon^3 u_{4(3)} + \ldots)^2 \\
&\quad + \beta_{25} (\varepsilon u_{1(1)} + \varepsilon^3 u_{1(3)} + \ldots) \times (\varepsilon u_{3(1)} + \varepsilon^3 u_{3(3)} + \ldots) \\
&\quad \times (\varepsilon u_{4(1)} + \varepsilon^3 u_{4(3)} + \ldots) = f_{12} \varepsilon^3 q
\end{aligned}
\tag{5-17}
$$

$$
\begin{aligned}
&(D_0{}^2 + 2\varepsilon D_0 D_1 + \varepsilon^2 (D_1{}^2 + 2D_0 D_2) + \ldots) \times (\varepsilon u_{3(1)} + \varepsilon^3 u_{3(3)} + \ldots) \\
&\quad + \varepsilon^2 \tilde{C} \times (D_0 + \varepsilon D_1 + \varepsilon^2 D_2 + \ldots) \times (\varepsilon u_{3(1)} + \varepsilon^3 u_{3(3)} + \ldots) \\
&\quad + \varepsilon^2 \tilde{k} \times (D_0{}^{\alpha} + \varepsilon \alpha D_0{}^{\alpha-1} D_1 + \varepsilon^2 \alpha(\alpha-1) D_0{}^{\alpha-2} D_2 + \ldots) \\
&\quad \times (\varepsilon u_{3(1)} + \varepsilon^3 u_{3(3)} + \ldots) + \omega_{21}{}^2 \times (\varepsilon u_{3(1)} + \varepsilon^3 u_{3(3)} + \ldots) \\
&\quad + \beta_{31} \times (\varepsilon u_{3(1)} + \varepsilon^3 u_{3(3)} + \ldots) \times (\varepsilon u_{1(1)} + \varepsilon^3 u_{1(3)} + \ldots)^2 \\
&\quad + \beta_{32} (\varepsilon u_{3(1)} + \varepsilon^3 u_{3(3)} + \ldots) \times (\varepsilon u_{2(1)} + \varepsilon^3 u_{2(3)} + \ldots)^2 \\
&\quad + \beta_{33} \times (\varepsilon u_{3(1)} + \varepsilon^3 u_{3(3)} + \ldots)^3 \\
&\quad + \beta_{34} (\varepsilon u_{3(1)} + \varepsilon^3 u_{3(3)} + \ldots) \times (\varepsilon u_{4(1)} + \varepsilon^3 u_{4(3)} + \ldots)^2 \\
&\quad + \beta_{35} (\varepsilon u_{1(1)} + \varepsilon^3 u_{1(3)} + \ldots) \times (\varepsilon u_{2(1)} + \varepsilon^3 u_{2(3)} + \ldots) \\
&\quad \times (\varepsilon u_{4(1)} + \varepsilon^3 u_{4(3)} + \ldots) = f_{21} \varepsilon^3 q
\end{aligned}
\tag{5-18}
$$

$$
\begin{aligned}
&(D_0{}^2 + 2\varepsilon D_0 D_1 + \varepsilon^2 (D_1{}^2 + 2D_0 D_2) + \ldots) \times (\varepsilon u_{4(1)} + \varepsilon^3 u_{4(3)} + \ldots) \\
&\quad + \varepsilon^2 \tilde{C} \times (D_0 + \varepsilon D_1 + \varepsilon^2 D_2 + \ldots) \times (\varepsilon u_{4(1)} + \varepsilon^3 u_{4(3)} + \ldots) \\
&\quad + \varepsilon^2 \tilde{k} \times (D_0{}^{\alpha} + \varepsilon \alpha D_0{}^{\alpha-1} D_1 + \varepsilon^2 \alpha(\alpha-1) D_0{}^{\alpha-2} D_2 + \ldots) \\
&\quad \times (\varepsilon u_{4(1)} + \varepsilon^3 u_{4(3)} + \ldots) + \omega_{22}{}^2 \times (\varepsilon u_{4(1)} + \varepsilon^3 u_{4(3)} + \ldots) \\
&\quad + \beta_{41} \times (\varepsilon u_{4(1)} + \varepsilon^3 u_{4(3)} + \ldots) \times (\varepsilon u_{1(1)} + \varepsilon^3 u_{1(3)} + \ldots)^2 \\
&\quad + \beta_{42} (\varepsilon u_{4(1)} + \varepsilon^3 u_{4(3)} + \ldots) \times (\varepsilon u_{2(1)} + \varepsilon^3 u_{2(3)} + \ldots)^2 \\
&\quad + \beta_{43} (\varepsilon u_{4(1)} + \varepsilon^3 u_{4(3)} + \ldots) \times (\varepsilon u_{3(1)} + \varepsilon^3 u_{3(3)} + \ldots)^2 \\
&\quad + \beta_{44} \times (\varepsilon u_{4(1)} + \varepsilon^3 u_{4(3)} + \ldots)^3 \\
&\quad + \beta_{45} (\varepsilon u_{1(1)} + \varepsilon^3 u_{1(3)} + \ldots) \times (\varepsilon u_{2(1)} + \varepsilon^3 u_{2(3)} + \ldots) \\
&\quad \times (\varepsilon u_{3(1)} + \varepsilon^3 u_{4(3)} + \ldots) = f_{22} \varepsilon^3 q
\end{aligned}
\tag{5-19}
$$

Assuming the external force to have the following harmonic relationship:

$$
q = q_0 \, Cos(\Omega T_0), \tag{5-20}
$$

The primary resonance for each mode occurs when the frequency of the external excitation moves closer to the natural frequency of that mode. Consequently, the following relationship can be assumed for the frequency of the external force:

$$
\Omega \to \omega_{nm} \;\Rightarrow\; \Omega = \omega_{nm} + \varepsilon \, \sigma_i \tag{5-21}
$$

where σ_i is the detuning parameter for each mode of vibration of the system.

Considering Eq. (5-20) and by eliminating the coefficients of ε^1 and ε^3 from Eqs. (5-16)-(5-19), the following respective equations can be obtained as:

For the coefficient ε^1 :

$$D_0{}^2 u_{1(1)}(T_0,T_2,...) + \omega_{11}{}^2 u_{1(1)}(T_0,T_2,...) = 0 \tag{5-22}$$

$$D_0{}^2 u_{2(1)}(T_0,T_2,...) + \omega_{12}{}^2 u_{2(1)}(T_0,T_2,...) = 0 \tag{5-23}$$

$$D_0{}^2 u_{3(1)}(T_0,T_2,...) + \omega_{21}{}^2 u_{2(1)}(T_0,T_2,...) = 0 \tag{5-24}$$

and

$$D_0{}^2 u_{4(1)}(T_0,T_2,...) + \omega_{22}{}^2 u_{4(1)}(T_0,T_2,...) = 0 \tag{5-25}$$

and for the coefficient ε^3 :

$$\begin{aligned} D_0{}^2 u_{1(3)} + \omega_{11}{}^2 u_{1(3)} = & -\tilde{C}\, D_0 u_{1(1)} - D_1{}^2 u_{1(1)} - 2 D_1 D_0 u_{1(1)} - \tilde{k}\, D_0{}^{\alpha} u_{1(1)} \\ & - \beta_{11}\, u_{1(1)}{}^3 - \beta_{12}\, u_{1(1)}\, u_{2(1)}{}^2 - \beta_{13}\, u_{1(1)}\, u_{3(1)}{}^2 - \beta_{14}\, u_{1(1)}\, u_{4(1)}{}^2 \\ & - \beta_{15}\, u_{2(1)}\, u_{3(1)}\, u_{4(1)} + f_{11}\, q_0\, Cos\,(\,\Omega\, T_0\,) \end{aligned} \tag{5-26}$$

$$\begin{aligned} D_0{}^2 u_{2(3)} + \omega_{12}{}^2 u_{2(3)} = & -\tilde{C}\, D_0 u_{2(1)} - D_1{}^2 u_{2(1)} - 2 D_1 D_0 u_{2(1)} - \tilde{k}\, D_0{}^{\alpha} u_{2(1)} \\ & - \beta_{21}\, u_{2(1)}\, u_{1(1)}{}^2 - \beta_{22}\, u_{2(1)}{}^3 - \beta_{23}\, u_{2(1)}\, u_{3(1)}{}^2 - \beta_{24}\, u_{2(1)}\, u_{4(1)}{}^2 \\ & - \beta_{25}\, u_{1(1)}\, u_{3(1)}\, u_{4(1)} + f_{12}\, q_0\, Cos\,(\,\Omega\, T_0\,) \end{aligned} \tag{5-27}$$

$$\begin{aligned} D_0{}^2 u_{3(3)} + \omega_{21}{}^2 u_{3(3)} = & -\tilde{C}\, D_0 u_{3(1)} - D_1{}^2 u_{3(1)} - 2 D_1 D_0 u_{3(1)} - \tilde{k}\, D_0{}^{\alpha} u_{3(1)} \\ & - \beta_{31}\, u_{3(1)}\, u_{1(1)}{}^2 - \beta_{32}\, u_{3(1)}\, u_{2(1)}{}^2 - \beta_{33}\, u_{3(1)}{}^3 - \beta_{34}\, u_{3(1)}\, u_{4(1)}{}^2 \\ & - \beta_{35}\, u_{1(1)}\, u_{2(1)}\, u_{4(1)} + f_{21}\, q_0\, Cos\,(\,\Omega\, T_0\,) \end{aligned} \tag{5-28}$$

and

$$
\begin{aligned}
D_0{}^2 u_{4(3)} + \omega_{22}{}^2 u_{4(3)} = & -\tilde{C}\, D_0 u_{4(1)} - D_1{}^2 u_{4(1)} - 2 D_1 D_0 u_{4(1)} - \tilde{k}\, D_0{}^{\alpha} u_{4(1)} \\
& - \beta_{41}\, u_{4(1)}\, u_{1(1)}{}^2 - \beta_{42}\, u_{4(1)}\, u_{2(1)}{}^2 - \beta_{43}\, u_{4(1)}\, u_{3(1)}{}^2 - \beta_{44}\, u_{4(1)}{}^3 \\
& - \beta_{45}\, u_{1(1)}\, u_{2(1)}\, u_{3(1)} + f_{22}\, q_0\, Cos\,(\Omega T_0)
\end{aligned}
\tag{5-29}
$$

The solutions of Eqs. (5-22)-(5-25) can be written as:

$$
u_{1(1)}(T_0, T_2, \ldots) = A_1(T_2)\, e^{i\,\omega_{11}\,T_0} + \bar{A}_1(T_2)\, e^{-i\,\omega_{11}\,T_0}, \tag{5-30}
$$

$$
u_{2(1)}(T_0, T_2, \ldots) = A_2(T_2)\, e^{i\,\omega_{12}\,T_0} + + \bar{A}_2(T_2)\, e^{-i\,\omega_{12}\,T_0}, \tag{5-31}
$$

$$
u_{3(1)}(T_0, T_2, \ldots) = A_3(T_2)\, e^{i\,\omega_{21}\,T_0} + \bar{A}_3(T_2)\, e^{-i\,\omega_{21}\,T_0}, \tag{5-32}
$$

and

$$
u_{4(1)}(T_0, T_2, \ldots) = A_4(T_2)\, e^{i\,\omega_{22}\,T_0} + \bar{A}_4(T_2)\, e^{-i\,\omega_{22}\,T_0}, \tag{5-33}
$$

where A_i $(i = 1,2,3,4)$ is the unknown complex function and $\bar{A}_i$ is the complex conjugate of A_i.

Considering Eqs. (5-30)-(5-33), and after some mathematical simplifications, the Eqs. (5-26)-(5-29) can be rewritten as:

$$
\begin{aligned}
D_0{}^2 u_{1(3)} + \omega_{11}{}^2 u_{1(3)} = & -i\,\tilde{C}\,\omega_{11} A_1 - 2i\,\omega_{11} A_1' - \tilde{k}\, A_1 (i\omega_{11})^{\alpha} \\
& - 3\beta_{11}\, A_1{}^2 \bar{A}_1 - 2\beta_{12}\, A_1 A_2 \bar{A}_2 - 2\beta_{13}\, A_1 A_3 \bar{A}_3 - 2\beta_{14}\, A_1 A_4 \bar{A}_4 \\
& + \frac{1}{2} f_{11}\, q_0\, e^{i\,\Omega\,T_0} + c.c
\end{aligned}
\tag{5-34}
$$

$$
\begin{aligned}
&D_0^{\,2}u_{2(3)} + \omega_{12}^{\,2}u_{2(3)} = -i\,\tilde{C}\,\omega_{12}A_2 - 2i\,\omega_{12}A_2' - \tilde{k}\,A_2(i\omega_{12})^{\alpha} \\
&\quad -2\beta_{21}\,A_2A_1\bar{A}_1 - 3\beta_{22}\,A_2^{\,2}\bar{A}_2 - 2\beta_{23}\,A_2A_3\bar{A}_3 - 2\beta_{24}\,A_2A_4\bar{A}_4 \\
&\quad +\frac{1}{2}f_{12}\,q_0\,e^{i\Omega T_0} + c.c
\end{aligned}
\tag{5-35}
$$

$$
\begin{aligned}
&D_0^{\,2}u_{3(3)} + \omega_{21}^{\,2}u_{3(3)} = -i\,\tilde{C}\,\omega_{21}A_3 - 2i\,\omega_{21}A_3' - \tilde{k}\,A_3(i\omega_{21})^{\alpha} \\
&\quad -2\beta_{31}\,A_3A_1\bar{A}_1 - 2\beta_{32}\,A_3A_2\bar{A}_2 - 3\beta_{33}\,A_3^{\,2}\bar{A}_3 - 2\beta_{34}\,A_3A_4\bar{A}_4 \\
&\quad +\frac{1}{2}f_{21}\,q_0\,e^{i\Omega T_0} + c.c
\end{aligned}
\tag{5-36}
$$

and

$$
\begin{aligned}
&D_0^{\,2}u_{4(3)} + \omega_{22}^{\,2}u_{4(3)} = -i\,\tilde{C}\,\omega_{22}A_4 - 2i\,\omega_{22}A_4' - \tilde{k}\,A_4(i\omega_{22})^{\alpha} \\
&\quad -2\beta_{41}\,A_4A_1\bar{A}_1 - 2\beta_{42}\,A_4A_2\bar{A}_2 - 2\beta_{43}\,A_4A_3\bar{A}_3 - 3\beta_{44}\,A_4^{\,2}\bar{A}_4 \\
&\quad +\frac{1}{2}f_{22}\,q_0\,e^{i\Omega T_0} + c.c
\end{aligned}
\tag{5-37}
$$

where $c.c$ represents the complex conjugate of the preceding terms.

5. 4. Primary Resonance

The primary resonance of the system for the first case occurs when the frequency of the external force moves closer to the natural frequency of the first mode of the system, i.e. $\Omega \to \omega_{11}$. Therefore, by defining the detuning parameter σ_1 and eliminating the secular terms from Eqs. (5-34)-(5-37), we will get:

$$
\begin{aligned}
&i\,\tilde{C}\,\omega_{11}A_1 + 2i\,\omega_{11}A_1' + \tilde{k}\,A_1(i\omega_{11})^{\alpha} + 3\beta_{11}\,A_1^{\,2}\bar{A}_1 + 2\beta_{12}\,A_1A_2\bar{A}_2 \\
&+2\beta_{13}\,A_1A_3\bar{A}_3 + 2\beta_{14}\,A_1A_4\bar{A}_4 - \frac{1}{2}f_{11}\,q_0\,e^{i\sigma_1 T_2} = 0
\end{aligned}
\tag{5-38}
$$

$$i\,\tilde{C}\,\omega_{12}A_2 + 2i\,\omega_{12}A_2' + \tilde{k}\,A_2(i\omega_{12})^{\alpha} + 2\beta_{21}\,A_2A_1\bar{A}_1 + 3\beta_{22}\,A_2{}^2\bar{A}_2 + 2\beta_{23}\,A_2A_3\bar{A}_3 + 2\beta_{24}\,A_2A_4\bar{A}_4 = 0 \tag{5-39}$$

$$i\,\tilde{C}\,\omega_{21}A_3 + 2i\,\omega_{21}A_3' + \tilde{k}\,A_3(i\omega_{21})^{\alpha} + 2\beta_{31}\,A_3A_1\bar{A}_1 + 2\beta_{32}\,A_3A_2\bar{A}_2 + 3\beta_{33}\,A_3{}^2\bar{A}_3 + 2\beta_{34}\,A_3A_4\bar{A}_4 = 0 \tag{5-40}$$

and

$$i\,\tilde{C}\,\omega_{22}A_4 + 2i\,\omega_{22}A_4' + \tilde{k}\,A_4(i\omega_{22})^{\alpha} + 2\beta_{41}\,A_4A_1\bar{A}_1 + 2\beta_{42}\,A_4A_2\bar{A}_2 + 2\beta_{43}\,A_4A_3\bar{A}_3 + 3\beta_{44}\,A_4{}^2\bar{A}_4 = 0 \tag{5-41}$$

Expanding the polar notation for the unknown complex function of A_i as:

$$A_i(T_2) = a_i(T_2)\,e^{i\,\theta_i(T_2)} \tag{5-42}$$

and by separating the real and the imaginary parts of Eqs. (5-38)-(5-41), the following expressions are obtained where $\gamma_1 = \sigma_1 T_2 - \theta_1$:

$$4\omega_{11}a_1' + 2\,\tilde{C}\,\omega_{11}a_1 + 2\tilde{k}\,a_1\,\omega_{11}{}^{\alpha}\,\mathrm{Sin}\left(\alpha\,\arg(i\omega_{11})\right) + f_{11}\,q_0\,Sin(\gamma_1) = 0 \tag{5-43}$$

$$2\,\omega_{12}a_2' + \tilde{C}\,\omega_{12}a_2 + \tilde{k}\,a_2\,\omega_{11}{}^{\alpha}\,\mathrm{Sin}\left(\alpha\,\arg(i\omega_{12})\right) = 0 \tag{5-44}$$

$$2\,\omega_{21}a_3' + \tilde{C}\,\omega_{21}a_3 + \tilde{k}\,a_3\,\omega_{21}{}^{\alpha}\,\mathrm{Sin}\left(\alpha\,\arg(i\omega_{21})\right) = 0 \tag{5-45}$$

$$2\,\omega_{22}a_4' + \tilde{C}\,\omega_{22}a_4 + \tilde{k}\,a_4\,\omega_{22}{}^{\alpha}\,\mathrm{Sin}\left(\alpha\,\arg(i\omega_{22})\right) = 0 \tag{5-46}$$

$$-4\,\omega_{11}a_1\sigma_1 + 2\tilde{k}\,a_1\,\omega_{11}{}^{\alpha}\,Cos\left(\alpha\,\arg(i\omega_{11})\right) + 6\beta_{11}\,a_1{}^3 + 4\beta_{12}\,a_1a_2{}^2 + 4\beta_{13}\,a_1a_3{}^2 + 4\beta_{14}\,a_1a_4{}^2 - f_{11}\,q_0\,Cos(\gamma_1) = 0 \tag{5-47}$$

$$-2\,\omega_{12}\theta_2' + \tilde{k}\,\omega_{12}{}^{\alpha}\,Cos\left(\alpha\,\arg(i\omega_{12})\right) + 2\beta_{21}a_1{}^2 + 3\beta_{22}\,a_2{}^2 + 2\beta_{23}a_3{}^2 + 2\beta_{24}\,a_4{}^2 = 0 \tag{5-48}$$

$$-2\,\omega_{21}\theta_3' + \tilde{k}\,\omega_{21}{}^{\alpha}\,Cos\left(\alpha\,\arg(i\omega_{21})\right) + 2\beta_{31}a_1{}^2 + 2\beta_{32}a_2{}^2 + 3\beta_{33}a_3{}^2 + 2\beta_{34}a_4{}^2 = 0 \tag{5-49}$$

and

$$-2\,\omega_{22}\theta_4' + \tilde{k}\,\omega_{22}{}^{\alpha}\,Cos\left(\alpha\,\arg(i\omega_{22})\right) + 2\beta_{41}a_1{}^2 + 2\beta_{42}a_2{}^2 + 2\beta_{43}a_3{}^2 + 3\beta_{44}a_4{}^2 = 0 \tag{5-50}$$

For the steady-state response of the system, the parameters $\acute{a_\iota}$ and $\acute{\theta_\iota}$ are set to zero and therefore, by applying few mathematical simplifications, the following relationship between the detuning parameter, amplitude of vibration and the physical parameters of the system can be obtained, which describes the amplitude-frequency behavior for the first mode of the system under the primary resonance:

$$\sigma_1 = \frac{2\tilde{k}\;\omega_{11}{}^{\alpha}\,Cos\left(\alpha\,\arg(i\omega_{11})\right) + 6\beta_{11}\,a_1{}^2}{4\omega_{11}} \pm \frac{1}{a_1}\sqrt{\left(f_{11}\,q_0\right)^2 - \left(2\,\tilde{C}\,\omega_{11}a_1\right)^2 - 8\tilde{k}\,\tilde{C}\,a_1{}^2\,\omega_{11}{}^{\alpha+1}\,\mathrm{Sin}\left(\alpha\,\arg(i\omega_{11})\right) - \left(2\tilde{k}\,a_1\,\omega_{11}{}^{\alpha}\right)^2 + 2\tilde{k}^2\,a_1{}^2\,\omega_{11}{}^{2\alpha}\,Cos\left(2\alpha\,\arg(i\omega_{11})\right)} \tag{5-51}$$

Repeating the same procedure, while the external force frequency is getting closer to the natural frequency of the second mode, the amplitude-frequency relationship for the second modes will be found as:

$$\sigma_2 = \frac{2\tilde{k}\ \omega_{12}{}^{\alpha}\ Cos\left(\alpha \arg(i\omega_{12})\right) + 6\beta_{22}\ a_2{}^2}{4\omega_{12}} \pm \frac{1}{a_2}\sqrt{\left(f_{12}\ q_0\right)^2 - \left(2\,\tilde{C}\ \omega_{12} a_2\right)^2 - 8\tilde{k}\ \tilde{C}\ a_2{}^2\ \omega_{12}{}^{\alpha+1}\,\mathrm{Sin}\left(\alpha \arg(i\omega_{12})\right) - \left(2\tilde{k}\ a_2\ \omega_{12}{}^{\alpha}\right)^2 + 2\tilde{k}^2\ a_2{}^2\ \omega_{12}{}^{2\alpha}\ Cos\left(2\alpha \arg(i\omega_{12})\right)} \tag{5-52}$$

Similar expressions can be obtained for the third and the fourth modes of vibration as the primary resonances:

$$\sigma_3 = \frac{2\tilde{k}\ \omega_{32}{}^{\alpha}\ Cos\left(\alpha \arg(i\omega_{32})\right) + 6\beta_{33}\ a_3{}^2}{4\omega_{21}} \pm \frac{1}{a_3}\sqrt{\left(f_{21}\ q_0\right)^2 - \left(2\,\tilde{C}\ \omega_{21} a_3\right)^2 - 8\tilde{k}\ \tilde{C}\ a_3{}^2\ \omega_{21}{}^{\alpha+1}\,\mathrm{Sin}\left(\alpha \arg(i\omega_{21})\right) - \left(2\tilde{k}\ a_3\ \omega_{21}{}^{\alpha}\right)^2 + 2\tilde{k}^2\ a_3{}^2\ \omega_{21}{}^{2\alpha}\ Cos\left(2\alpha \arg(i\omega_{21})\right)} \tag{5-53}$$

$$\sigma_4 = \frac{2\tilde{k}\ \omega_{22}{}^{\alpha}\ Cos\left(\alpha \arg(i\omega_{22})\right) + 6\beta_{44}\ a_4{}^2}{4\omega_{22}} \pm \frac{1}{a_4}\sqrt{\left(f_{22}\ q_0\right)^2 - \left(2\,\tilde{C}\ \omega_{22} a_4\right)^2 - 8\tilde{k}\ \tilde{C}\ a_4{}^2\ \omega_{22}{}^{\alpha+1}\,\mathrm{Sin}\left(\alpha \arg(i\omega_{22})\right) - \left(2\tilde{k}\ a_4\ \omega_{22}{}^{\alpha}\right)^2 + 2\tilde{k}^2\ a_4{}^2\ \omega_{22}{}^{2\alpha}\ Cos\left(2\alpha \arg(i\omega_{22})\right)} \tag{5-54}$$

5. 5. Results and Discussions

Forced vibration analysis of the plate with fractional derivative subjected to a harmonic excitation is studied numerically. Based on the frequency responses derived

analytically in the previous section as Eqs. (5-51)-(5-54), the numerical amplitude-frequency figures are plotted and explained for different values of the parameters of the system.

5.5.1. Effect of Fractional Derivation Order, α

The frequency responses of the first four modes of vibration for various values of the fractional derivative order are illustrated in **Figure 5-1** to **Figure 5-4**. The damping effect of the fractional order clearly follows the previous results obtained for the free vibration of the system, i.e., as the magnitude of parameter α increases, the system damping becomes stronger. Also, it can be seen that as the order of the fractional derivative increases from $\alpha = 0.1$ to $\alpha = 0.9$, the maximum amplitude of the frequency response decreases and hence, the nonlinear behavior of the system changes from the nonlinear hardening to linear one.

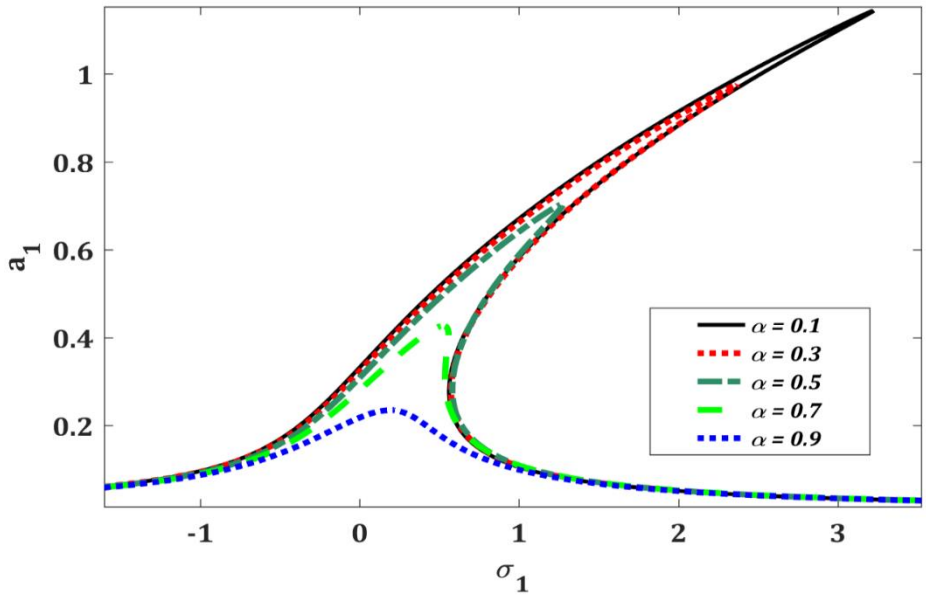

Figure 5-1- Frequency response of first mode for different values of α

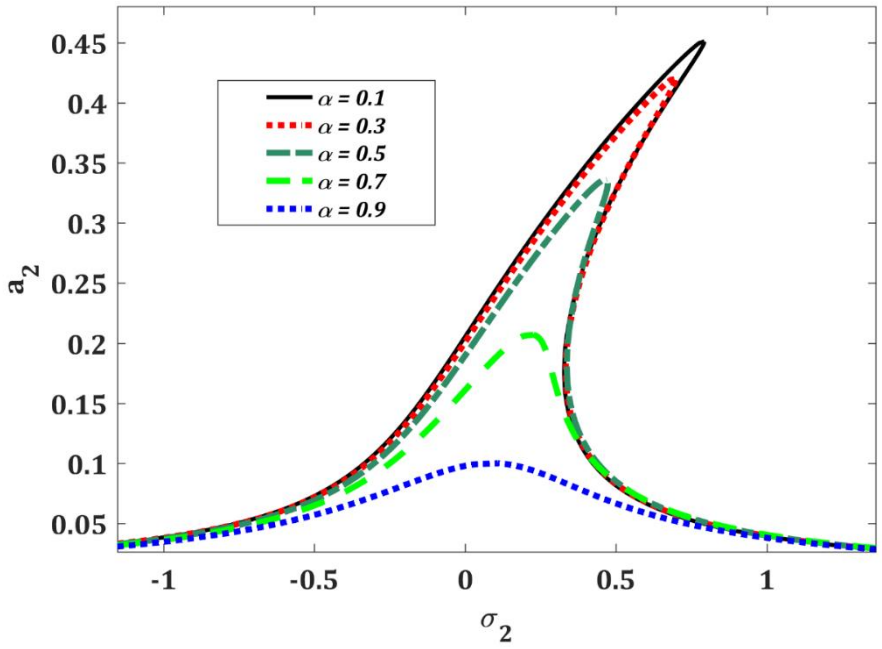

Figure 5-2- Frequency response of second mode for different values of α

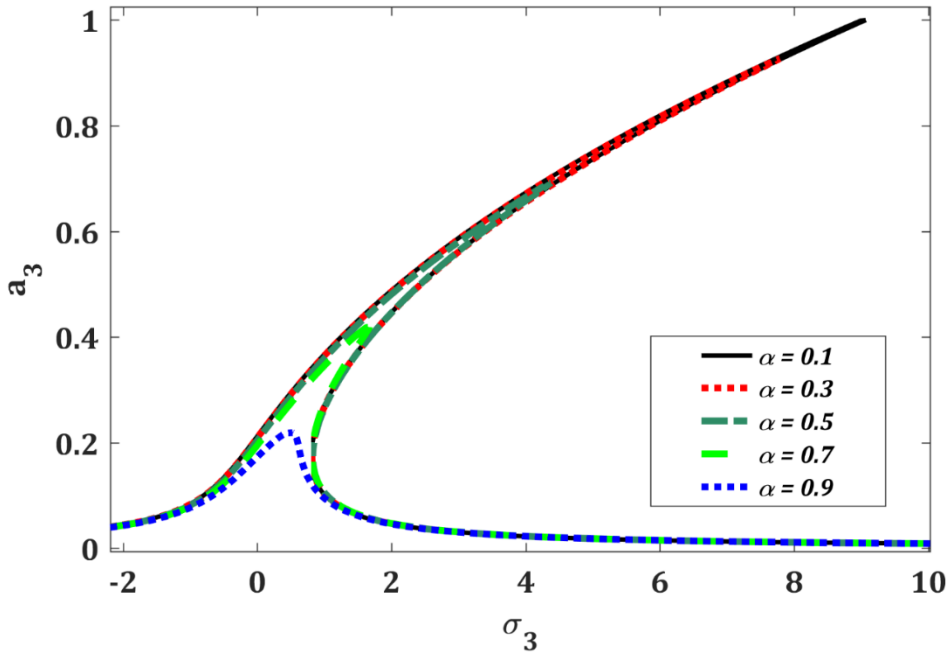

Figure 5-3- Frequency response of third mode for different values of α

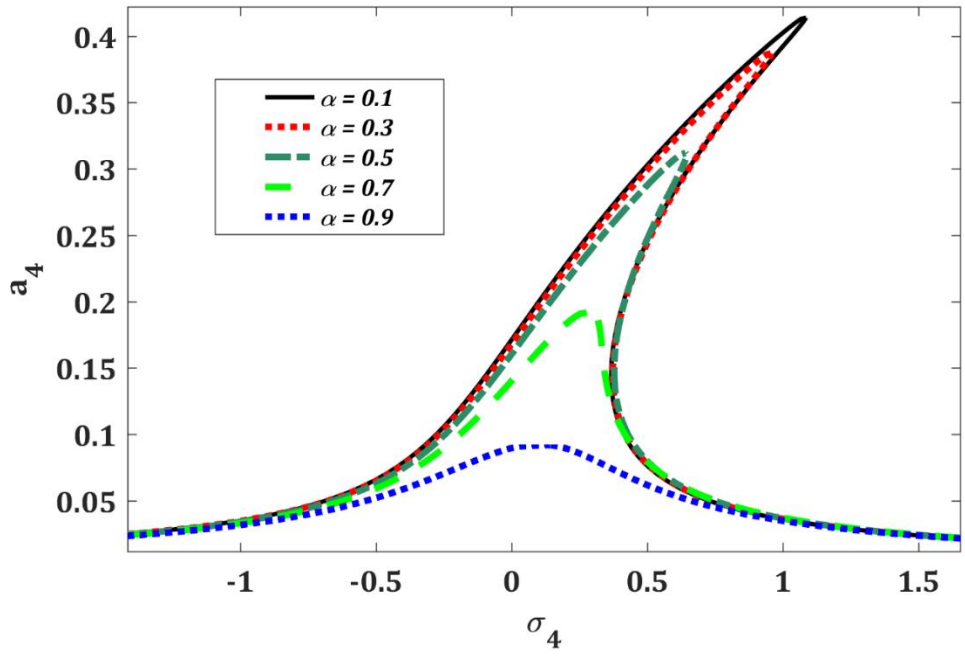

Figure 5-4- Frequency response of fourth mode for different values of α

By comparing the frequency responses, obtained for each mode of the system, it can be found that the third mode of the system has the strongest hardening nonlinearity behavior and the fourth mode has the weakest hardening behavior among the four modes of the system.

5.5.2. Effect of Fractional Derivative Coefficient, k

Nonlinear vibration behavior of the plate under influence of different values of the fractional derivative coefficient and various orders of the fractional derivative has been investigated in this section.

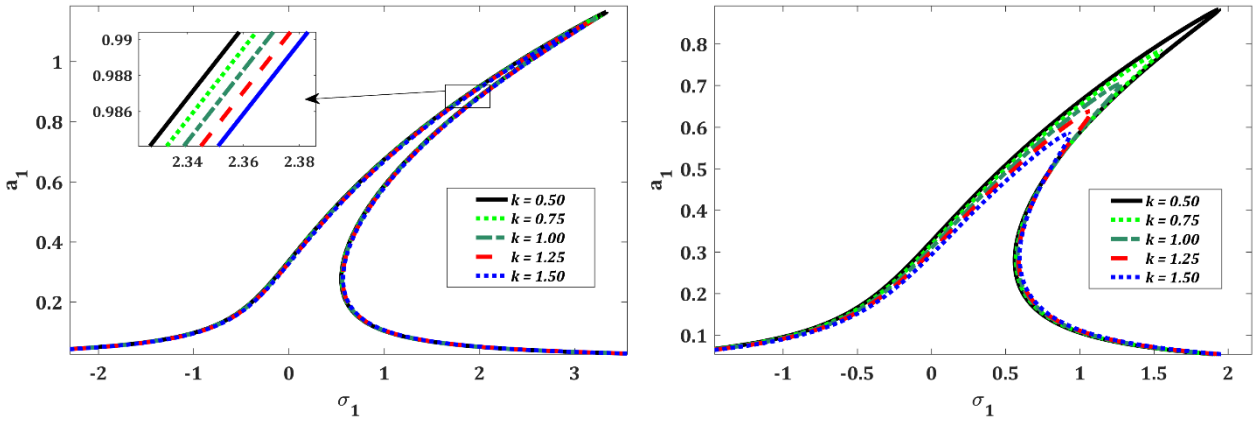

(a)

(b)

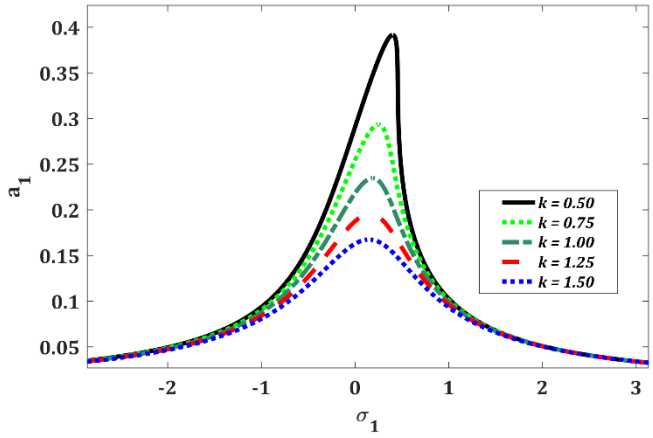

(c)

Figure 5-5- Vibration behavior of the first mode for different values of k : (a) $\alpha = 0.1$, (b) $\alpha = 0.5$, and (c) $\alpha = 0.9$

Figure 5-5 represents the frequency response of the first mode for three different values of α. As can be seen from each subfigure the value of k varies from $k = 0.50$ to $k = 1.50$, and as this value increases, the damping effect of the fractional derivative will increase. By comparing these three subfigures, it can be concluded that the system with smaller values of α has a higher nonlinear hardening behavior and as α increases,

the vibration behavior of the system changes from hardening nonlinear into linear ones.

Similar nonlinear behavior has been observed for the three other natural modes of the system, which are presented in **Figure 5-6** to **Figure 5-8**. It can be seen that all four modes of vibration have nonlinear hardening behavior for small values of α, but the strength of this hardening nonlinearity varies for each mode.

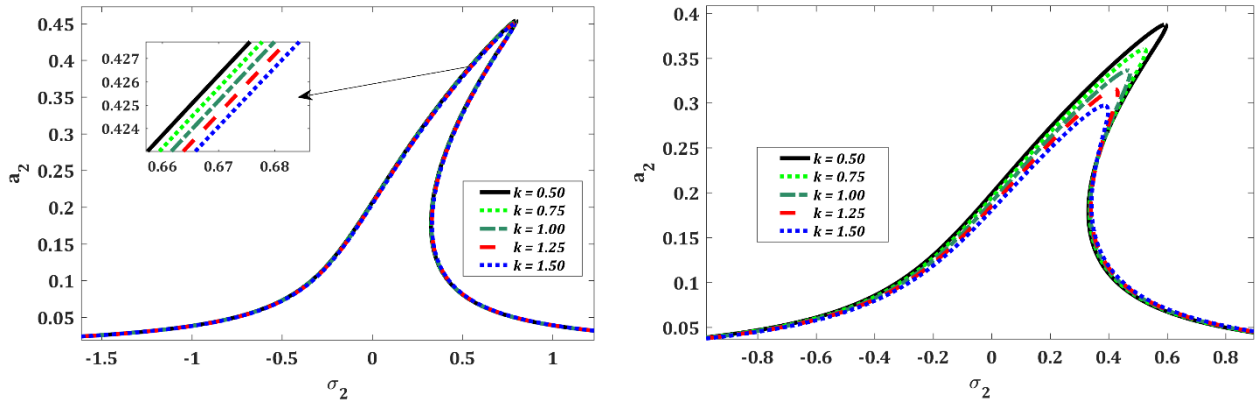

(a) (b)

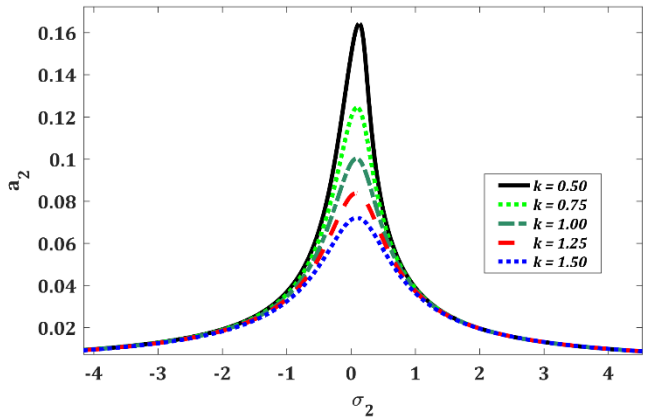

(c)

Figure 5-6- Vibration behavior of second mode for different values of k : (a) $\alpha = 0.1$, (b) $\alpha = 0.5$, and (c) $\alpha = 0.9$

Another important point that should be mentioned is about the influence of k on the nonlinearity of the system. Whenever the value of α approaches to the highest limit of 1, ($0 < \alpha < 1$) the effect of the parameter k becomes stronger for all four modes of vibration.

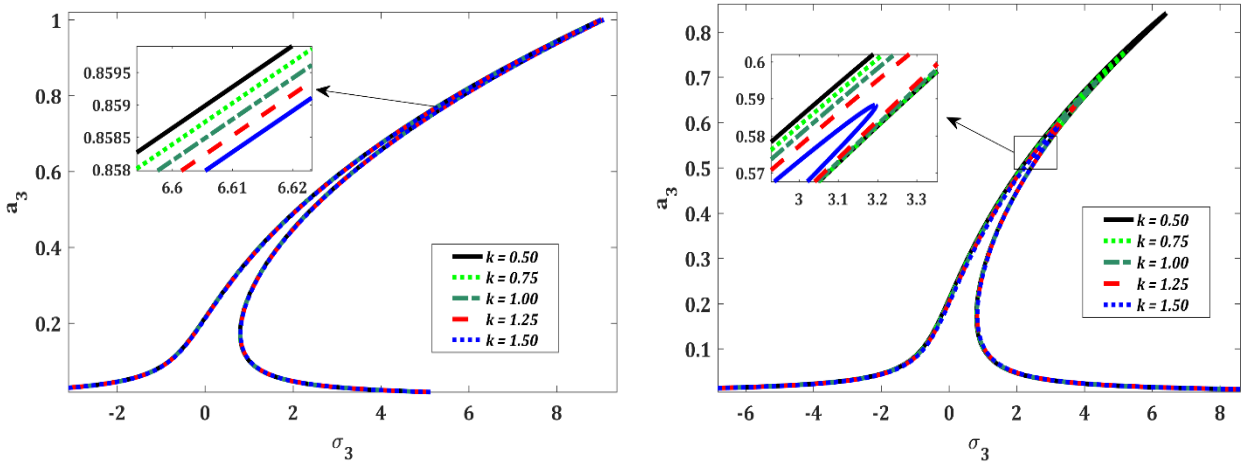

(a) (b)

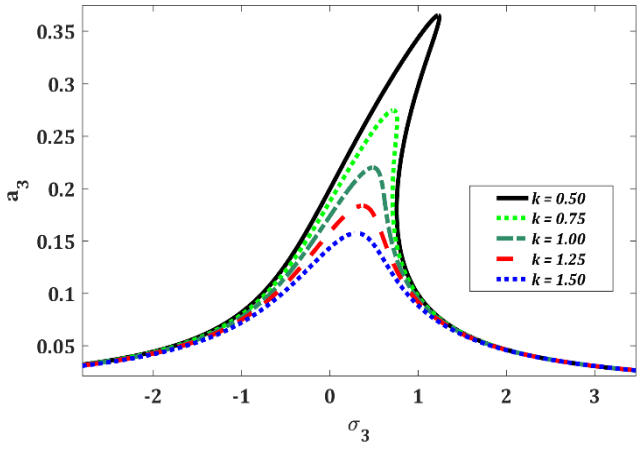

(c)

Figure 5-7- Vibration behavior of the third mode for different values of k : (a) $\alpha = 0.1$, (b) $\alpha = 0.5$, and (c) $\alpha = 0.9$

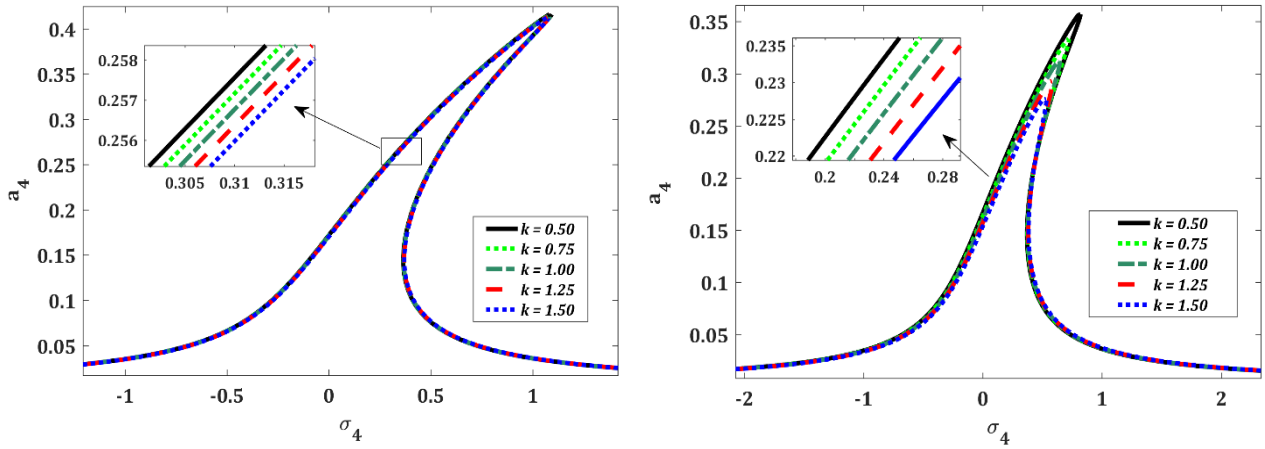

(a)

(b)

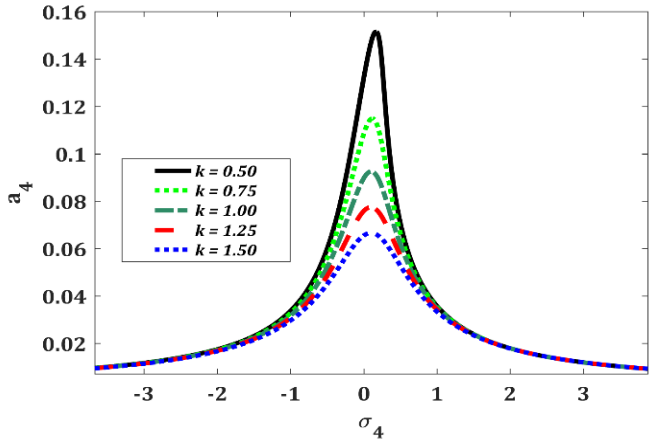

(c)

Figure 5-8- Vibration behavior of the fourth mode for different values of k : (a) $\alpha = 0.1$, (b) $\alpha = 0.5$, and (c) $\alpha = 0.9$

5.5.3. Effect of Aspect Ratio, r

In order to investigate the effect of the geometry of the plate on the vibration behavior of the system, the aspect ratio $r = {}^{a}/_{b}$ has been studied in this part. Three different values have been assumed for r and the results have been obtained for various values of α.

(a)

(b)

(c)

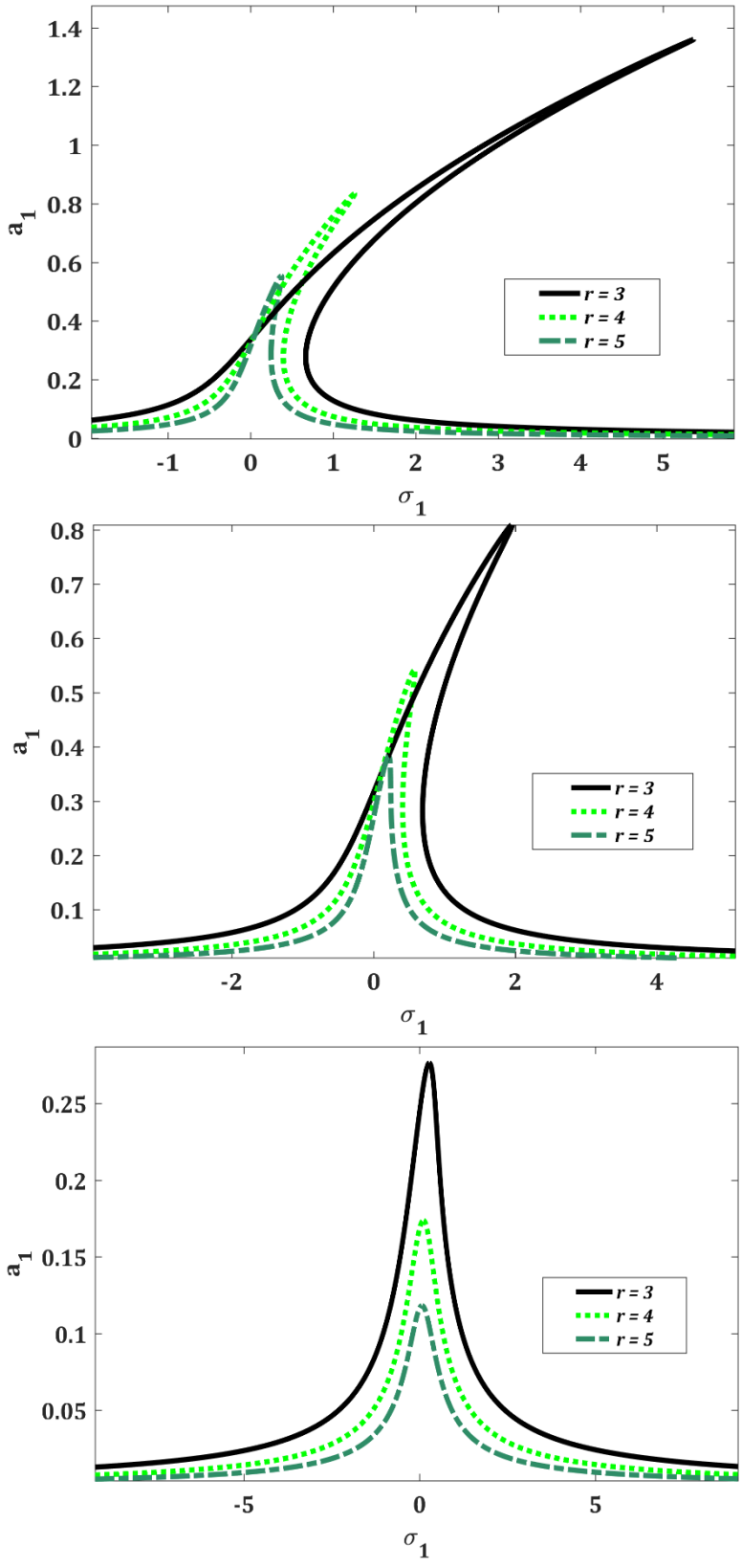

Figure 5-9- Vibration behavior of first mode for different aspect ratios under conditions of: (a) $\alpha = 0.1$, (b) $\alpha = 0.5$, and (c) $\alpha = 0.9$

Figure 5-9 illustrates the simultaneous effect of r and α on the frequency response of the first natural mode of the system. It was shown in Section 4.4.2 that as the aspect ratio increases, the natural frequency of the system would increase. **Figure 5-9** shows that as the aspect ratio increases, the system nonlinearity changes from the nonlinear hardening behavior to the linear ones and also, the maximum amplitude for each curve decreases. Similar to the previous observations, the parameter α increases the damping efficiency, but this effect does not have any specific influence on the outcome of having different values of aspect ratio. The same investigation have been repeated for the mode one-two, two-one, and two-two and similar behavior has been observed. The obtained results for other three modes of vibration of the system are included in Appendix B as **Figure B-4** to **Figure B-6**.

5.5.4. Effect of Elasticity Ratio

Elasticity ratio is defined as the non-dimensional parameter E_x/E_y that will be investigated in this section. **Figure 5-10** illustrates that any changes in the elasticity ratio will affect the frequency response of the system. In Section 4.4.3, the influence of this parameter on the free vibration of the system and also on the natural frequencies were studied and the exact numerical results were presented in **Table 4-3**. In the case of nonlinear forced vibration, it is observed that any increase in the elasticity ratio has an inverse effect on both the natural frequencies and the nonlinear hardening behavior of the system and will decrease these parameters. On the other hand, as the elasticity ratio increases, the maximum amplitude of the amplitude-frequency curves will increase to its higher values.

(a)

(b)

(c)

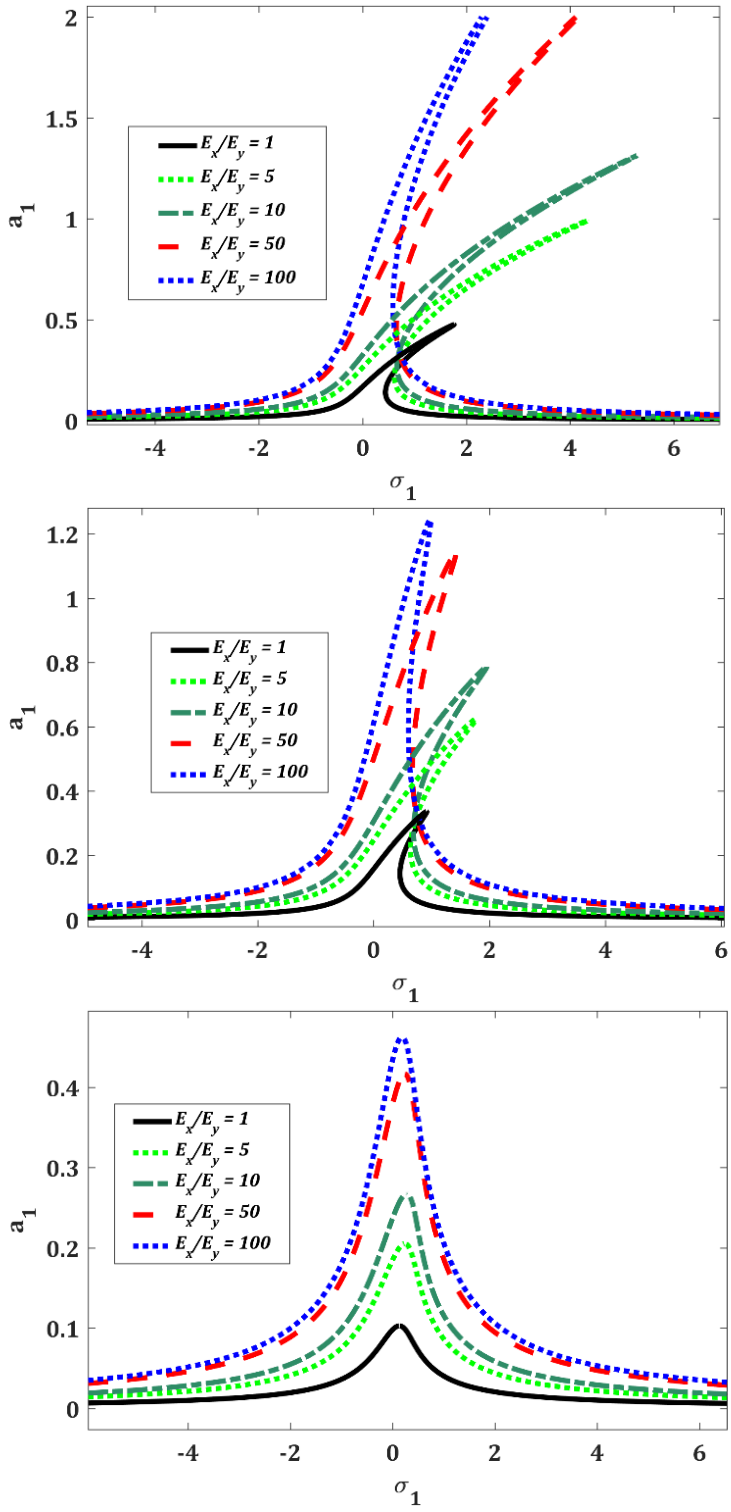

Figure 5-10- Frequency response of first mode for different elasticity ratios under conditions of: (a) $\alpha = 0.1$, (b) $\alpha = 0.5$, and (c) $\alpha = 0.9$

All the conclusions mentioned above for the first vibration mode can be seen in the vibration behavior of other three vibration modes of the system. For further investigations on the three other modes, one could examine the available figures included in Appendix B as **Figure B-7** to **Figure B-9**.

Chapter 6 - Conclusion

6. 1. Conclusion Remarks

The overall conclusions of this research work are presented in this section. Two methodologies chosen in this study were the variational iteration method for the nonlinear free vibration analysis and the multiple time-scales method for the nonlinear forced vibration, respectively. The von Kármán plate theory was applied to develop the partial differential equations of motion. The governing time-dependent ordinary differential equations for each mode of the system, based on the Galerkin procedure, was obtained. The fractional derivative in this investigation was defined based on the Caputo's fractional derivative definition.

The nonlinear free vibration analysis of the plate with the fractional viscoelasticity was studied and the variational iteration method for damped nonlinear free vibration was utilized to solve the time dependent nonlinear ordinary differential equations. The effect of the fractional derivative order was presented and found that as α increased, the system damping effect increased. It was observed that as the aspect ratio

increased, the natural frequencies of the system increased too. Comparing the effect of aspect ratio on different modes showed that aspect ratio does not affect the system damping. Results obtained for various elasticity ratio and fractional derivative order showed that as the elasticity ratio increased, the system frequencies will decrease.

The nonlinear forced vibration analysis of the plate with fractional viscoelasticity under excitation of a harmonic force was investigated. The method of multiple time-scales was applied to derive the amplitude-frequency relationships for each mode of the system, analytically. The effect of various values of α on the frequency responses were presented and it was concluded that as the fractional derivative order increased, the system damping increased and changed the system nonlinearity from a nonlinear hardening into a linear behavior.

The parametric studies performed on the primary resonances showed the effects of fractional derivative coefficient, the aspect ratio, and the elasticity ratio on the frequency responses. Based on the obtained results, as the coefficient of fractional derivative increased, the system damping increased and therefore decreased the pick amplitudes of the amplitude-frequency curves. The parameter α intensifies the influence of parameter k and therefore, maximum damping effect could be seen at the frequency response curves with highest values of k and α. Parametric study showed that as aspect ratio (r) increases, the maximum amplitude would decrease and hence, the system behavior will change from a strong nonlinear hardening to a weak nonlinear one with smaller amplitude. Also, it could be seen that although increasing the value of α amplified the damping effect, but the effect of aspect ratio on the system

behavior remained unchanged. The elasticity ratio was another parameter under investigation. It was found that as the elasticity ratio increased, the natural frequency will decrease and as a result, the frequency response of the system will change from a nonlinear hardening to a linear behavior.

Numerical results confirmed the sensitivity of vibration behavior to the fractional derivative order, and from a design point of view, any types of resonance or undesired vibration behavior can be avoided by choosing an optimum value of fractional derivative order.

6. 2. Suggestions for Future Research

Although fractional calculus has the same history as classic calculus, but applications of this concept in different engineering fields and modeling simulation are a new topic. Nevertheless, the exact physical meaning of fractional derivatives is still quite an open question for many real-world problems. For future research work, specifically in vibration analysis of plates with fractional viscoelastic properties, following topics are suggested:

1. Different type of plates such as triangular and circular with fractional viscoelastic properties and considering different boundary conditions can be investigated.

2. Studies can be done at the nano and micro scales by utilizing the fractional derivative properties in the NEMS (Nanoelectromechanical systems) and MEMS (Microelectromechanical systems) applications.
3. In solving nonlinear free vibration, based on the variational iteration method, the first iteration of the correction functional equation was considered. One could enhance the iteration formula analytically to the second or higher iterations.
4. The thermal effect has been neglected in this thesis. One could consider the effect of thermal variations on the viscoelastic behavior of the plate.

References

[1] Y. Xing and B. Liu, "New exact solutions for free vibrations of thin orthotropic rectangular plates," Composite Structures, vol. 89, pp. 567-574, 2009.

[2] J. R. Y. W. Chao, "Nonlinear oscillations of laminated, anisotropic rectangular plates," ASME J. appl. Mech, vol. 49, pp. 396-402, 1972.

[3] Y. A. Rossikhin and M. V. Shitikova, "Application of fractional calculus for analysis of nonlinear damped vibrations of suspension bridges," Journal of Engineering Mechanics, vol. 124, pp. 1029-1036, 1998.

[4] R. Szilard, "Theory and analysis of plates," 1974.

[5] L. Meirovitch, Elements of vibration analysis: McGraw-Hill, 1975.

[6] R. Bhat, "Natural frequencies of rectangular plates using characteristic orthogonal polynomials in Rayleigh-Ritz method," Journal of Sound and Vibration, vol. 102, pp. 493-499, 1985.

[7] C. A. Fletcher, "Computational galerkin methods," in Computational Galerkin Methods, ed: Springer, 1984, pp. 72-85.

[8] T. Wierzbicki and G. Nurick, "Large deformation of thin plates under localised impulsive loading," International Journal of Impact Engineering, vol. 18, pp. 899-918, 1996.

[9] M. Amabili, Nonlinear vibrations and stability of shells and plates: Cambridge University Press, 2008.

[10] A. C. Ugural, Stresses in beams, plates, and shells: CRC Press, 2009.

[11] E. Car, S. Oller, and E. Oñate, "A large strain plasticity model for anisotropic materials—composite material application," International Journal of Plasticity, vol. 17, pp. 1437-1463, 2001.

[12] R. L. Bagley and J. TORVIK, "Fractional calculus-a different approach to the analysis of viscoelastically damped structures," AIAA journal, vol. 21, pp. 741-748, 1983.

[13] Z. Odibat and S. Momani, "Numerical methods for nonlinear partial differential equations of fractional order," Applied Mathematical Modelling, vol. 32, pp. 28-39, 2008.

[14] K. Oldham and J. Spanier, The fractional calculus theory and applications of differentiation and integration to arbitrary order vol. 111: Elsevier, 1974.

[15] S. G. Samko, A. A. Kilbas, and O. I. Marichev, "Fractional integrals and derivatives," Theory and Applications, Gordon and Breach, Yverdon, vol. 1993, 1993.

[16] Z. Odibat and S. Momani, "Application of variational iteration method to nonlinear differential equations of fractional order," International Journal of Nonlinear Sciences and Numerical Simulation, vol. 7, pp. 27-34, 2006.

[17] J.-H. He and X.-H. Wu, "Variational iteration method: new development and applications," Computers & Mathematics with Applications, vol. 54, pp. 881-894, 2007.

[18] J.-H. He, "Variational iteration method for autonomous ordinary differential systems," Applied Mathematics and Computation, vol. 114, pp. 115-123, 2000.

[19] J. He, "A new approach to nonlinear partial differential equations," Communications in Nonlinear Science and Numerical Simulation, vol. 2, pp. 230-235, 1997.

[20] J. He, "Variational iteration method for delay differential equations," Communications in Nonlinear Science and Numerical Simulation, vol. 2, pp. 235-236, 1997.

[21] J.-H. He, "Variational iteration method–a kind of non-linear analytical technique: some examples," International journal of non-linear mechanics, vol. 34, pp. 699-708, 1999.

[22] A. H. Nayfeh and D. T. Mook, Nonlinear oscillations: John Wiley & Sons, 2008.

[23] M. Sadri and D. Younesian, "Nonlinear harmonic vibration analysis of a plate-cavity system," Nonlinear Dynamics, vol. 74, pp. 1267-1279, 2013.

[24] M. Sadri and D. Younesian, "Nonlinear free vibration analysis of a plate-cavity system," Thin-Walled Structures, vol. 74, pp. 191-200, 2014.

[25] J. Nowinski and I. A. Ismail, "Large oscillations of an anisotropic triangular plate," Journal of the Franklin Institute, vol. 280, pp. 417-424, 1965.

[26] H. Askari, Z. Saadatnia, E. Esmailzadeh, and D. Younesian, "Multi-frequency excitation of stiffened triangular plates for large amplitude oscillations," Journal of Sound and Vibration, vol. 333, pp. 5817-5835, 2014.

[27] W. N. Findley and F. A. Davis, Creep and relaxation of nonlinear viscoelastic materials: Courier Corporation, 2013.

[28] R. M. Jones, Mechanics of composite materials: CRC press, 1998.

[29] J. Woo and S. Meguid, "Nonlinear analysis of functionally graded plates and shallow shells," International Journal of Solids and structures, vol. 38, pp. 7409-7421, 2001.

[30] J.-S. Park, J.-H. Kim, and S.-H. Moon, "Vibration of thermally post-buckled composite plates embedded with shape memory alloy fibers," Composite Structures, vol. 63, pp. 179-188, 2004.

[31] Z.-X. Wang and H.-S. Shen, "Nonlinear vibration of nanotube-reinforced composite plates in thermal environments," Computational Materials Science, vol. 50, pp. 2319-2330, 2011.

[32] W. Chen, K. Y. Lee, and H. Ding, "On free vibration of non-homogeneous transversely isotropic magneto-electro-elastic plates," Journal of Sound and Vibration, vol. 279, pp. 237-251, 2005.

[33] G.-c. Wu and E. Lee, "Fractional variational iteration method and its application," Physics Letters A, vol. 374, pp. 2506-2509, 2010.

[34] J.-H. He, "A short remark on fractional variational iteration method," Physics Letters A, vol. 375, pp. 3362-3364, 2011.

[35] S. Das, "Solution of fractional vibration equation by the variational iteration method and modified decomposition method," International Journal of Nonlinear Sciences and Numerical Simulation, vol. 9, pp. 361-366, 2008.

[36] H. Yaghoobi and M. Torabi, "An analytical approach to large amplitude vibration and post-buckling of functionally graded beams rest on non-linear elastic foundation," Journal of Theoretical and Applied Mechanics, vol. 51, pp. 39-52, 2013.

[37] M. Ansari, E. Esmailzadeh, and D. Younesian, "Internal-external resonance of beams on non-linear viscoelastic foundation traversed by moving load," Nonlinear Dynamics, vol. 61, pp. 163-182, 2010.

[38] P. Joshi, N. Jain, and G. Ramtekkar, "Analytical modeling for vibration analysis of thin rectangular orthotropic/functionally graded plates with an internal crack," Journal of Sound and Vibration, vol. 344, pp. 377-398, 2015.

[39] H. Askari, E. Esmailzadeh, and A. Barari, "A unified approach for nonlinear vibration analysis of curved structures using non-uniform rational B-spline representation," Journal of Sound and Vibration, vol. 353, pp. 292-307, 2015.

[40] Y. A. Rossikhin and M. Shitikova, "Analysis of free non-linear vibrations of a viscoelastic plate under the conditions of different internal resonances," International Journal of Non-Linear Mechanics, vol. 41, pp. 313-325, 2006.

[41] Y. Rossikhin and M. Shitikova, "Nonlinear dynamic response of a thin plate in a fractional viscoelastic medium under internal resonance 1: 1: 2," in Applied Mechanics and Materials, 2014, pp. 60-65.

[42] Y. A. Rossikhin and M. V. Shitikova, "A new approach for studying nonlinear dynamic response of a thin fractionally damped plate with 2: 1 and 2: 1: 1 internal resonances," in Shell and Membrane Theories in Mechanics and Biology, ed: Springer, 2015, pp. 267-288.

[43] M. Du, Z. Wang, and H. Hu, "Measuring memory with the order of fractional derivative," Scientific reports, vol. 3, 2013.

[44] H. F. Brinson and L. C. Brinson, Polymer engineering science and viscoelasticity: Springer, 2008.

[45] C. Zhang, Viscoelastic fracture mechanics: Science Press, 2006.

[46] B. Carmichael, H. Babahosseini, S. Mahmoodi, and M. Agah, "The fractional viscoelastic response of human breast tissue cells," Physical biology, vol. 12, p. 046001, 2015.

[47] F. Meral, T. Royston, and R. Magin, "Fractional calculus in viscoelasticity: an experimental study," Communications in Nonlinear Science and Numerical Simulation, vol. 15, pp. 939-945, 2010.

[48] S. Kaul, "Influence of Fractional Damping and Time Delay on Maxwell-Voigt Model for Vibration Isolation," in ASME 2016 International Mechanical Engineering Congress and Exposition, 2016, pp. V04BT05A061-V04BT05A061.

[49] J. L. Horbach, R. Ikehata, and R. C. Charão, "Optimal decay rates and asymptotic profile for the plate equation with structural damping," Journal of Mathematical Analysis and Applications, vol. 440, pp. 529-560, 2016.

[50] P. Litewka and R. Lewandowski, "Steady-state non-linear vibrations of plates using Zener material model with fractional derivative," Computational Mechanics, pp. 1-22, 2017.

Appendix A

Coefficients of the Ordinary Differential Equations as Eqs. (3-39)-(3-42) are reported in appendix A as Eqs. (A-1)-(A-28) as follow:

$$\omega_{11} = \pi^2 \sqrt{1 + 2\,\alpha_1\, r^2 + \bar{\bar{E}}\, r^4}\,, \tag{A-1}$$

$$\omega_{12} = \pi^2 \sqrt{1 + 8\,\alpha_1\, r^2 + 16\bar{\bar{E}}\, r^4}\,, \tag{A-2}$$

$$\omega_{21} = \pi^2 \sqrt{16 + 8\,\alpha_1\, r^2 + \bar{\bar{E}}\, r^4}\,, \tag{A-3}$$

$$\omega_{22} = 2\,\pi^2 \sqrt{1 + 2\,\alpha_1\, r^2 + \bar{\bar{E}}\, r^4}\,, \tag{A-4}$$

$$\beta_{11} = \frac{512\,\alpha_3\,\bar{\bar{E}}\, r^4}{9\left(\bar{\bar{E}} + \bar{\bar{E}}\,\alpha_2 + r^4\right)}, \tag{A-5}$$

$$\beta_{12} = \frac{2084\,\alpha_3\,\bar{\bar{E}}\,r^4\left(\left(31+36\,\alpha_2\right)\bar{\bar{E}}+56\,r^4\right)}{25\left(\bar{\bar{E}}+\bar{\bar{E}}\,\alpha_2+r^4\right)\left(\bar{\bar{E}}+4\bar{\bar{E}}\,\alpha_2+16\,r^4\right)}, \tag{A-6}$$

$$\beta_{13} = \frac{2084\,\alpha_3\,\bar{\bar{E}}\,r^4\left(4\bar{\bar{E}}\left(22+7\,\alpha_2\right)+13\,r^4\right)}{75\left(\bar{\bar{E}}+\bar{\bar{E}}\,\alpha_2+r^4\right)\left(16\,\bar{\bar{E}}+4\bar{\bar{E}}\,\alpha_2+r^4\right)}, \tag{A-7}$$

$$\beta_{14} = \frac{57344\,\alpha_3\,\bar{\bar{E}}\,r^4}{225\left(\bar{\bar{E}}+\bar{\bar{E}}\,\alpha_2+r^4\right)}, \tag{A-8}$$

$$\beta_{15} = \frac{180224\,\alpha_3\,\bar{\bar{E}}\,r^4}{1125}\left(\begin{array}{l}\dfrac{1}{\bar{\bar{E}}+\bar{\bar{E}}\,\alpha_2+r^4}+\dfrac{4}{16\bar{\bar{E}}+4\bar{\bar{E}}\,\alpha_2+r^4}\\ +\dfrac{44}{\bar{\bar{E}}+4\bar{\bar{E}}\,\alpha_2+16\,r^4}\end{array}\right), \tag{A-9}$$

$$f_{11} = 4\,Sin(\pi X_0)\,Sin(\pi Y_0) \tag{A-10}$$

$$\beta_{21} = \frac{2084\,\alpha_3\,\bar{\bar{E}}\,r^4\left(\bar{\bar{E}}\left(3+4\,\alpha_2\right)+8\,r^4\right)}{5\left(\bar{\bar{E}}+\bar{\bar{E}}\,\alpha_2+r^4\right)\left(\bar{\bar{E}}+4\bar{\bar{E}}\,\alpha_2+16\,r^4\right)}, \tag{A-11}$$

$$\beta_{22} = \frac{8192\,\alpha_3\,\bar{\bar{E}}\,r^4}{25\left(\bar{\bar{E}}+\bar{\bar{E}}\,\alpha_2+r^4\right)}, \tag{A-12}$$

$$\beta_{23} = \frac{3825664\,\alpha_3\,\bar{\bar{E}}\,r^4}{5625\left(\bar{\bar{E}}+\bar{\bar{E}}\,\alpha_2+r^4\right)}, \tag{A-13}$$

$$\beta_{24} = \frac{32768\,\alpha_3\,\bar{\bar{E}}\,r^4\left(4\bar{\bar{E}}\left(122+47\,\alpha_2\right)+113\,r^4\right)}{1875\left(\bar{\bar{E}}+\bar{\bar{E}}\,\alpha_2+r^4\right)\left(16\,\bar{\bar{E}}+4\bar{\bar{E}}\,\alpha_2+r^4\right)}, \tag{A-14}$$

$$\beta_{25} = \frac{16384\,\alpha_3\,\bar{E}\,r^4}{1125}\left(\begin{array}{l}\dfrac{11}{\bar{E}+\bar{E}\,\alpha_2+r^4}+\dfrac{36}{16\bar{E}+4\bar{E}\,\alpha_2+r^4}\\ +\dfrac{220}{\bar{E}+4\bar{E}\,\alpha_2+16\,r^4}\end{array}\right), \tag{A-15}$$

$$f_{12} = 4\,Sin(\pi X_0)\,Sin(2\pi Y_0), \tag{A-16}$$

$$\beta_{31} = \frac{2084\,\alpha_3\,\bar{E}\,r^4\left(4\bar{E}\left(22+7\,\alpha_2\right)+13\,r^4\right)}{75\left(\bar{E}+\bar{E}\,\alpha_2+r^4\right)\left(16\bar{E}+4\bar{E}\,\alpha_2+r^4\right)}, \tag{A-17}$$

$$\beta_{32} = \frac{3825664\,\alpha_3\,\bar{E}\,r^4}{5625\left(\bar{E}+\bar{E}\,\alpha_2+r^4\right)}, \tag{A-18}$$

$$\beta_{33} = \frac{8192\,\alpha_3\,\bar{E}\,r^4}{25\left(\bar{E}+\bar{E}\,\alpha_2+r^4\right)}, \tag{A-19}$$

$$\beta_{34} = \frac{32768\,\alpha_3\,\bar{E}\,r^4}{5625}\left(\frac{75}{\bar{E}+\bar{E}\,\alpha_2+r^4}+\frac{1672}{\bar{E}+4\bar{E}\,\alpha_2+16\,r^4}\right), \tag{A-20}$$

$$\beta_{35} = \frac{16384\,\alpha_3\,\bar{E}\,r^4}{1125}\left(\begin{array}{l}\dfrac{11}{\bar{E}+\bar{E}\,\alpha_2+r^4}+\dfrac{44}{16\bar{E}+4\bar{E}\,\alpha_2+r^4}\\ +\dfrac{228}{\bar{E}+4\bar{E}\,\alpha_2+16\,r^4}\end{array}\right), \tag{A-21}$$

$$f_{21} = 4\,Sin(2\pi X_0)\,Sin(\pi Y_0), \tag{A-22}$$

$$\beta_{41} = \frac{57344\,\alpha_3\,\bar{E}\,r^4}{225\left(\bar{E}+\bar{E}\,\alpha_2+r^4\right)}, \tag{A-23}$$

$$\beta_{42} = \frac{32768\,\alpha_3\,\bar{E}\,r^4\left(4\bar{E}\left(122+47\,\alpha_2\right)+113\,r^4\right)}{1875\left(\bar{E}+\bar{E}\,\alpha_2+r^4\right)\left(16\bar{E}+4\bar{E}\,\alpha_2+r^4\right)}, \tag{A-24}$$

$$\beta_{43} = \frac{32768\,\alpha_3\,\bar{E}\,r^4}{5625}\left(\frac{75}{\bar{E}+\bar{E}\,\alpha_2+r^4}+\frac{1144}{\bar{E}+4\bar{E}\,\alpha_2+16\,r^4}\right), \tag{A-25}$$

$$\beta_{44} = \frac{131072\,\alpha_3\,\bar{E}\,r^4}{225\left(\bar{E}+\bar{E}\,\alpha_2+r^4\right)}, \tag{A-26}$$

$$\beta_{45} = \frac{16384\,\alpha_3\,\bar{E}\,r^4}{1125}\left(\begin{array}{l}\dfrac{11}{\bar{E}+\bar{E}\,\alpha_2+r^4}+\dfrac{36}{16\bar{E}+4\bar{E}\,\alpha_2+r^4}\\ +\dfrac{156}{\bar{E}+4\bar{E}\,\alpha_2+16\,r^4}\end{array}\right), \tag{A-27}$$

$$f_{22} = 4\,Sin(2\pi X_0)\,Sin(2\pi Y_0) \tag{A-28}$$

Appendix B

Time responses of the free vibration of modes one-two, two-one and two-two have been presented in appendix B. Effect of the elasticity ratio on the time response are shown as **Figure B-1** to **Figure B-3**.

Frequency responses of the second, third and fourth modes of the system under various aspect ratios and elasticity ratios are presented as **Figure B-4** to **Figure B-9**.

(a)

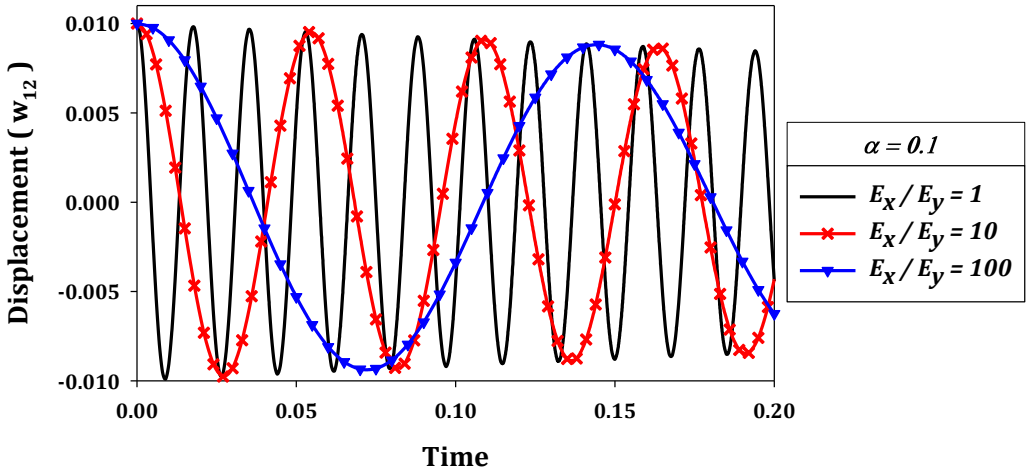

(b)

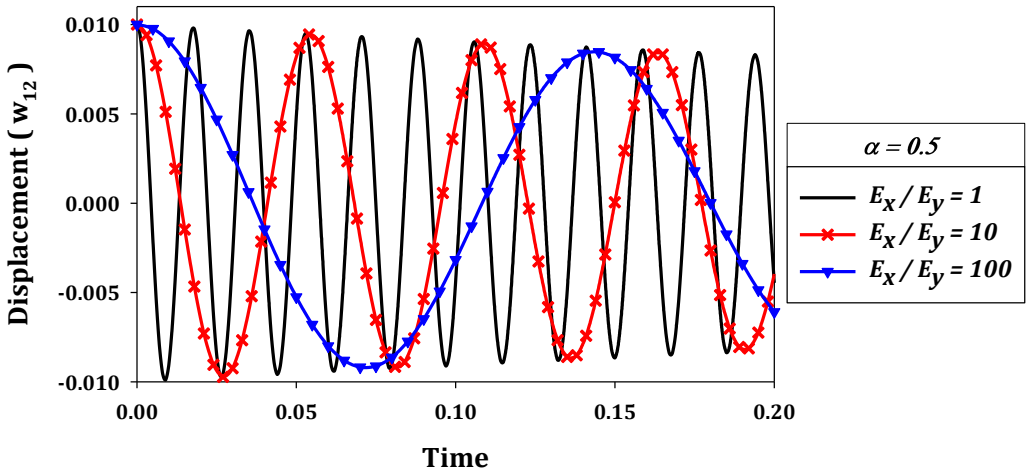

(c)

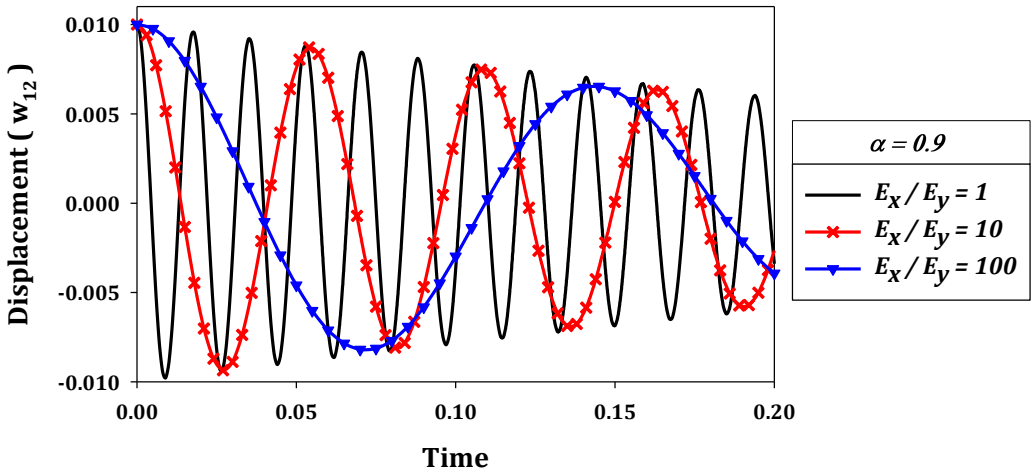

Figure B-1- Time responses of second mode for different elasticity ratios under conditions of: (a) $\alpha = 0.1$, (b) $\alpha = 0.5$, and (c) $\alpha = 0.9$

(a)

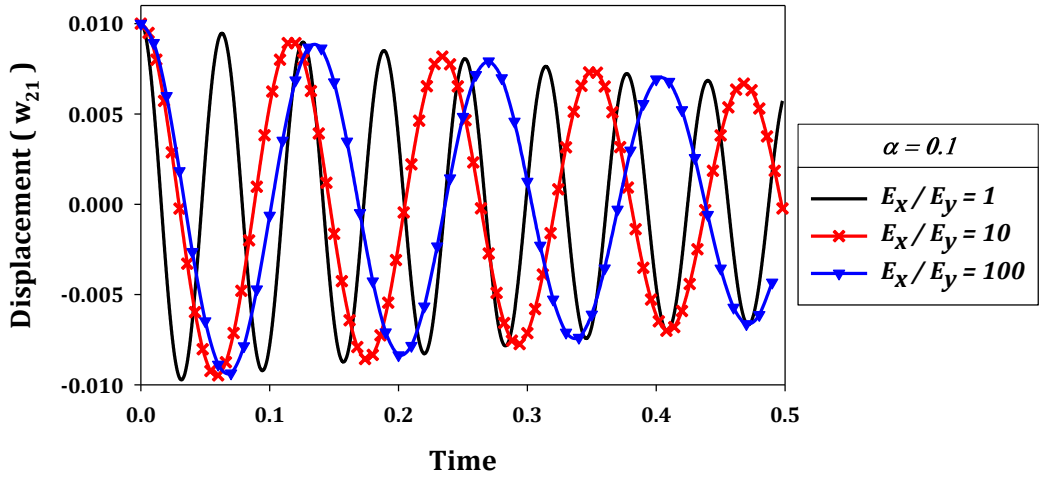

(b)

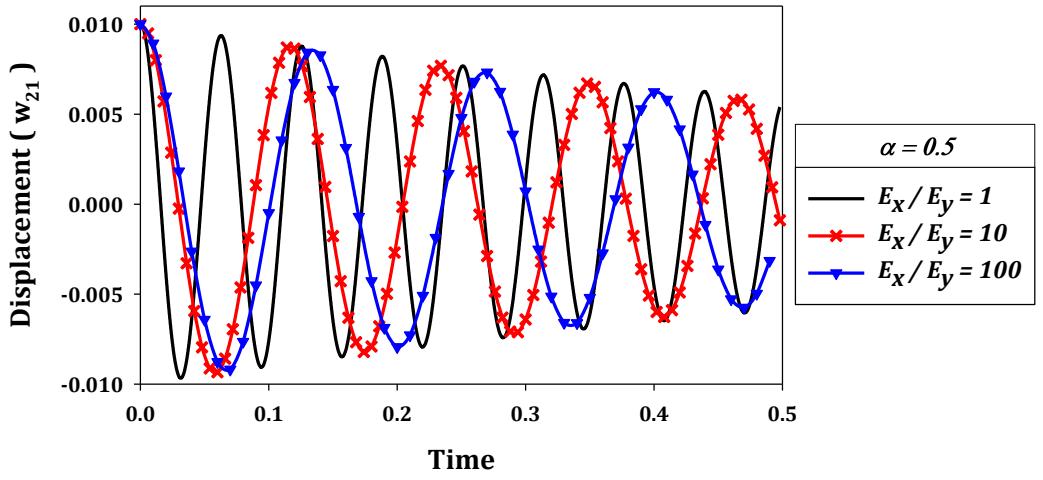

(c)

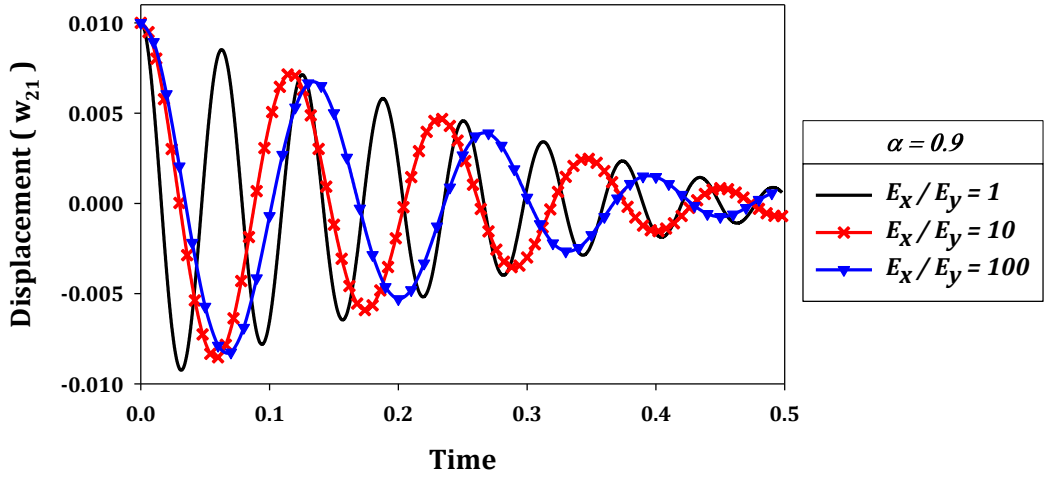

Figure B-2- Time responses of third mode for different elasticity ratios under conditions of: (a) $\alpha = 0.1$, (b) $\alpha = 0.5$, and (c) $\alpha = 0.9$

(a)

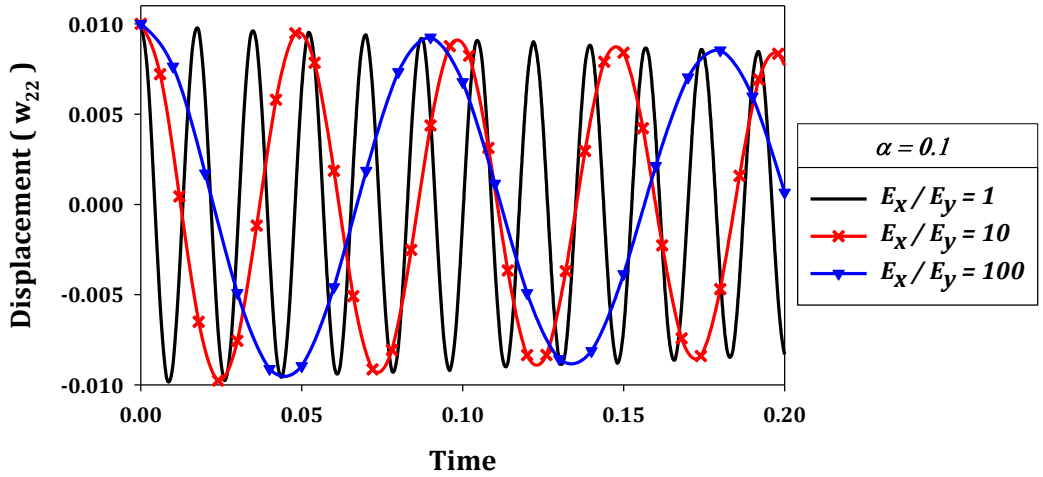

(b)

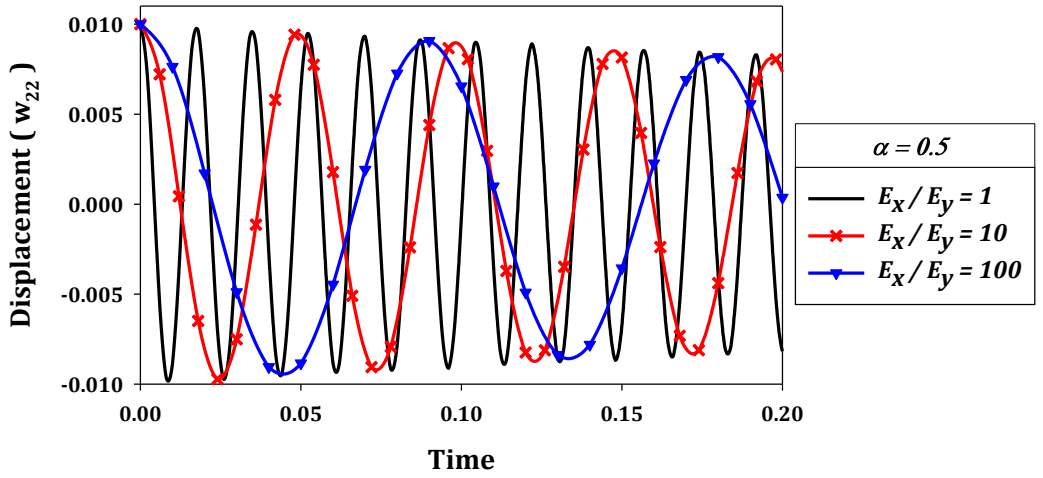

(c)

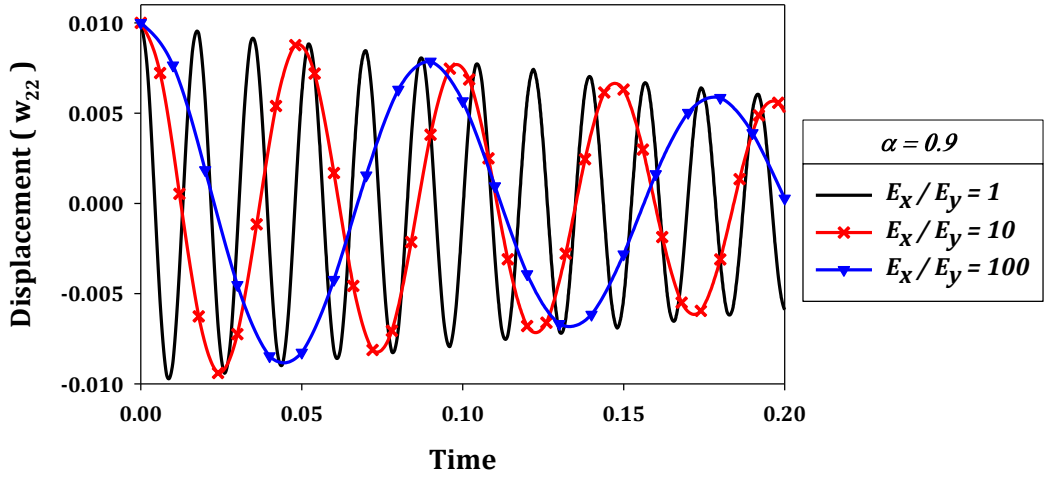

Figure B-3- Time responses of fourth mode for different elasticity ratios under conditions of: (a) $\alpha = 0.1$, (b) $\alpha = 0.5$, and (c) $\alpha = 0.9$

(a)

(b)

(c)

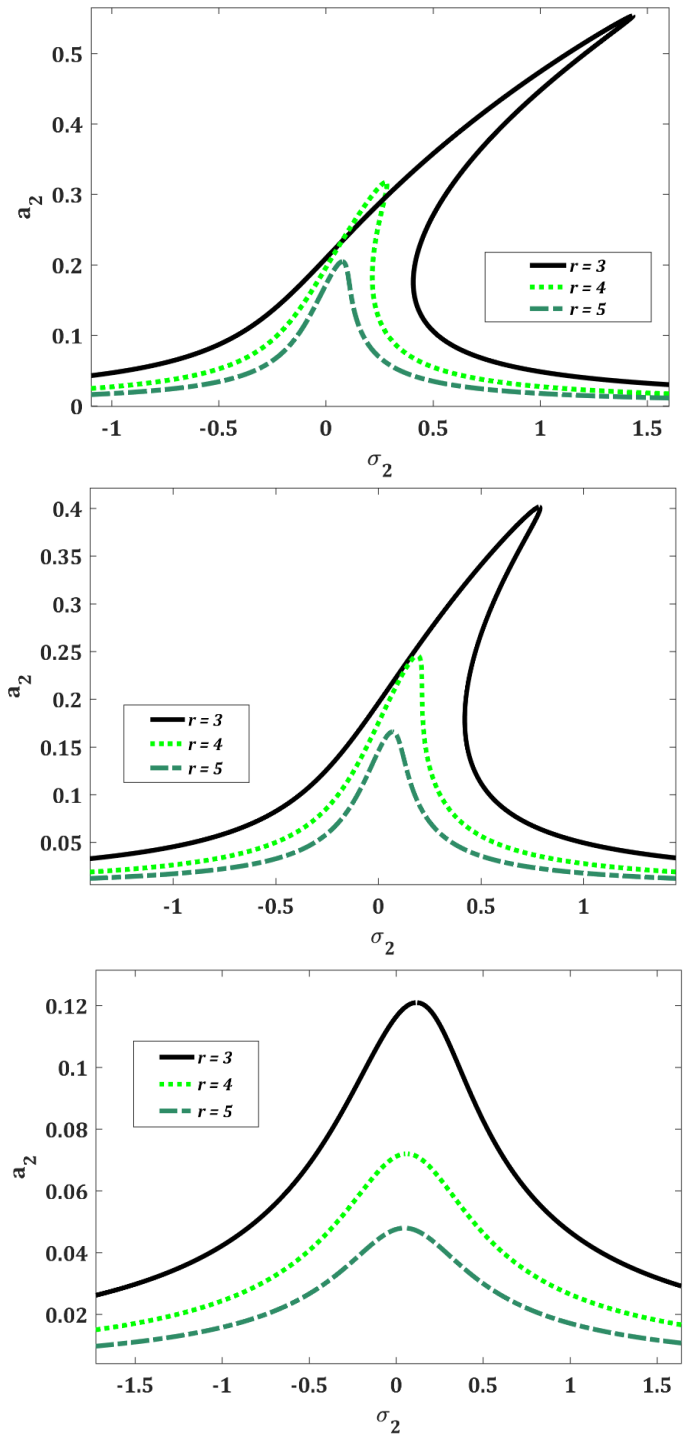

Figure B-4- Frequency response of second mode for different aspect ratios under conditions of: (a) $\alpha = 0.1$, (b) $\alpha = 0.5$, and (c) $\alpha = 0.9$

Frequency response of the third mode for different aspect ratios:

(a)

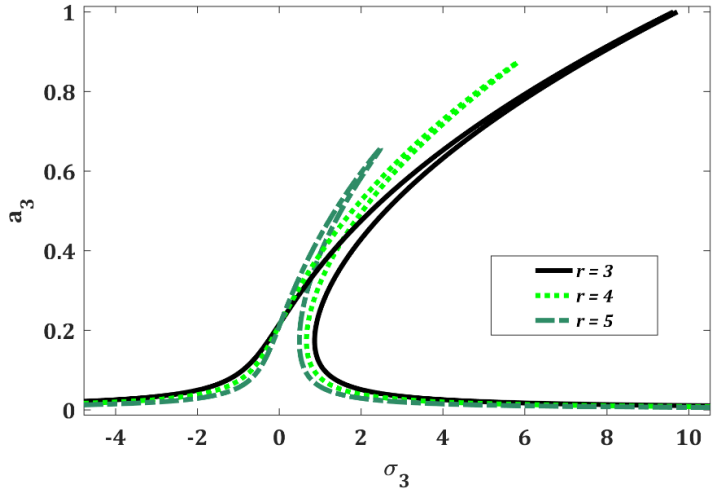

(b)

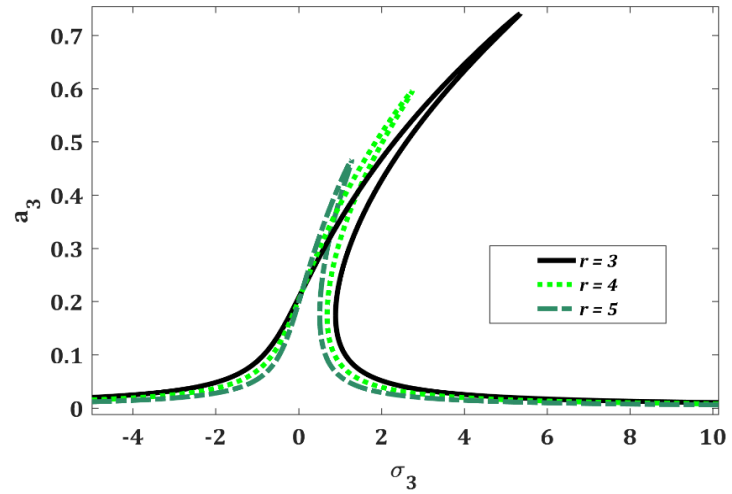

(c)

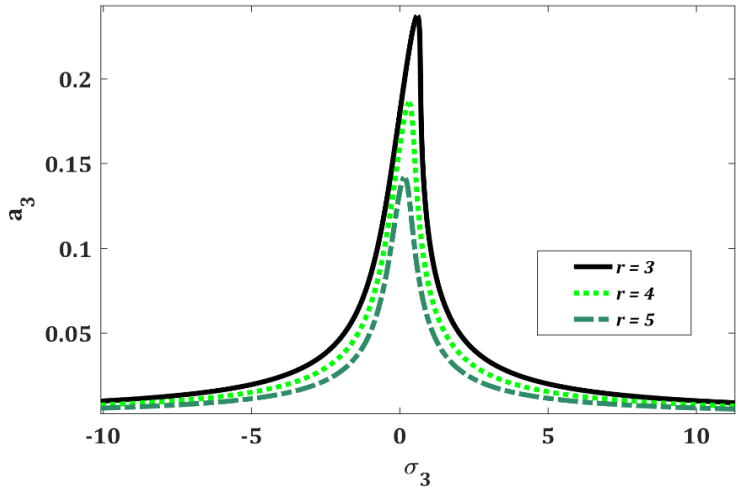

Figure B-5- Frequency response of third mode for different aspect ratios under conditions of: (a) $\alpha = 0.1$, (b) $\alpha = 0.5$, and (c) $\alpha = 0.9$

Frequency response of fourth mode for different aspect ratios:

(a)

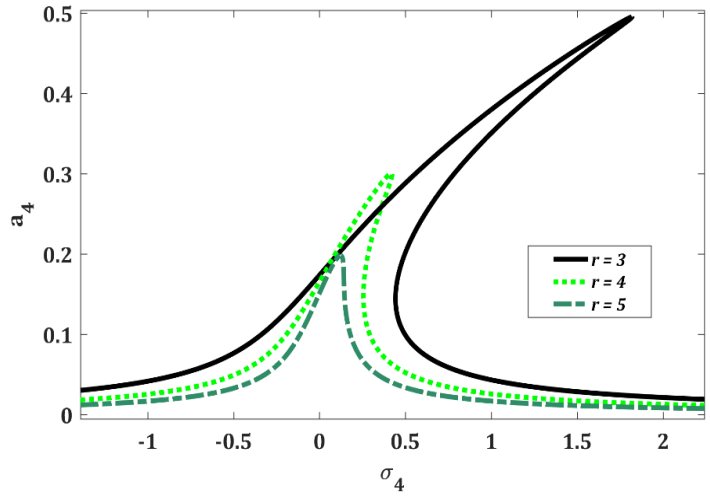

(b)

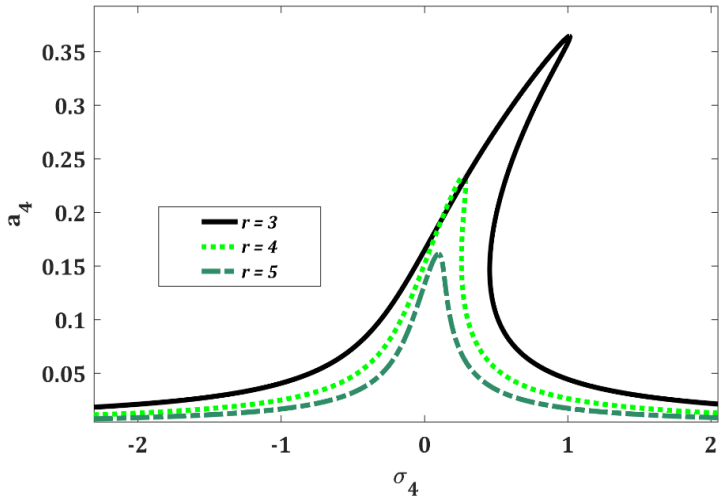

(c)

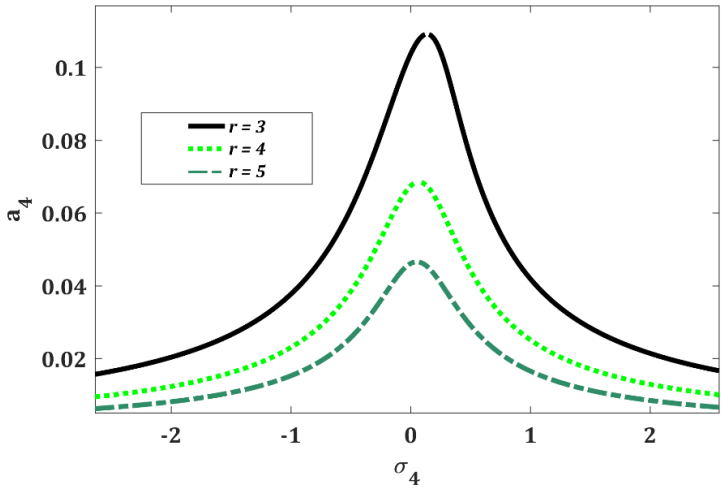

Figure B-6- Frequency response of fourth mode for different aspect ratios under conditions of: (a) $\alpha = 0.1$, (b) $\alpha = 0.5$, and (c) $\alpha = 0.9$

Frequency response of the second mode for different elasticity ratios:

(a)

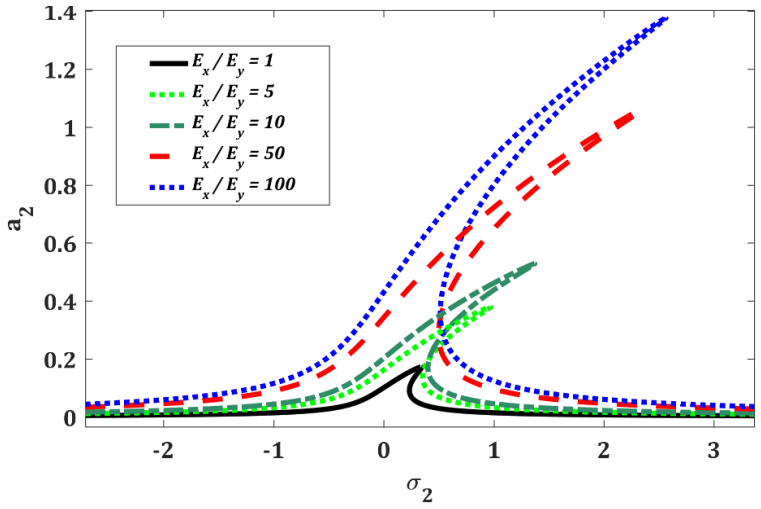

(b)

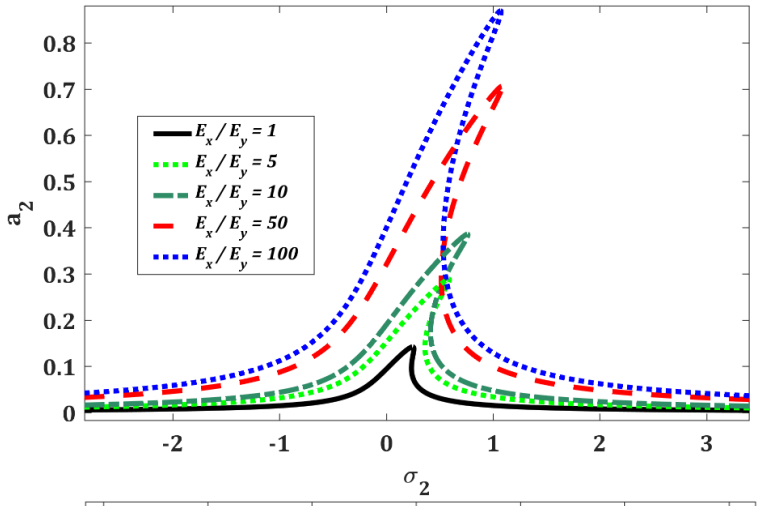

(c)

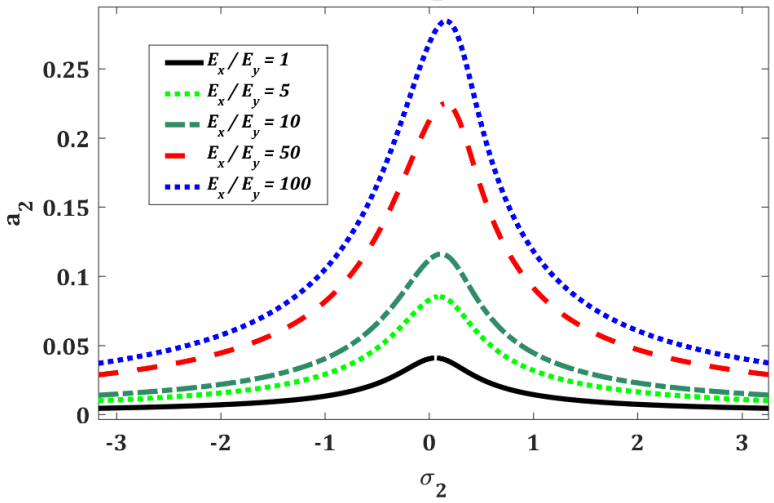

Figure B-7- Frequency response of second mode for different elasticity ratios under conditions of: (a) $\alpha = 0.1$, (b) $\alpha = 0.5$, and (c) $\alpha = 0.9$

Frequency response of the third mode for different elasticity ratios:

(a)

(b)

(c)

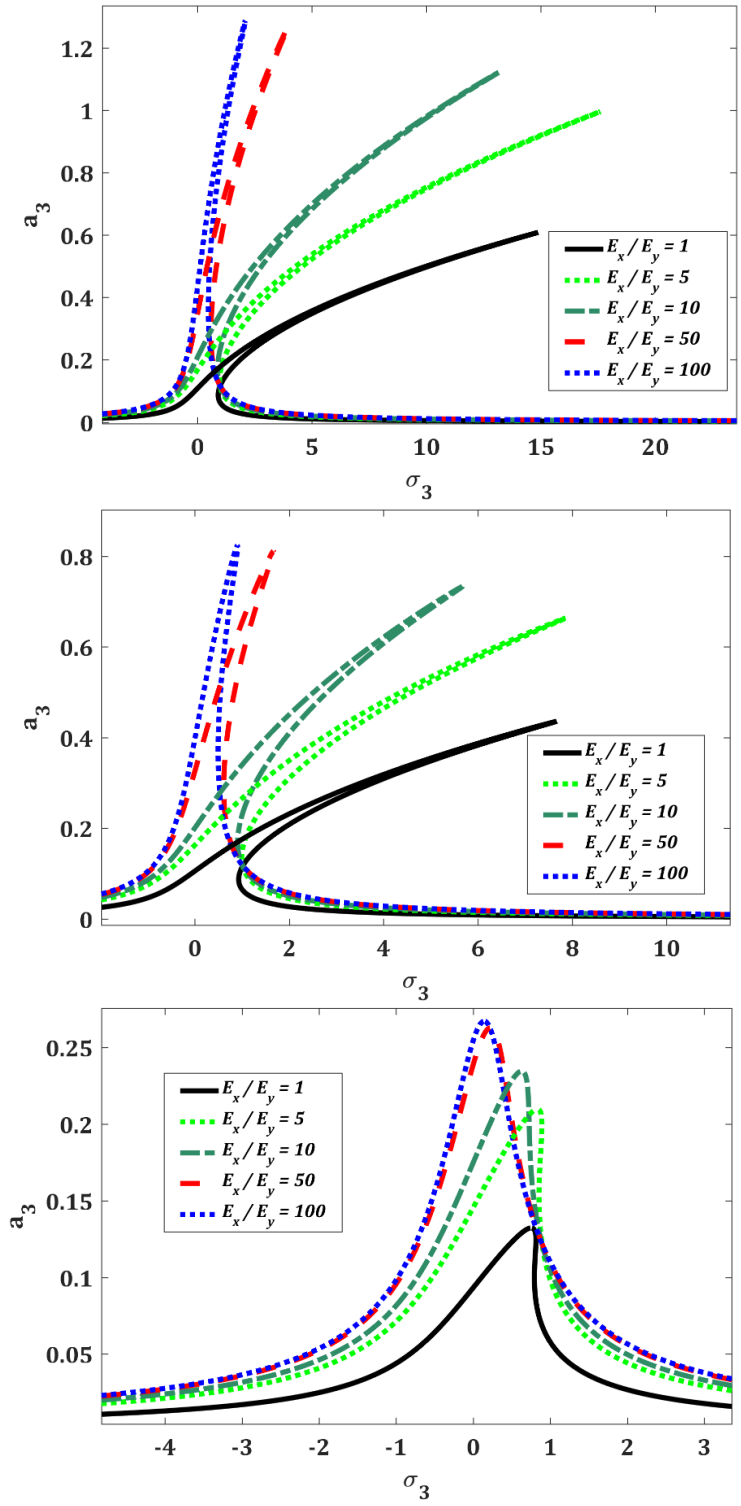

Figure B-8- Frequency response of third mode for different elasticity ratios under conditions of: (a) $\alpha = 0.1$, (b) $\alpha = 0.5$, and (c) $\alpha = 0.9$

Frequency response of the fourth mode for different elasticity ratios:

(a)

(b)

(c)

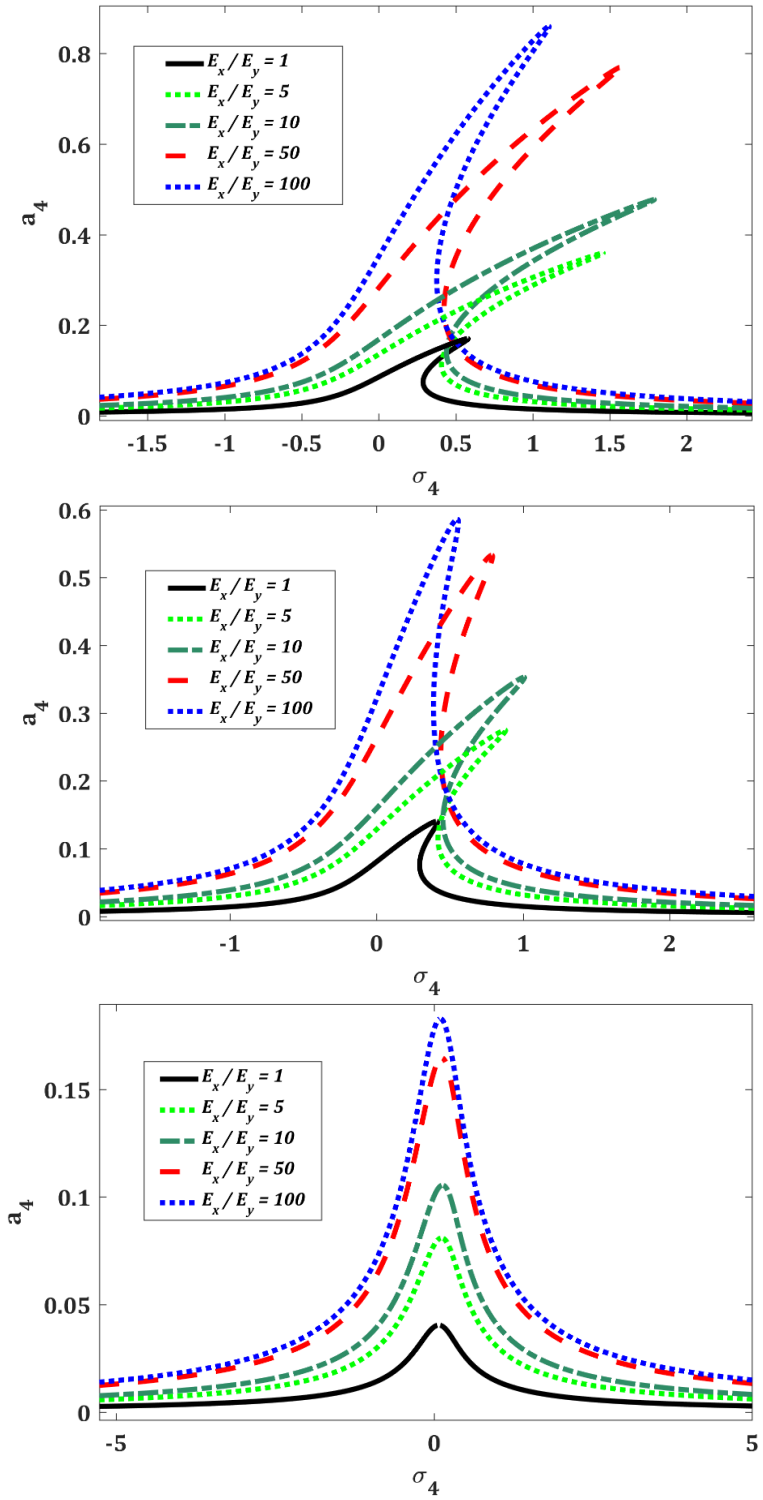

Figure B-9- Frequency response of fourth mode for different elasticity ratios under conditions of: (a) $\alpha = 0.1$, (b) $\alpha = 0.5$, and (c) $\alpha = 0.9$